

Supplementary Material to the submission EGU25-1
EGU General Assembly 2025, Vienna, Austria

THEORETICAL REFERENCE ESTIMATE

for the components of the global energy balance



Miklos Zagoni

EOTVOS LORAND UNIVERSITY, BUDAPEST, HUNGARY

2025

TABLE OF CONTENTS

Section	Page
Abstract	3
TRE (Theoretical Reference Estimate) on CMIP (Wild 2020, Fig. 13)	4
TRE on CMIP (Wild 2020, Table 1)	5
TRE on reanalyses (Wild and Bosilovich 2024, Table 1)	6
TRE on surface radiation budget (Li, Li, Wild and Jones, 2024, Fig. 2)	6
TRE on CERES EBAF TOA (Stackhouse et al. 2024, Table 2.9)	7
TRE on GEWEX Surface Radiation Budget (SRB) (Stackhouse et al., EGU 2023)	7
Derivation of TRE Eq. (1) and Eq. (2) from an idealized atmosphere (Schär, 2007)	8
Original: Karl Schwarzschild (1906) (Deutsch; English translation: 1966)	10
First appearance: Robert Emden (1913)	12
Early works: Milne (1930), Ostriker (1963)	13
Books with Eq. (1) (Goody 1964, Goody and Yung 1989, Houghton 1977)	14
Derivation in Houghton (1977, 1986, 2002)	15
Books with Eq. (1) (Chamberlain 1978, Hartmann 1994, Visconti 2001, Vardavas and Taylor 2007)	17
Books with Eq. (1) (Marshall and Plumb 2008, Pierrehumbert 2010, Andrews, 2012, Salby 2012, Ambaum 2021)	21
University lecture notes with Eq. (1) (Stephens, Emanuel, Tokyo, Toronto, Tyndall)	23
University lecture notes with Eq. (1) (University of Arizona, Harvard, Manchester, UK)	30
Schwarzschild (1906) equations in a university exam	31
Books with Eq. (1)	32
Books without Eq. (1)	32
TRE basics: The four equations from Schwarzschild (1906)	33
Early verification of Eqs. (1) and (2)	34
Recent verification of the four equations (CERES EBAF Ed4.1, Ed4.2)	35
The simplest greenhouse geometry	36
CERES EBAF Ed4.1 (April 2000 – March 2022) data in MS Excel table	37
The all-sky integer structure and Eqs.(3) and (4) on Hartmann (2016) Fig. 2.4	38
The all-sky integer structure on Stephens et al. (2012)	39
The all-sky integer structure, Eqs.(3)-(4) and albedo on Stephens et al. (2023, GEWEX, BAMS)	40
An independent estimate: all-sky Eqs. (3) and (4) on L’Ecuyer et al. (2015)	41
An independent estimate: clear-sky greenhouse effect in GFDL AM4	41
A case study: surface solar radiation, all-sky (Stackhouse, Trentmann, Kato, Wild)	42
A case study: surface solar radiation, all-sky (Hakuba, Loeb)	43
Attribution of global warming: greenhouse effect?	44
What are the drivers of global warming? ASR/ULW	45
TRE in earlier presentations (CERES STM 2017)	46
Geometric Summary	47
The Physical Science Basis: Trenberth’s Greenhouse Geometry	48
An Unresolved Mystery: Albedo (all-sky)	49
An Unresolved Mystery: Albedo (clear-sky)	50
TOA Net CRE and Clear-sky Atmospheric Window	51
Transfer Function and Clear-sky Atmospheric Window	52
Contemplating on the Hows ...	53
... And Whys	54
CERES EBAF Ed4.2.1, 24 years (288 monthly global mean), 2000 October – 2024 September	55



Theoretical reference estimate for the components of the global energy balance

Abstract

Wild (2020), and Wild and Bosilovich (2024) provide estimates of global mean energy balance components as represented in climate models and reanalyses, with reference estimates from Loeb et al. (2018), Wild et al. (2015, 2019), L'Ecuyer et al. (2015) and Kato et al. (2018). Here we add a theoretical reference estimate (TRE) based on four radiative transfer equations and geometric considerations as detailed in Zagoni (2025). The equations do not refer to the atmospheric gaseous composition or the reflective properties of the surface or clouds. The first equation is a clear-sky constraint relationship on the net radiation at the surface (R_N), following from the two-stream approximation of Schwarzschild's (1906-Eq.11) radiative transfer equation as given in standard university textbooks on atmospheric physics and radiation (Goody, Oxford, 1964_Eq.2.115; Houghton, Cambridge, 1977_Eq.2.13; Hartmann, Academic Press 1994, Eqs. 3.51-3.54; Ambaum, Royal Met Soc, 2021_Eq.10.56), and in university lecture notes (Stephens 2003): $R_N = \text{OLR}/2$. The second equation is a clear-sky constraint relationship on the total radiation at the surface (R_T), following from the simplest greenhouse geometry (Hartmann 1994, Fig.2.3): $R_T = 2\text{OLR}$. The third and fourth equations are all-sky versions of the first pair: $R_N(\text{all-sky}) = (\text{OLR} - \text{LWCRE})/2$, and $R_T(\text{all-sky}) = 2\text{OLR} + \text{LWCRE}$. Two decades of CERES observations (EBAF Ed4.1 April 2000–March 2022) give -2.33 , -2.82 , 2.71 and 2.44 [Wm^{-2}] deviations for the four equations, respectively, with a mean difference of 0.00 . The all-sky equations are justified by an independent estimate of GEWEX within 0.1 Wm^{-2} (Zagoni 2024). The solution can be given in small integer ratios relative to LWCRE as the unit flux; the best fit is 1 unit = 26.68 Wm^{-2} , see Table1 (highres figures and other info about TRE available at TABLELINK). Some of the most remarkable precisions are in TOA SW up all-sky ($=100$) and clear-sky ($=53$). – Li, Li, Wild and Jones (2024) provide a global radiation budget from a surface perspective from 34 CMIP6 models for 2000-2022, with differences from the TRE integer positions less than 1 Wm^{-2} in SW down radiation, Thermal down Surface and the convective flux (Sensible heat + Latent heat); less than 2 Wm^{-2} in Thermal up Surface; and less than 3 Wm^{-2} in Reflect by surface; each within the noted ranges of uncertainty. Stackhouse et al. (2024) give Earth radiation budget at top-of-atmosphere; TRE differ from 2001-22 Climatological Mean in OLR, TSI and RSW by 0.23 , 0.03 and 1.05 [Wm^{-2}], see details in TABLELINK in References.

References

- Li, X., Li, Q., Wild, M. and Jones, P. (2024) An intensification of surface EEI. *Nature Comm E&E*, <https://www.nature.com/articles/s43247-024-01802-z>
- Stackhouse, P., et al. (2024) State of the Climate 2023, *Bull. Am. Met. Soc.* **105**:8, <https://journals.ametsoc.org/view/journals/bams/105/8/2024BAMSStateoftheClimate.1.xml>
- Stephens, G. (2003) Colorado_State_University_AT622_Section 6_Eqs. (6.10a)-(6.10b), Example 6.3, Fig. 6.3a, https://reef.atmos.colostate.edu/~odell/AT622/stephens_notes/AT622_section06.pdf
- Wild, M. (2020) The global energy balance as represented in CMIP6 climate models. *Climate Dynamics* 55:553–577, <https://doi.org/10.1007/s00382-020-05282-7>
- Wild, M., Bosilovich, M. (2024) The global energy balance as represented in reanalyses. *Surv Geophys*, <https://link.springer.com/article/10.1007/s10712-024-09861-9>
- Zagoni, M. (2024) Modeling and Observing Global Energy and Water Cycles by GEWEX. AGU Fall Meeting, <https://agu.confex.com/agu/agu24/meetingapp.cgi/Paper/1535956>
- Zagoni, M. (2025) Trenberth's Greenhouse Geometry. AMS Annual Meeting, <https://ams.confex.com/ams/105ANNUAL/meetingapp.cgi/Paper/445222>
- See also the updated Supplementary Material video:
https://www.earthenergyflows.com/Zagoni-EGU2024-Trenberths-Greenhouse-Geometry_Full-v03-480.mp4

TABLELINK (this document): <https://earthenergyflows.com/TRE20.pdf>

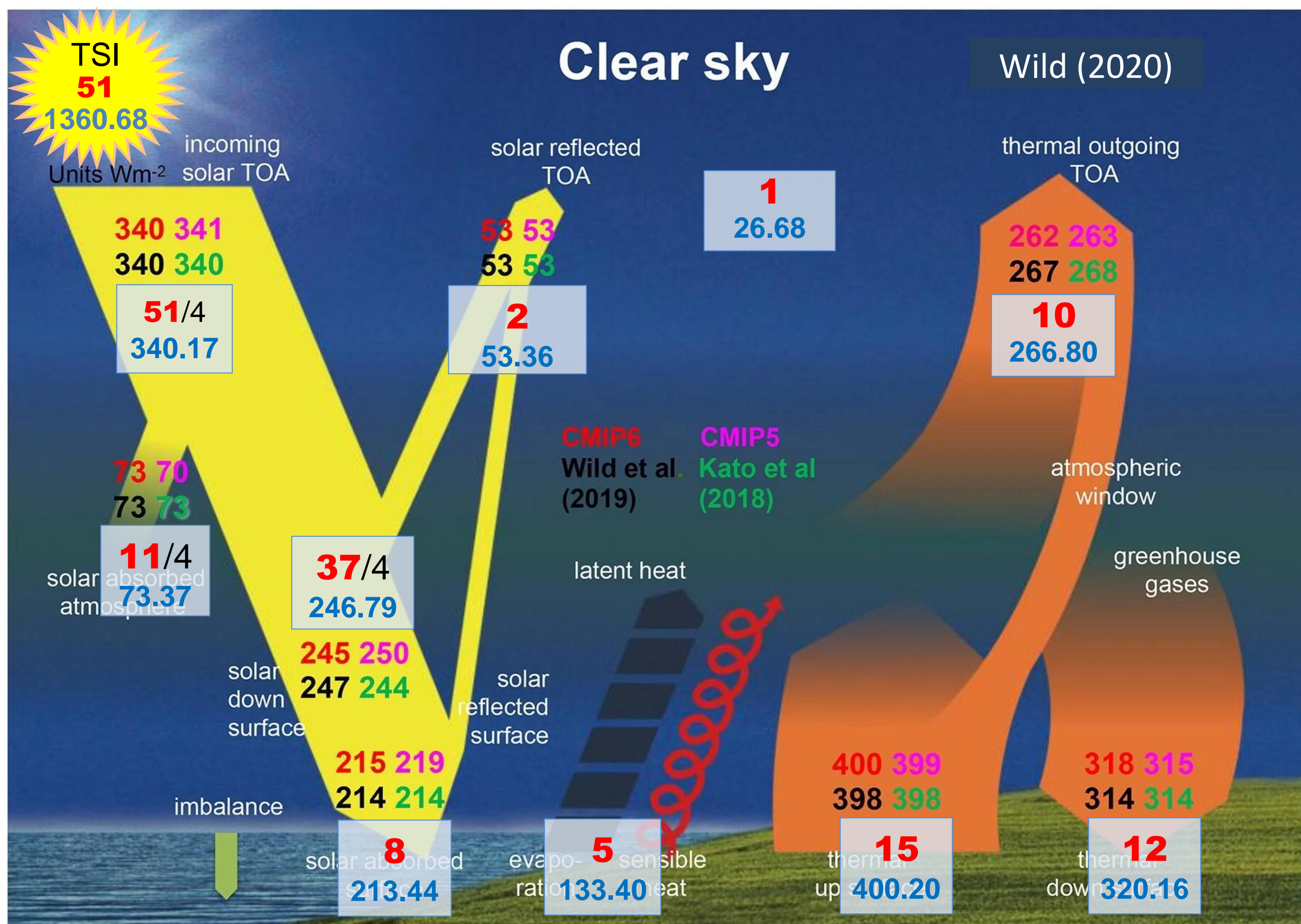
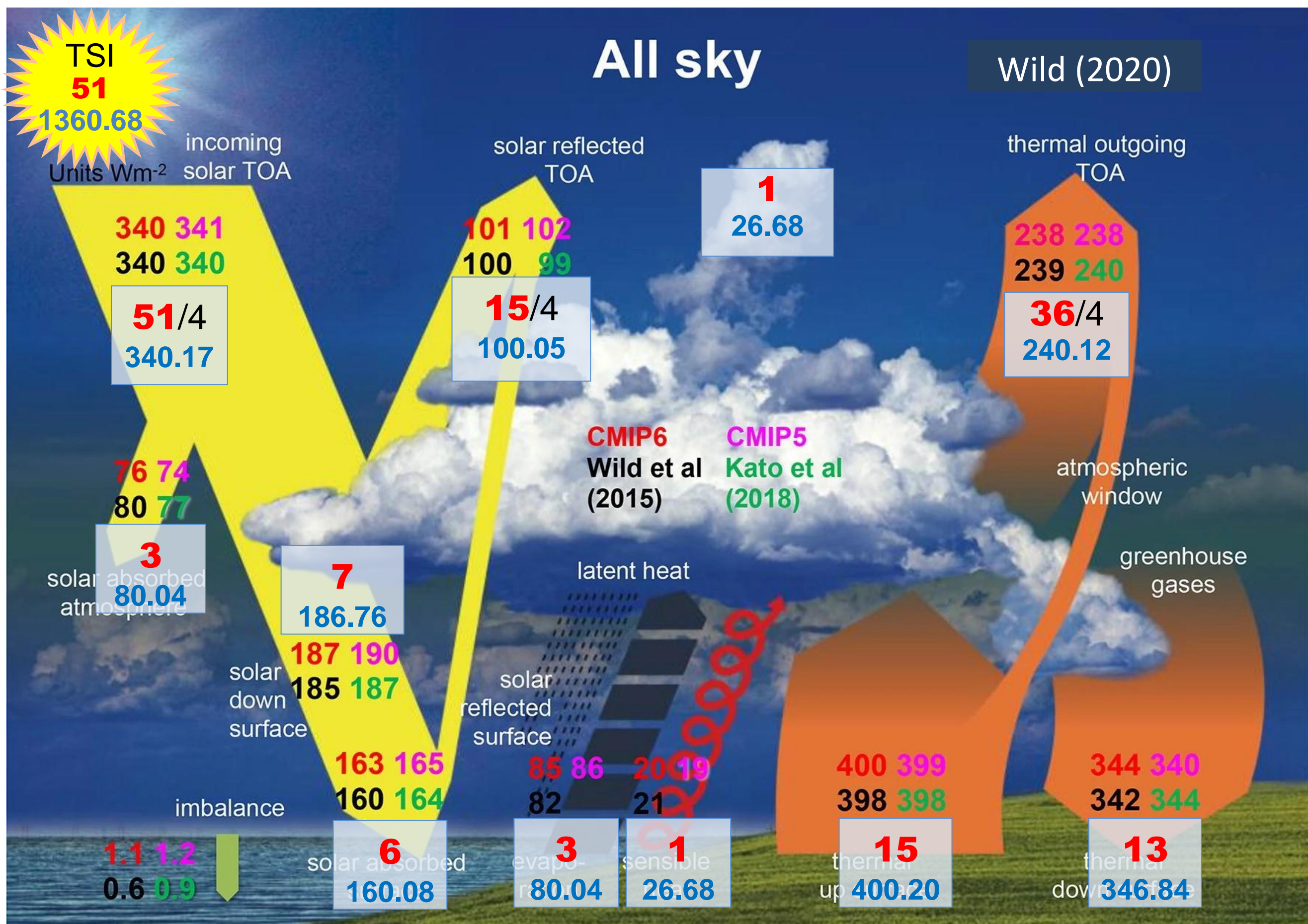


Fig.1a, b Theoretical reference estimate (TRE) projected on Wild (2020, Fig.13) all-sky and clear-sky, in textboxes. Values in upper rows (red bold typeface) are integer multiples of the unit flux of 26.68 Wm^{-2} ; values in the lower rows (blue) are in Wm^{-2} . The colored numbers in the original diagram are reference estimates from four different sources as specified in Wild (2020). Total solar irradiance is shown as $\text{TSI} = 51 \text{ units} = 1360.68 \text{ Wm}^{-2}$ [the most accurate community consensus value is $1360.8 \pm 0.5 \text{ Wm}^{-2}$, Kopp and Lean 2011]. Recently, the solar minimum value was increased by 0.294 Wm^{-2} (G. Kopp, August 2023); the most current estimate of TSI for 2003-2024 mean from SORCE and TSIS-1 TIM is 1361.96 Wm^{-2} . This value, with a geodetic weighting factor of 4.0034 (as in CERES EBAF), corresponds to $1 \text{ unit} = 26.682 \text{ Wm}^{-2}$. I use $\mathbf{1} = 26.68 \text{ Wm}^{-2}$ throughout this study, belonging to TSI of 51 units = 1361.84 Wm^{-2} . — With this solar-based unit flux, there are several, remarkably accurate fits, one of the most unexpected is solar reflected TOA, both all-sky and clear-sky, having 100 Wm^{-2} and 53 Wm^{-2} , resp., without any reference to cloudy or surface reflective properties. Notice that in the all-sky, TRE albedo = $15/51 = 0.294$; c.f. “The CERES flying on the Terra and Aqua satellites confirm that Earth’s albedo is 29.4% ($\pm 0.3\%$)” [Ackerman, L’Ecuyer, Loeb et al. 2019, AMS Met Monographs].

Below: Theoretical reference estimate (**N** and **N** × unit) compared to Wild (2020, Table 1), and Wild and Bosilovich (2024, Table 1) (next page).

TOA	Reference estimates	N	N × unit	CMIP6 mean
SW down TOA	340 ^a , 340 ^b , 340 ^c	51/4	340.17	340.2
SW up all-sky TOA	− 99 ^a , − 100 ^b , − 102 ^c	-15/4	-100.05	− 100.6
SW absorbed all-sky TOA	241 ^a , 240 ^b , 238 ^c	36/4	240.12	239.5
SW up clear-sky TOA	− 53 ^a , − 53 ^b	-8/4	-53.36	− 53.0
SW absorbed clear-sky TOA	287 ^a , 287 ^b	43/4	286.81	287.3
SW CRE TOA	− 46 ^a , − 47 ^b	-7/4	-46.69	− 47.8
LW up (OLR) all-sky TOA	− 240 ^a , − 239 ^b , − 238 ^c	-9	-240.12	− 238.3
LW up (OLR) clear-sky TOA	− 268 ^a , − 267 ^b	-10	-266.80	− 262.4
LW CRE TOA	28 ^a , 28 ^b	1	26.68	24.1
Net CRE TOA	− 18 ^a , − 19 ^b	-3/4	-20.01	− 23.6
Imbalance TOA	0.7 ^a	0		1.1
Atmosphere				
SW absorbed all-sky atmos.	80 ^b , 74 ^c , 77 ^d	3	80.04	76.0
SW absorbed clear-sky atmos.	73 ^b , 73 ^d	11/4	73.37	72.8
SW CRE atmos.	7 ^b , 4 ^d	1/4	6.67	3.2
LW net all-sky atmos.	− 183 ^b , − 180 ^c , − 187 ^d	-7	-186.76	− 182.1
LW net clear-sky atmos.	− 183 ^b , − 184 ^d	-7	-186.76	− 180.9
LW CRE atmos.	0 ^b , − 3 ^d			− 1.3
Net CRE atmos.	7 ^b , 1 ^d	1/4	6.67	1.9
Surface				
SW down all-sky surface	185 ^b , 186 ^c , 187 ^d	7	186.76	187.4
SW up all-sky surface	− 25 ^b , − 22 ^c , − 23 ^d	-1	-26.68	− 23.9
SW absorbed all-sky surface	160 ^b , 164 ^c , 164 ^d	6	160.08	163.4
SW down clear-sky surface	247 ^b , 244 ^d	37/4	246.79	244.8
SW up clear-sky surface	33 ^b , 30 ^d	5/4	33.35	30.2
SW absorbed clear-sky surface	214 ^b , 214 ^d	8	213.44	214.6
SW CRE surface	− 54 ^b , − 50 ^d	-2	-53.36	− 51.2
LW down all-sky surface	342 ^b , 341 ^c , 344 ^d	13	346.84	343.8
LW up all-/clear-sky surface	398 ^b , 399 ^c , 398 ^d	15	400.20	− 399.9
LW net all-sky surface	− 56 ^b , − 58 ^c , − 54 ^d	-2	-53.36	− 56.2
LW down clear-sky surface	314 ^b , 314 ^d	12	320.16	318.0
LW net clear-sky surface	− 84 ^b , − 84 ^d	-3	-80.04	− 81.7
LW CRE surface	28 ^b , 30 ^d	1	26.68	25.5
Net CRE surface	− 26 ^b , − 20 ^d	-1	-26.68	− 25.4
Net radiation surface	104 ^b , 106 ^c , 110 ^d	14	106.72	107.2
Latent heat flux	− 82 ^b , − 81 ^c	-3	-80.04	− 85.3
Sensible heat flux	− 21 ^b , − 25 ^c	-1	-26.68	− 20.1
Surface Imbalance	0.6 ^b , 0.5 ^c	0		1.5

The Global Energy Balance as Represented in Atmospheric Reanalyses

Martin Wild · Michael G. Bosilovich

Surveys in Geophysics 2024
https://doi.org/10.1007/s10712-024-09861-9

Energy balance component	Reference Estimates Wm^{-2}	Recent Reanal Reanal Wm^{-2}	N	N ×unit	Energy balance component	Reference Estimates Wm^{-2}	Recent Reanal Reanal Wm^{-2}	N	N ×unit
<i>TOA</i>					<i>Surface</i>				
SW down	340 ^a , 340 ^b , 340 ^c	340.9 340.8	51 /4	340.17	SW down all-sky	185 ^b , 186 ^c , 187 ^d	187.8 189.2	7	186.76
SW up all-sky	−99 ^a , −100 ^b , −102 ^c	−101.3 −100.7	−15 /4	−100.05	SW up all-sky	−25 ^b , −22 ^c , −23 ^d	−24.4 −25.0	−1	−26.68
SW absorbed all-sky	241 ^a , 240 ^b , 238 ^c	239.6 240.1	36 /4	240.12	SW absorbed all-sky	160 ^b , 164 ^c , 164 ^d	163.4 164.2	6	160.08
SW up clear-sky	−53 ^a , −53 ^b	−51.3 −52.5	−8 /4	−53.36	SW down clear-sky*	247 ^b , 244 ^d	246.8 247.8	37 /4	246.79
SW absorbed clear-sky	287 ^a , 287 ^b	289.4 288.2	43 /4	286.81	SW up clear-sky*	33 ^b , 30 ^d	31.0 32.4	−5 /4	−33.35
SW CRE	−46 ^a , −47 ^b	−48.8 −47.7	−7 /4	−46.69	SW absorbed clear-sky	214 ^b , 214 ^d	215.8 215.3	8	213.44
LW up (OLR) all-sky	−240 ^a , −239 ^b , −238 ^c	−243.4 −241.5	−9	−240.12	SW CRE	−54 ^b , −50 ^d	−51.5 −50.8	−2	−53.36
LW up (OLR) clear-sky	−268 ^a , −267 ^b	−265.8 −265.2	−10	−266.80	LW down all-sky	342 ^b , 341 ^c , 344 ^d	339.1 338.2	13	346.84
LW CRE	28 ^a , 28 ^b	22.4 23.9	1	26.68	LW up all-sky/clear-sky	−398 ^b , −399 ^c , −398 ^c	−398.3 −398.1	−15	−400.20
Net CRE	−18 ^a , −19 ^b	−26.5 −23.8	−3 /4	−20.01	LW net all-sky	−56 ^b , −58 ^c , −54 ^d	−59.3 −59.9	−2	−53.36
Imbalance	0.7 ^a	−3.9 −1.5	0	0	LW down clear-sky	314 ^b , 314 ^d	314.7 314.3	12	320.16
<i>Atmosphere</i>					<i>Surface</i>				
SW absorbed all-sky	80 ^b , 74 ^c , 77 ^d	76.1 75.9	3	80.04	LW net clear-sky	−84 ^b , −84 ^d	−83.9 −83.9	−3	−80.04
SW absorbed clear-sky	73 ^b , 73 ^d	73.6 72.8	11 /3	73.37	LW CRE	28 ^b , 30 ^d	23.7 23.6	1	26.68
SW CRE	7 ^b , 4 ^d	2.7 3.1	1 /4	6.67	Net CRE	−26 ^b , −20 ^d	−27.7 −27.2	−1	−26.68
LW net all-sky	−183 ^b , −180 ^c , −187 ^d	−184.2 −181.6	−7	−186.76	Net radiation	104 ^b , 106 ^c , 110 ^d	104.1 104.3	4	106.72
LW net clear-sky	−183 ^b , −184 ^d	−182.0 −181.4	−7	−186.76	Latent heat flux	−82 ^b , −81 ^c	−88.7 −86.0	−3	−80.04
LW CRE	0 ^b , −3 ^d	−1.4 0.3	0	0	Sensible heat flux	−21 ^b , −25 ^c	16.0 −17.5	−1	−26.68
Net CRE	7 ^b , 1 ^d	1.3 3.4	1 /4	6.67	Surface Imbalance	0.6 ^b , 0.5 ^c	−0.6 0.7	0	0

An intensification of surface Earth's energy imbalance since the late 20th century

X. Li, Q. Li, M. Wild, P. Jones (2024)

<https://doi.org/10.1038/s43247-024-01802-z>

Article

Fig. 2 | The global Radiation Budget from a surface perspective in this study. The numbers indicate the best estimates and their uncertainties (at 95% confidence level) for the magnitudes of the globally averaged energy balance components, obtained using the BMA method constrained by observational data from 34 CMIP6 models during 2000–2022, representing present-day climate conditions since the start of the 21st century. Downward shortwave radiation is constrained by reconstructed SSR data from Jiao et al. 2023, while upward shortwave and longwave radiation are constrained using GEBA observational station data. Due to the lack of observational data for latent and sensible heat fluxes, SME results are used directly. Uncertainties are calculated from the weighted ensemble standard deviation of the models.

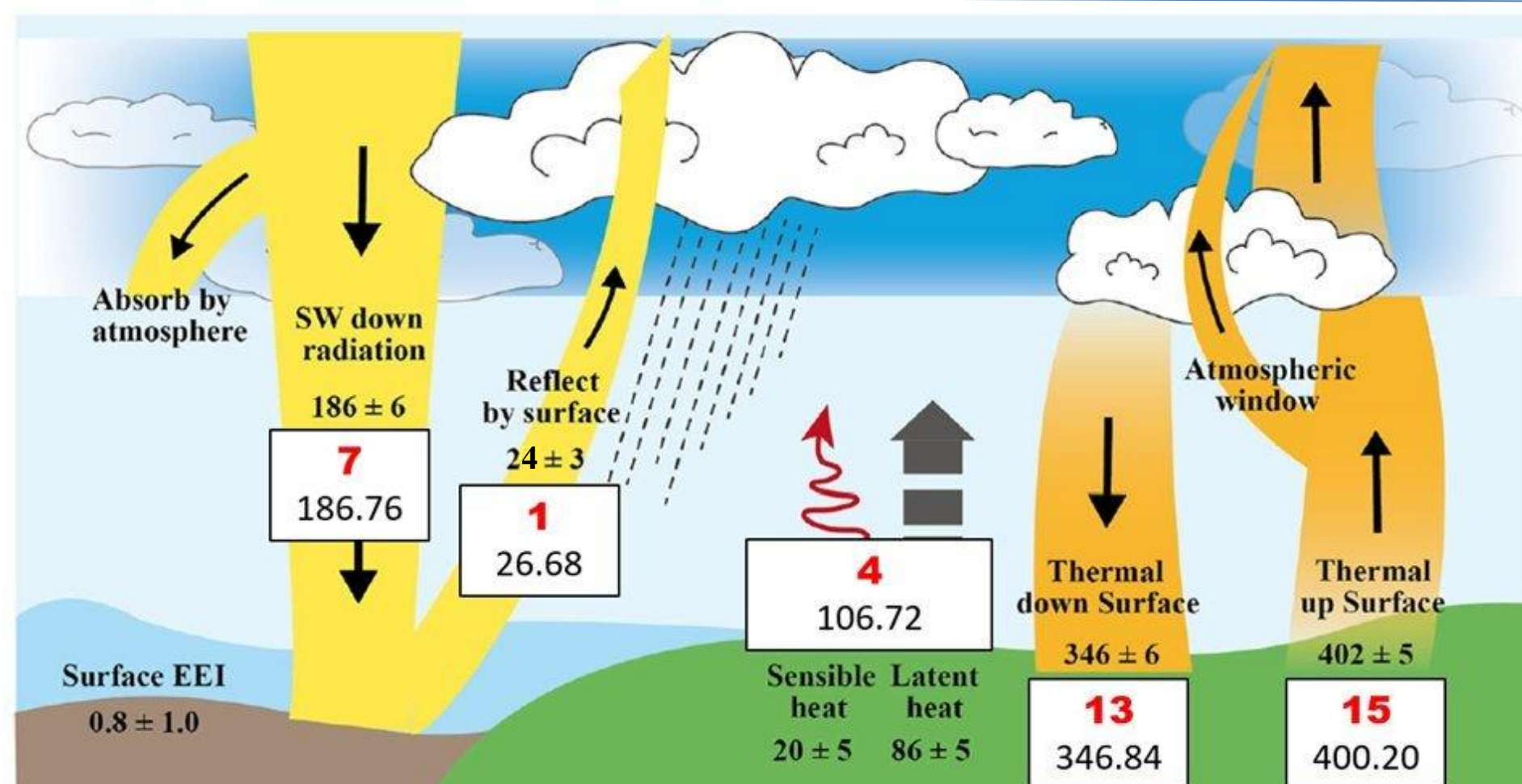


Fig. 2 Theoretical Reference Estimate (TRE) projected on the global radiation budget from a surface perspective (Li, Li, Wild and Jones, 2024) in form of integer positions and values in textboxes. The accuracy of their estimate to the GHG-independent theoretical expectation is within the acknowledged ranges of uncertainty; the differences are 0.76, 2.68, 0.72, 0.84 and 1.80 Wm^{-2} . The convective flux at the surface is $20 + 86 = 106 \text{ Wm}^{-2}$, the net radiation (R_N) is the same, 106 Wm^{-2} ; the total absorbed radiation at the surface is $R_T = 186 - 24 + 346 = 508 \text{ Wm}^{-2}$. My reference estimate gives $R_N = 4$ units which, with 1 unit = 26.68 Wm^{-2} , yields R_N (theory) = 106.72 Wm^{-2} , the difference is 0.72 Wm^{-2} ; and my reference estimate for $R_T = 6 + 13 = 19$ units, yielding R_T (theory) = 506.92 Wm^{-2} ; difference is 1.08 Wm^{-2} , showing the accuracy of the Earth's system sitting on its stationary geometric equilibrium position, far within the stated uncertainty. — Since the energy released by the surface is $402 + 20 + 86 = 508 \text{ Wm}^{-2}$, and its total absorption is the same, $186 - 24 + 346 = 508 \text{ Wm}^{-2}$, this surface energy balance represents a surface in equilibrium, that is, a zero EEI, being in evident contradiction to the indicated EEI = 0.8 and with the title of the article. [In a communication the Authors informed me about the values of the diagram in one decimal place, giving up the correct EEI = 0.8 Wm^{-2} , but these numbers are not presented in the paper.] — An easy solution could be to decrease 'Thermal up Surface' from 402 Wm^{-2} (which is unreasonably high, compared to Wild et al. (2015, 2019) = 398, CERES = 398.5 or CMIP6 = 399.9 for the examined period) to 401 Wm^{-2} , generating a positive (downward) 1 Wm^{-2} EEI, and satisfying the integer solution for this energy flow component by a difference of 0.8 Wm^{-2} .

On the other hand, $ULW = 402 \text{ Wm}^{-2}$ is strongly supported by the theoretical transfer function of $f(\text{all-sky}) = \text{ASR}/ULW = 9/15 = 0.6$, since with ASR climatological mean = 241.20 (see Stackhouse et al. 2024 below), $f(\text{observed}) = 241.20/402 \equiv 0.600$. — Note also that the most reliable assessment for components of the convective flux (Sensible heat, SH, and Latent heat, LH) is from the NEWS – NASA Energy and Water-cycle Study (Rodell et al. 2015, L'Ecuyer et al. 2015), proposing $SH = 25$ and $LH = 81$ ($R_N = 106 \text{ Wm}^{-2}$), and, after a second optimization (Stephens and L'Ecuyer 2015), $SH = 26$ and $LH = 82$ ($R_N = 108 \text{ Wm}^{-2}$). Notice that $1 = 26.68 \text{ Wm}^{-2}$ and $3 = 80.04 \text{ Wm}^{-2}$; hence these components occupy integer positions separately.

State of the Climate 2023 – August 2024 – BAMS

1. EARTH RADIATION BUDGET AT TOP-OF-ATMOSPHERE
—P. W. Stackhouse Jr., T. Wong, P. Sawaengphokhai, J. Garg, and N. G. Loeb

Table 2.9. Global annual mean top-of-atmosphere (TOA) radiative flux changes between 2022 and 2023, the 2023 global annual mean radiative flux anomalies relative to their corresponding 2001–22 mean climatological values, the mean 2001–22 climatological values, and the 2-sigma interannual variabilities of the 2001–22 global annual mean fluxes (all units in W m ⁻²) for the outgoing longwave radiation (OLR), total solar irradiance (TSI), reflected shortwave (RSW), absorbed solar radiation (ASR, determined from TSI – RSW), and total net fluxes. All flux values have been rounded to the nearest 0.05 W m ⁻² and only balance to that level of significance.						
Global	One Year Change (2023 minus 2022) (W m ⁻²)	2023 Anomaly (Relative to 2001–22) (W m ⁻²)	Climatological Mean (2001–22) (W m ⁻²)		Interannual Variability (2001–22) (W m ⁻²)	
OLR	+0.60	+0.85	36 /4 = 240.12	240.35	ΔOLR = +0.23	±0.65
TSI	+0.10	+0.25	51 /4 = 340.17	340.20	ΔTSI = +0.03	±0.15
RSW	–0.80	–1.50	15 /4 = 100.05	99.00	ΔRSW = –1.05	±1.05
ASR	+0.90	+1.75		241.20	ΔASR = +1.08	±1.05
Net	+0.30	+0.90		0.85	Net = +0.85	±0.85

Fig. 3 Theoretical reference estimate (TRE) projected on TOA radiation budget of CERES by Stackhouse et al. (2024), Table 2.9. Differences from OLR (Outgoing Longwave Radiation), TSI (Total Solar Irradiance) and RSW (Reflected Shortwave Radiation) climatological means (2001–22) are 0.23, 0.03 and -1.05 Wm⁻², respectively; each within the interannual variability for the same period. TRE Unit Flux **1** = 26.68 Wm⁻².

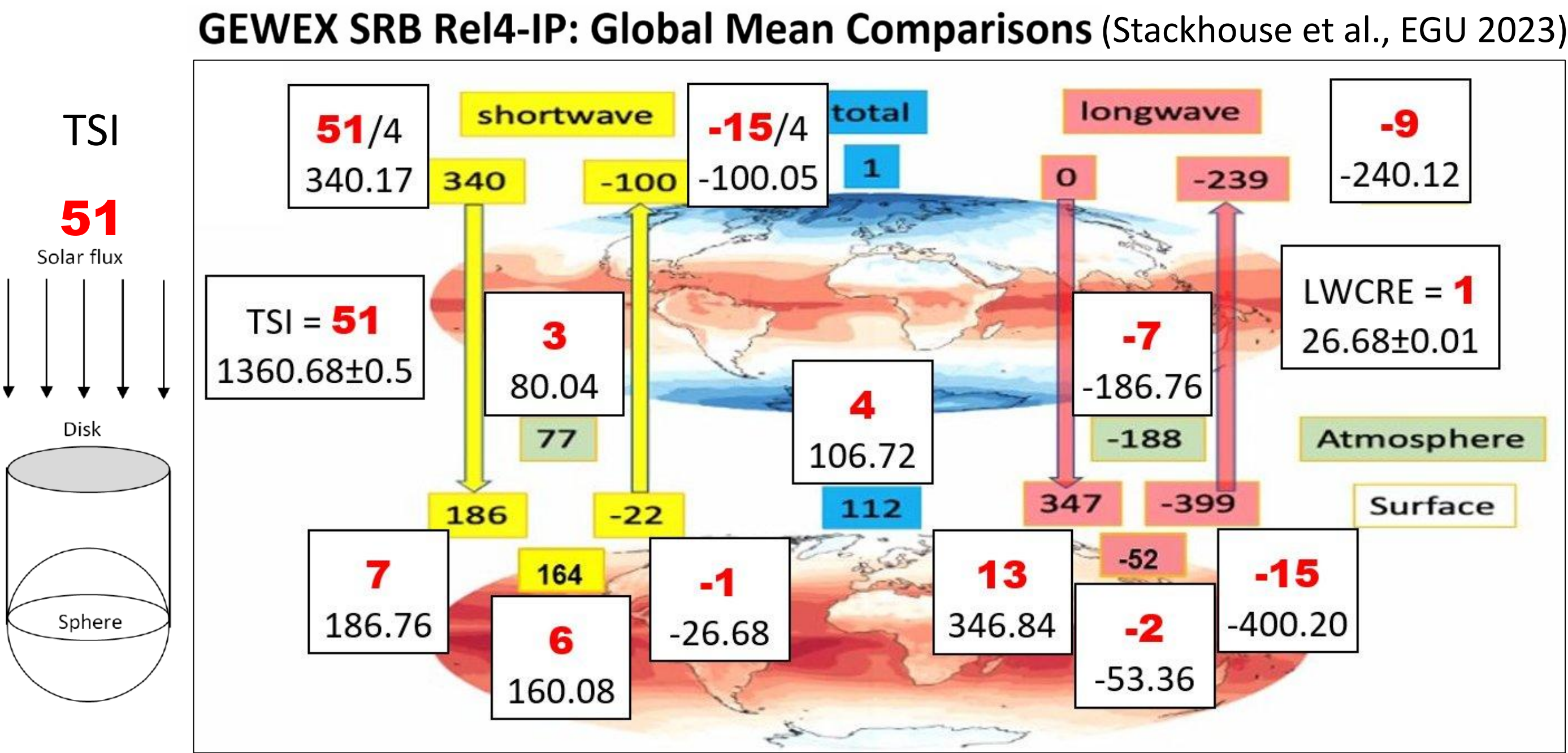
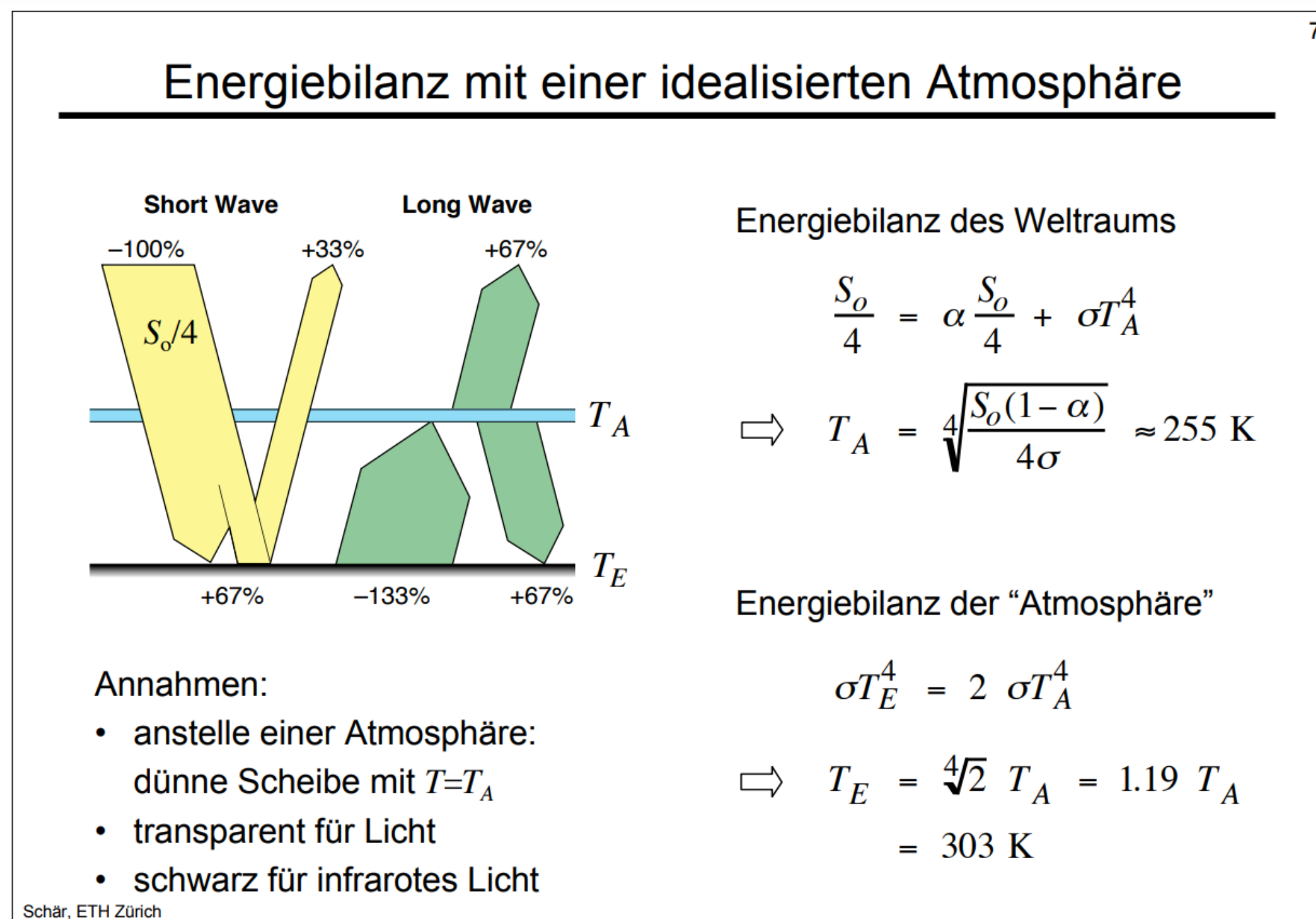


Fig. 4 TRE projected on SRB Surface Radiation Budget by GEWEX (Stackhouse et al. 2023, EGU)

Derivation of TRE Eq. (1) and Eq. (2) from an idealized atmosphere: Christoph Schär, ETH Zürich, Klimasystem und Wasserkreislauf, 2007

https://iacweb.ethz.ch/staff/schaer/etc/EuP/L2_Klima_HO.pdf



TRE Eq. (2) for the idealized atmosphere:

$$\text{Eq. (2)} \quad R_T (\text{clear-sky}) = \sigma T_E^4 = 2\sigma T_A^4$$

Notation: T_E
Temperatur der
Erdoberfläche

Now let's follow the logic of Hartmann (1994, Fig. 3.10-3.11, p.63):

A thin layer of atmosphere near the surface absorbs a fraction ϵ of the emission from above and below and emits in both directions. The temperature of the air adjacent to the surface, T_{SA} , may be derived from the energy balance there.

$$\epsilon \sigma T_E^4 + \epsilon \sigma T_A^4 = 2\epsilon \sigma T_{SA}^4.$$

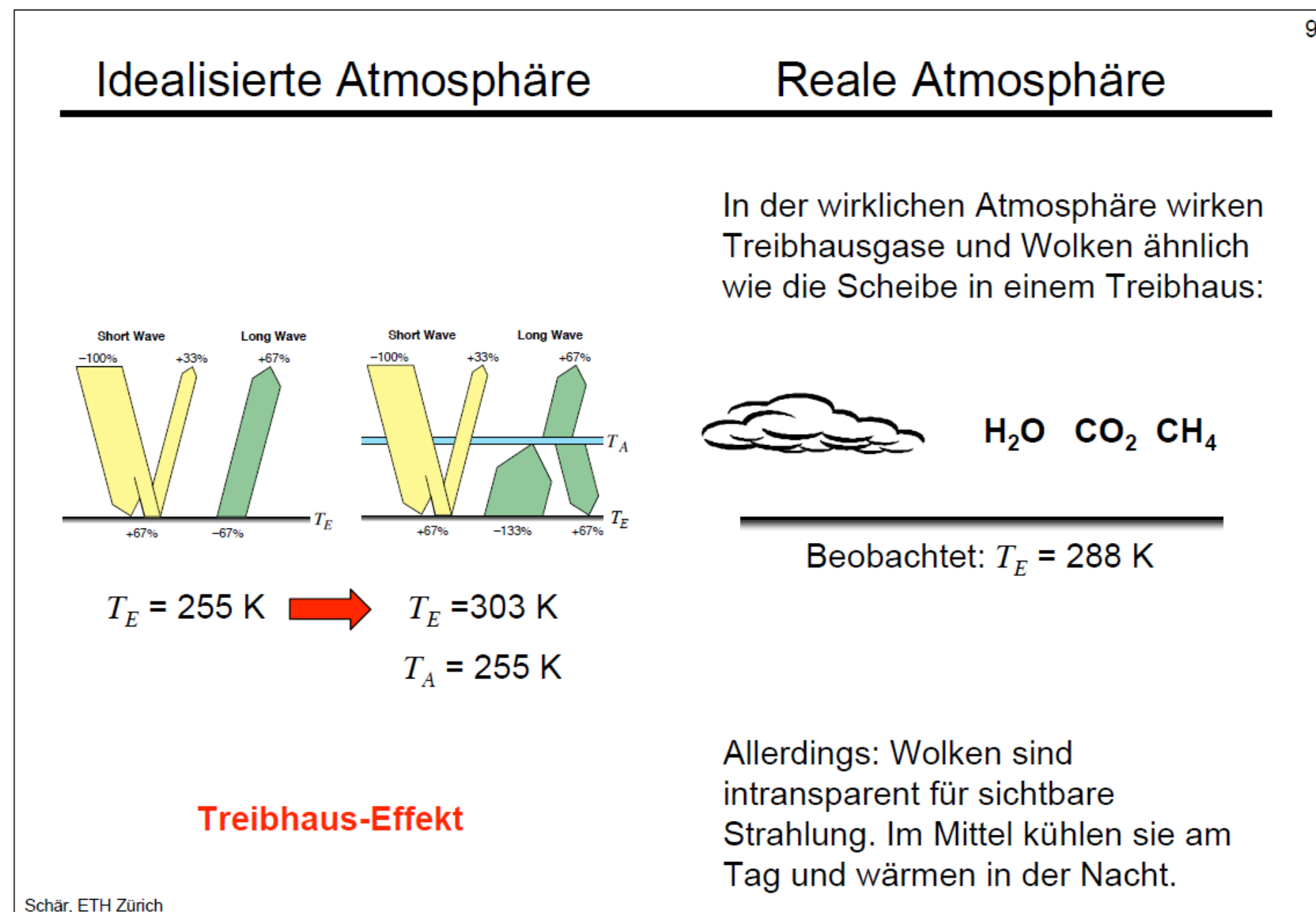
From Eq. (2) $\sigma T_E^4 = 2\sigma T_A^4$, we have $3\sigma T_A^4 = 2\sigma T_{SA}^4$,

that is, $\sigma T_{SA}^4 = (3/2) \sigma T_A^4 \Rightarrow$

TRE Eq. (1) for the idealized atmosphere:

$$\text{Eq. (1)} \quad R_N (\text{clear-sky}) = \sigma T_E^4 - \sigma T_{SA}^4 = \sigma T_A^4 / 2$$

Validation of Idealized Eqs. (1)-(2) on Real Atmosphere:



All-sky $T_A = 255 \text{ K} \Rightarrow$ All-sky OLR $= 239.74 \text{ Wm}^{-2} \Rightarrow T_E = 303.25 \text{ K}$

Clear-sky $T_A = 261.91 \text{ K} \Rightarrow$ Clear-sky OLR $= 266.80 \text{ Wm}^{-2} \Rightarrow T_E = 311.46 \text{ K}$

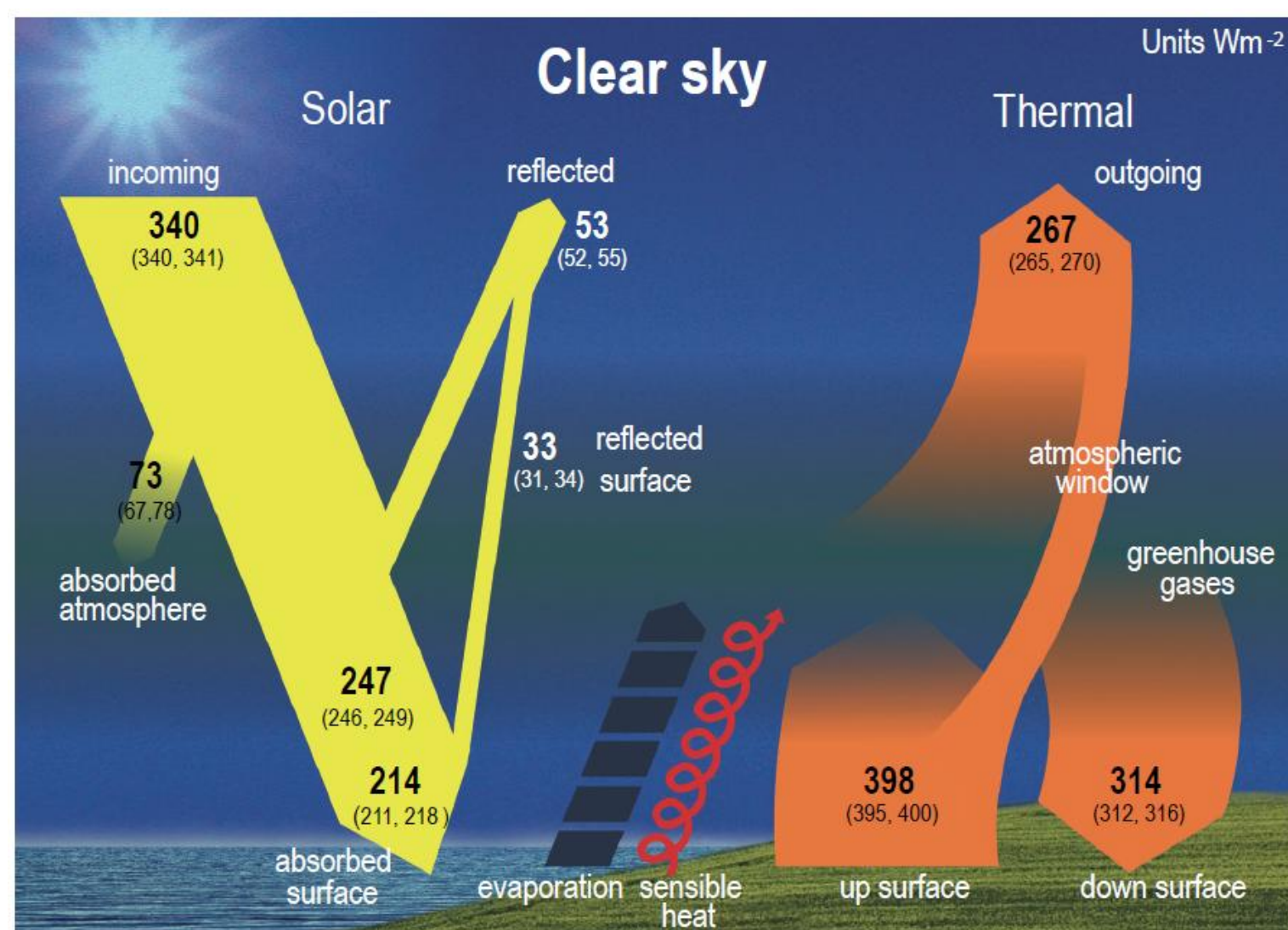
Treibhaus-Effekt:

$T_E = 255 \text{ K}$ → $T_E = 303 \text{ K}$, Beobachtet: $T_E = 288 \text{ K}$

Greenhouse effect, clear-sky: $T_E = 262 \text{ K} \Rightarrow T_E = 311.5 \text{ K}$, **Observed: $T_E = 288 \text{ K}$**

From TRE Eqs. (1) and (2): $\sigma T_{SA}^4 = (3/2) 266.80 \text{ Wm}^{-2} = 400.20 \text{ Wm}^{-2} \Rightarrow T_{SA} = 289.85 \text{ K}$ ✓

Idealized greenhouse effect, clear-sky: $G = 400.20 - 266.80 = 133.40 \text{ Wm}^{-2}$



Observed $G = 398 - 267 = 131 \text{ Wm}^{-2}$ ✓

TRE Equations (1) and (2) of the idealized atmosphere are satisfied by the real atmosphere's data.

Original: Karl Schwarzschild (1906)

Ueber das Gleichgewicht der Sonnenatmosphäre

Von

K. Schwarzschild.

Vorgelegt in der Sitzung vom 13. Januar 1906.

Man betrachte jetzt die Strahlungsenergie A , die durch die Sonnenatmosphäre an irgend einer Stelle nach außen wandert, und die Strahlungsenergie B , die (infolge der Strahlung der weiter außen liegenden Schichten) nach innen wandert.

Man verfolge zunächst die nach innen wandernde Energie B . Geht man um eine unendlich dünne Schicht dh nach innen, so geht von der von außen kommenden Energie B der Bruchteil $B \cdot a \, dh$ verloren, auf der anderen Seite kommt durch die nach der einen Seite gehende Eigenstrahlung der Schicht dh der Betrag $a E \, dh$ hinzu, es ergibt sich also im Ganzen:

$$(7) \quad \frac{dB}{dh} = a(E - B).$$

Völlig analog folgt für die nach außen gehende Strahlung:

$$(8) \quad \frac{dA}{dh} = -a(E - A).$$

Indem man sich das Absorptionsvermögen a als Funktion der Tiefe h gegeben denkt, bilde man die über der Tiefe h liegende „optische Masse“ der Atmosphäre:

$$(9) \quad m = \int^h a \, dh.$$

Dann lauten die Differentialgleichungen:

$$(10) \quad \frac{dB}{dm} = E - B, \quad \frac{dA}{dm} = A - E.$$

Wir fragen nach einem stationären Zustand der Temperaturverteilung. Derselbe ist bedingt durch die Forderung, daß jede Schicht ebensoviel Energie empfängt, als ausstrahlt, daß also gilt:

$$aA + a \cdot B = 2aE, \quad A + B = 2E.$$

Führt man dieser Bedingung entsprechend die Hilfsgröße γ ein durch:

$$A = E + \gamma, \quad B = E - \gamma,$$

Die Integrationskonstanten E_0 und γ wurden dadurch bestimmt, daß an der Außengrenze der Atmosphäre ($m = 0$) keine nach innen wandernde Energie B vorhanden ist und die nach außen wandernde Energie den zu beobachtenden Betrag A_0 hat. Es muß also für $m = 0$:

$$B = 0, \quad A = A_0$$

sein. Hiermit ergibt sich das Resultat:

$$(11) \quad E = \frac{A_0}{2}(1 + m), \quad A = \frac{A_0}{2}(2 + m), \quad B = \frac{A_0}{2}m.$$

Now, form the difference of the second and first term in Eq. (11), and we have the net radiation at the surface:

$$A - E = \Delta A = A_0/2.$$

**English translation in: Donald Menzel, ed., Selected papers on the transfer of radiation
Dover Publication, New York (1966)**

On the Equilibrium of the Sun's Atmosphere

by K. Schwarzschild

(Presented at the meeting of the Berlin Academy of Sciences on January 13, 1906)

Consider now, at some point in the solar atmosphere, the radiative energy A which is transmitted outward, and the radiative energy B , which (due to the radiation of outer layers) is transmitted inward.

Treat first the inward energy B . When traveling inward through an infinitesimally thin layer dh , the fraction $aBdh$ of B will be lost; on the other hand, the contribution $aEdh$ due to the lateral radiation of the layer itself will be added to B . All in all,

$$\frac{dB}{dh} = a(E - B). \quad (7)$$

In the case of the outward energy A , we proceed analogously and obtain

$$\frac{dA}{dh} = -a(E - A). \quad (8)$$

Given the absorption coefficient a as a function of depth h , define the "average optical depth"* of the atmosphere lying above the depth h by

$$\bar{\tau} = \int^h adh. \quad (9)$$

The differential equations then become

$$\frac{dB}{d\bar{\tau}} = E - B, \quad \frac{dA}{d\bar{\tau}} = A - E. \quad (10)$$

We want to find the temperature distribution under steady-state conditions. These require that each layer receives as much energy as it radiates, i.e., that

$$aA + aB = 2aE, \quad A + B = 2E.$$

Introducing the parameter ζ such that

$$A = E + \zeta, \quad B = E - \zeta,$$

we obtain the differential equations in the form

$$\frac{d\zeta}{d\bar{\tau}} = 0, \quad \frac{dE}{d\bar{\tau}} = \zeta,$$

and after integration we have

$$\begin{aligned} \zeta &= \text{const.} \\ E &= E_0 + \zeta\bar{\tau} \\ A &= E_0 + \zeta(1 + \bar{\tau}) \\ B &= E_0 + \zeta(\bar{\tau} - 1). \end{aligned}$$

The constants of integration E_0 and ζ are fixed by the requirements that there can be no inward radiation at the outer boundary of the atmosphere ($\bar{\tau} = 0$), and that the outward energy there must have the observed value A . Thus at $\bar{\tau} = 0$ we must have

$$B = 0, \quad A = A_0.$$

This leads to the final result

$$E = \frac{A_0}{2} (1 + \bar{\tau}), \quad A = \frac{A_0}{2} (2 + \bar{\tau}), \quad B = \frac{A_0}{2} \bar{\tau}. \quad (11)$$

Difference of the second and first term in Eq. (11) gives
the net radiation at the surface:

$$A - E = \Delta A = A_0/2.$$

First appearance: Robert Emden (1913)

ETH Zürich (1888), Physikalisches Laboratorium des eidgenössischen Polytechnikums Zürich

Brother-in-law of Karl Schwarzschild (married to Klara, sister of Karl)

Über Strahlungsgleichgewicht und atmosphärische Strahlung.

Ein Beitrag zur Theorie der oberen Inversion.

Von R. Emden.

Vorgelegt von S. Finsterwalder in der Sitzung am 1. Februar 1913.

Sitzungsberichte der mathematisch-physikalischen Klasse der

K. B. Akademie der Wissenschaften zu München (1913)

English translation: Monthly Weather Review (1916)

und die Lösung des Problems

$$(31) \quad \begin{cases} B = -k\gamma m + B_0 \\ A = -k\gamma m + A_0 \\ E = -k\gamma m + E_0. \end{cases}$$

B_0 und A_0 sind dem jeweiligen Spezialfalle anzupassende Integrationskonstanten. Stets ist

$$(32) \quad \gamma = \frac{B_0 - A_0}{2}; \quad E_0 = \frac{B_0 + A_0}{2}.$$

Ansatz und Lösung dieses Strahlungsproblems sind von K. Schwarzschild (loc. cit.) gegeben.

$$89) \quad T_{\text{Erde}} = 254^\circ \sqrt[4]{2,2} = 309^\circ = + 36^\circ.$$

An der Berührungsfläche Atmosphäre und Erde ergibt sich somit ein Temperatursprung von 20°C , der in Wirklichkeit durch äußere Wärmeleitung stark herabgesetzt wird, namentlich auf Wasser, wo der Wasserdampf mit der Temperatur der Oberfläche in die Atmosphäre übertritt. Auch diese Strahlungstemperatur der Erdoberfläche hat einen durchaus annehmbaren Wert.

“At the interface between the atmosphere and the earth, there is a temperature jump of 20°C , which is in reality greatly reduced by external heat conduction, especially on water, where the water vapor transfers into the atmosphere at the temperature of the surface. This radiation temperature of the earth's surface also has a perfectly acceptable value.”

The size of ‘Temperatursprung’ (discontinuity) is correctly computed; but the other side of the equation ($A_0/2$) is not explicitly given.

Edward Arthur Milne (1930)

Thermodynamics of the Stars

Handbuch der Astrophysik, Vol. 3. 1930

$$\frac{1}{2} \frac{dI}{d\tau} = I - B \quad (88)$$

and similarly

$$\frac{1}{2} \frac{dI'}{d\tau} = B - I'. \quad (89)$$

These equations may be described as the equations of “linear” or “tubular” flow of radiation. They may be derived from first principles by dividing the radiation into an outward and an inward beam, and assuming a coefficient of absorption $2k$ to allow for the mean obliquity of the rays to the direction of the axis. They have proved exceedingly useful in many approximate investigations.

The equation of radiative equilibrium (82) becomes

There is no radiation incident on the boundary. Hence $I'(0) = 0$. Hence

$$B_0 = \frac{1}{2} \mathfrak{F} \quad (92)$$

whence

$$B = \mathfrak{F}(\frac{1}{2} + \tau) \quad (93)$$

$$I = \mathfrak{F}(1 + \tau) \quad (94)$$

$$I' = \mathfrak{F}\tau. \quad (95)$$

We notice that $I(0) = \mathfrak{F}$, as it ought.

Jeremiah Ostriker (1963)

Radiative transfer in a finite gray atmosphere

Astrophysical Journal, vol. 138, p.281-290

and the temperature at the ground layer is

$$T(\tau_1) \equiv T_1 = T_b \left(\frac{\tau_1 + \frac{2}{3}}{\tau_1 + \frac{4}{3}} \right)^{1/4} = T_b \left[1 - \frac{1}{2} \left(\frac{T_e}{T_b} \right)^4 \right]^{1/4}. \quad (15)$$

Here we see that there will be a discontinuity in the temperature between the lowest layer of the atmosphere (T_1) and the ground (T_b). This discontinuity, although somewhat

a similar problem, Emden (1913) found the same type of discontinuity. One may note from the form of equation (15) that the magnitude of the discontinuity may be large if τ_1 is small but will tend toward zero as the total optical depth increases.

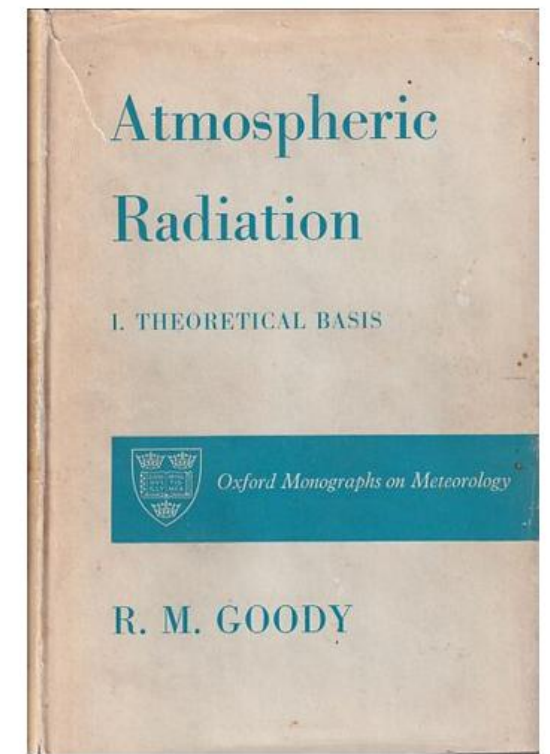
Some books with explanation of TRE Eq. (1):

R. Goody: Atmospheric radiation. Theoretical basis. Oxford, 1964

$$F_v/2\pi = J_v(0) - B_v^*(0) = B_v^*(\tau_v^*) - J_v(\tau_v^*). \quad (2.115)$$

Note that if the medium is in thermodynamic equilibrium ($J_v = B_v$), equation (2.115) requires a discontinuity in B_v (i.e. a *temperature discontinuity*) at both boundaries.

the step in B always equals $F/2\pi$



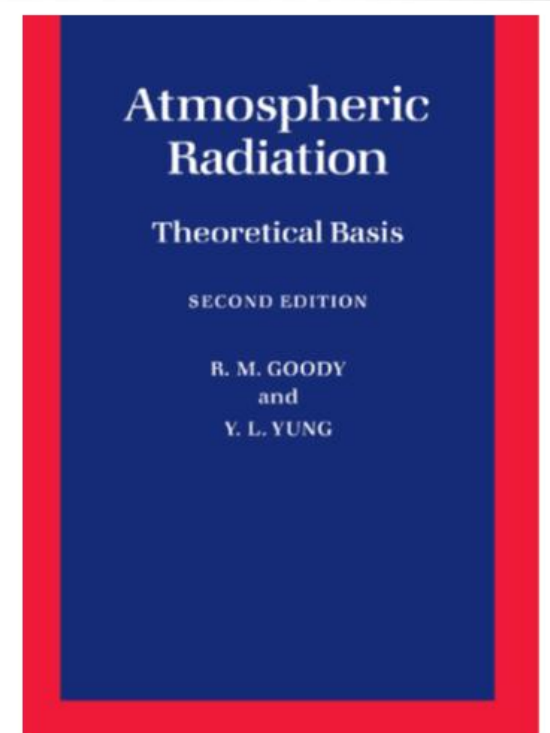
Goody – Yung: Atmospheric radiation. Theoretical basis. Oxford, 1989

$$F/2\pi = B(0) - B^*(0) = B^*(\tau_1) - B(\tau_1). \quad (2.146)$$

Equation (2.146) requires a discontinuity in the Planck function, implying a discontinuity of temperature, at the boundary.

2. There are discontinuities,

$$\Delta B = \frac{F_s}{2\pi} \quad \text{DISCONTINUITY} = \text{OLR}/2$$



23

John Houghton: The Physics of Atmospheres

Cambridge (1977, 1986, 2002) Eq. 2.13

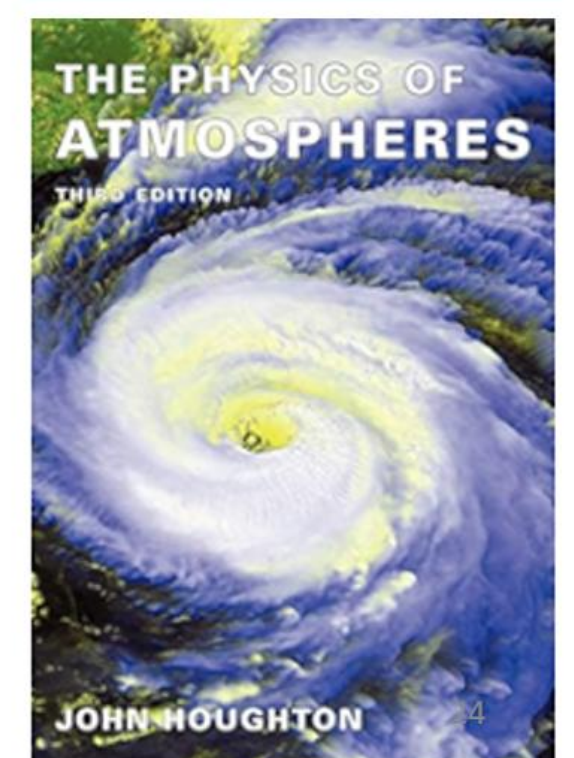
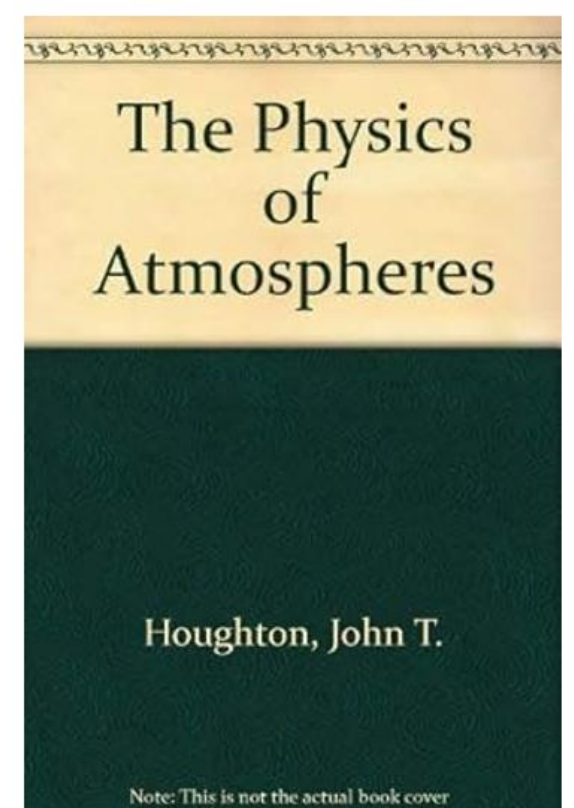
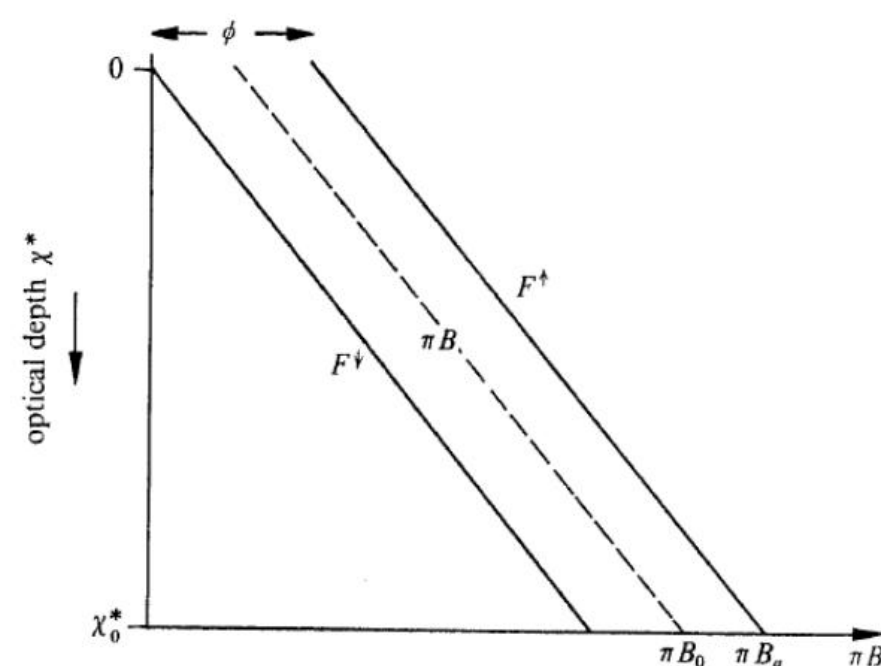
At the bottom of the atmosphere where $\chi^* = \chi_0^*$, $F^\uparrow = \pi B_g$, B_g being the black-body function at the temperature of the ground. It is easy to show that there must be a temperature discontinuity at the lower boundary, the black-body function for the air close to the ground being B_0 , and

$$B_g - B_0 = \frac{\phi}{2\pi}$$

DISCONTINUITY = OLR/2
(independent of the optical depth)

such a steep lapse rate is very unstable with respect to vertical motion, and will soon be destroyed by the process of *convection*

Discontinuity = Convection = OLR/2



Derivation in Houghton (1977, 1986, 2002)

In a plane parallel atmosphere,

$$dI = -Ik\rho dz \quad (2.1)$$

The equation for radiative transfer through the slab, which includes both absorption and emission, is sometimes known as *Schwarzschild's equation*

$$\begin{aligned} dI &= -Ik\rho dz + Bk\rho dz \\ \text{or} \quad \frac{dI}{d\chi} &= I - B \end{aligned} \quad (2.3)$$

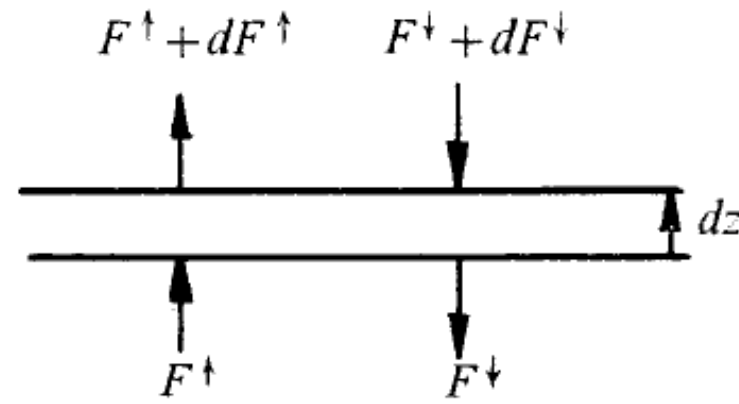


Fig. 2.3.

$$\frac{d}{dz}(F^{\downarrow} - F^{\uparrow}) = \rho c_p \frac{dT}{dt} \quad (2.4)$$

In equilibrium $dT/dt = 0$, and integration of (2.4) gives

$$F^{\uparrow} - F^{\downarrow} = \text{a constant } \phi, \text{ the net flux.} \quad (2.5)$$

Further, from (2.3) the transfer equations are

$$\left. \begin{aligned} \frac{dF^{\uparrow}}{d\chi^*} &= F^{\uparrow} - \pi B \\ -\frac{dF^{\downarrow}}{d\chi^*} &= F^{\downarrow} - \pi B \end{aligned} \right\} \quad (2.6)$$

where the star on the optical depth χ^* , which is measured from the top of the atmosphere, denotes that it is appropriate to hemispheric radiation (i.e. the factor 5/3 has been applied to dz in the expression for χ).

If

$$\psi = F^{\uparrow} + F^{\downarrow} \quad (2.7)$$

equations (2.6) may be written

$$\frac{d\psi}{d\chi^*} = \phi \quad (2.8)$$

$$\frac{d\phi}{d\chi^*} = \psi - 2\pi B \quad (2.9)$$

Since $\phi = \text{constant}$ (from (2.5)) $d\phi/d\chi^* = 0$

$$\text{and} \quad \psi = 2\pi B \quad (2.10)$$

which on substitution into (2.8) gives

$$B = \frac{\phi}{2\pi}\chi^* + \text{constant} \quad (2.11)$$

The boundary condition at the top of the atmosphere ($\chi^* = 0$) is $F^\downarrow = 0$, so that here $\psi = \phi$ and, from (2.10), the constant in (2.11) is $\phi/2\pi$, i.e.

$$B = \frac{\phi}{2\pi}(\chi^* + 1) \quad (2.12)$$

$$B = \frac{\phi}{2\pi}(\chi^* + 1) \quad (2.12)$$

At the bottom of the atmosphere where $\chi^* = \chi_0^*$, $F^\uparrow = \pi B_g$, B_g being the black-body function at the temperature of the ground. It is easy to show that there must be a temperature discontinuity at the lower boundary, the black-body function for the air close to the ground being B_0 , and

$$B_g - B_0 = \frac{\phi}{2\pi} \quad (2.13)$$

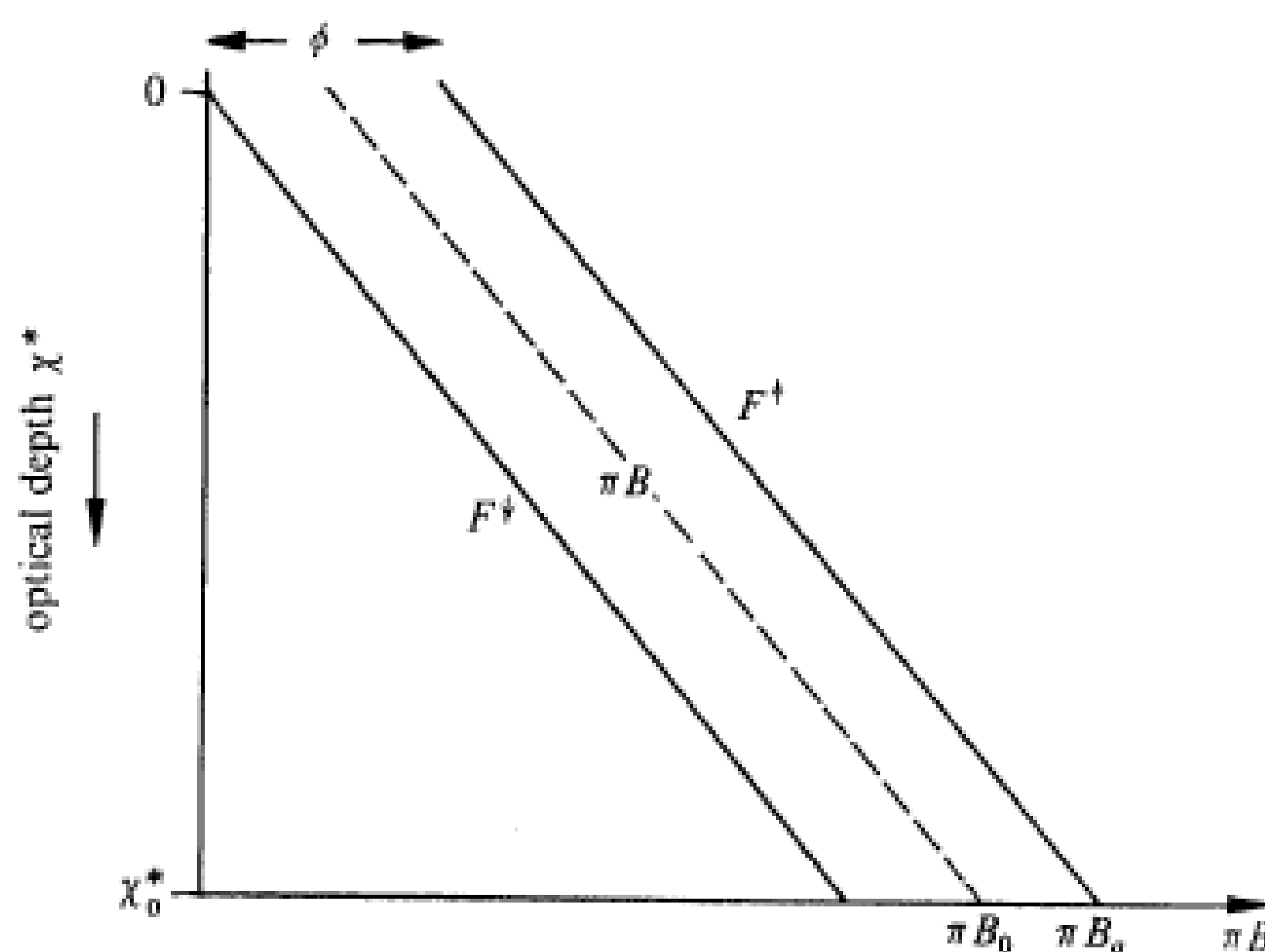
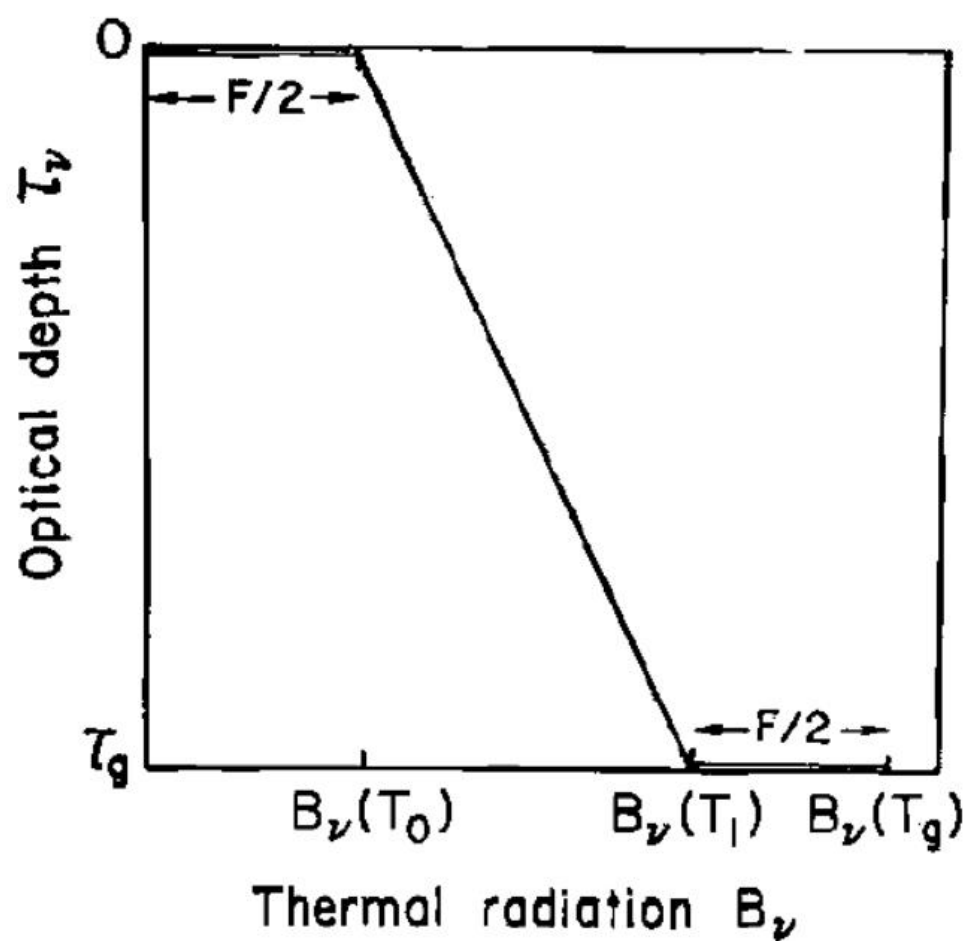


Fig. 2.4. Upward radiation flux F^\uparrow , downward flux F^\downarrow and black-body function πB at atmospheric temperature plotted against optical depth for radiative equilibrium atmosphere.

The black-body function B for such an atmosphere is plotted against χ^* in fig. 2.4. The equivalent diagram in terms of temperature and height is fig. 2.5. Notice that the lower part of the atmosphere possesses a very steep lapse rate of temperature, and at the surface itself there is a discontinuity in temperature. As was shown in § 1.4, such a steep lapse rate is very unstable with respect to vertical motion, and will soon be destroyed by the process of *convection* which will tend to establish a mean adiabatic lapse rate.



Joseph Chamberlain

Theory of Planetary Atmospheres (1978, 1987)

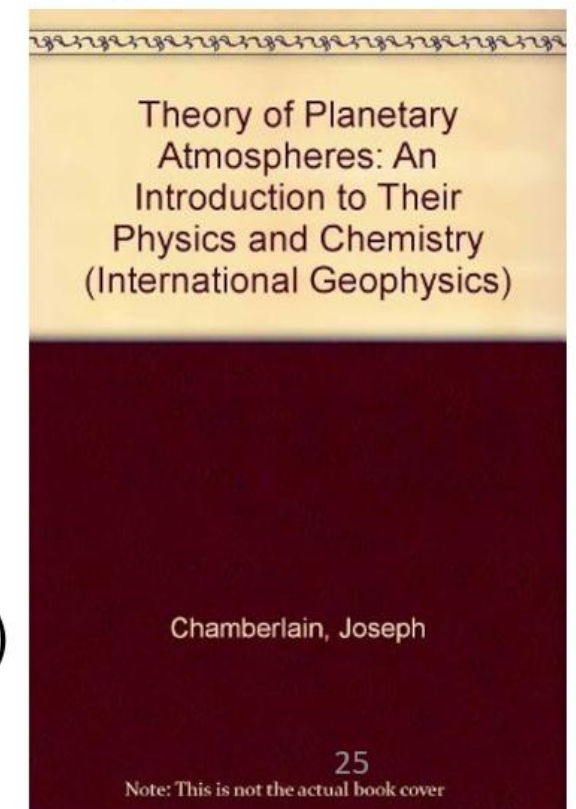
Academic Press, Fig. 1.4, Eq. 1.2.29

Fig. 1.4 The MRE solution for $T(\tau)$, presented as $B_v(T)$ vs. τ . Note the discontinuity at the ground and the finite skin temperature at $\tau = 0$.

DISCONTINUITY = OLR/2
(independent of τ)

Hence the upward intensity at the ground is

$$I_g^+ \equiv B_v(T_g) = B_v(T_1) + \frac{1}{2}F_v \quad (1.2.29)$$



Dennis Hartmann: Global Physical Climatology

Academic Press (1994, 2016) Fig. 3.10-3.11

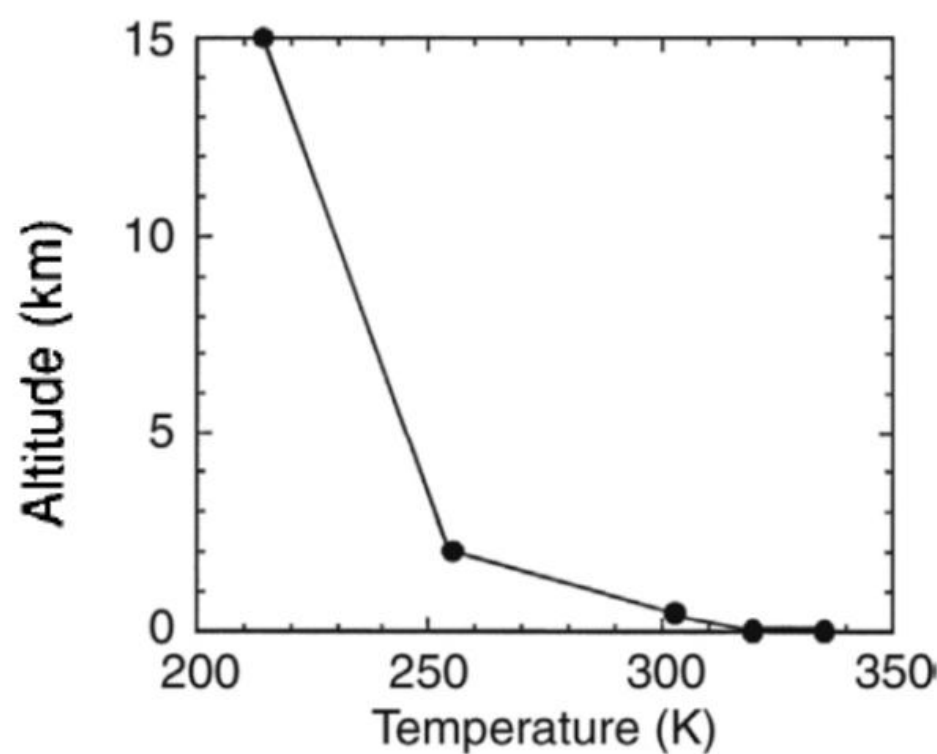
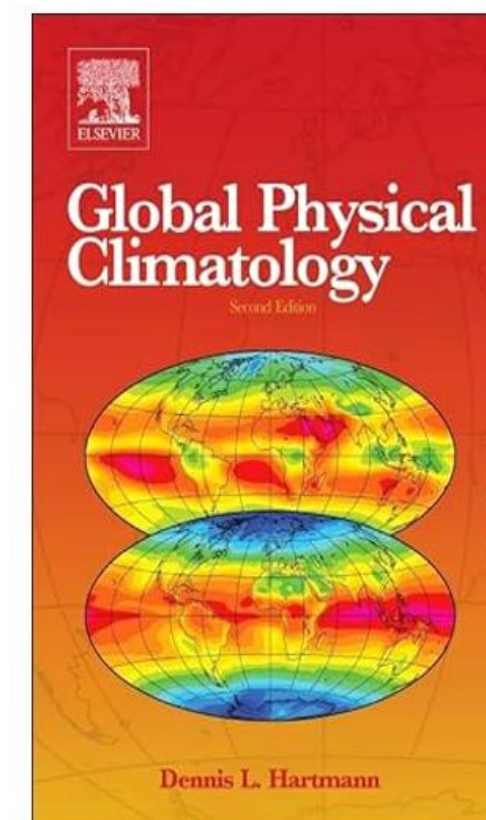
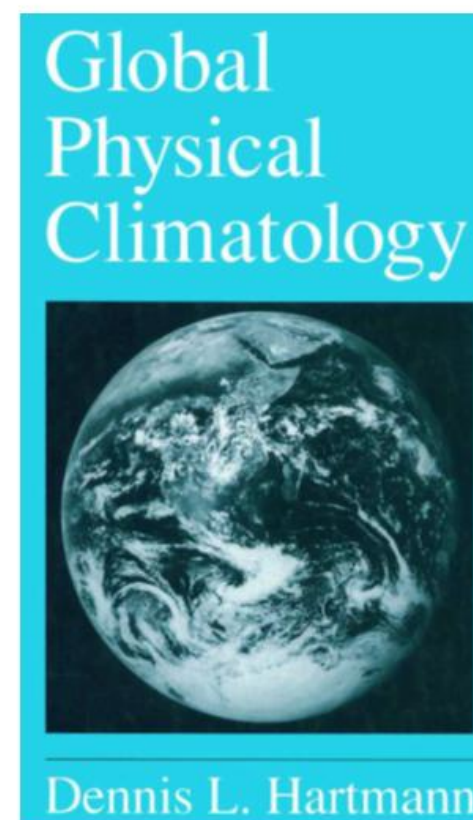


Fig. 3.11



With Hartmann's data, the equation is justified within 0.31 Wm^{-2}

Emission temperature $T_e = 255 \text{ K}$

Air adjacent to surface $T_{SA} = 320 \text{ K}$

Surface temperature $T_s = 335 \text{ K}$

σT_s^4	$- \sigma T_{SA}^4$	$= \sigma T_e^4 / 2$
5.67 [(3.35) ⁴ - (3.20) ⁴]		$= 5.67(2.55)^4 / 2$
714.11	$- 594.54 = 119.56$	$= 119.87 - 0.31 \text{ Wm}^{-2}$

Radiation and Climate

Vardavas and Taylor, Oxford University Press, 2007

THERMODYNAMICS OF MOIST AIR

47

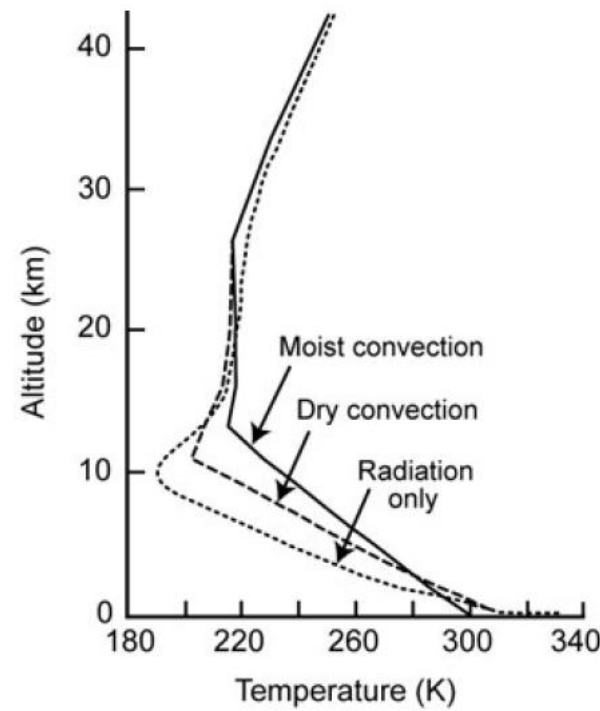
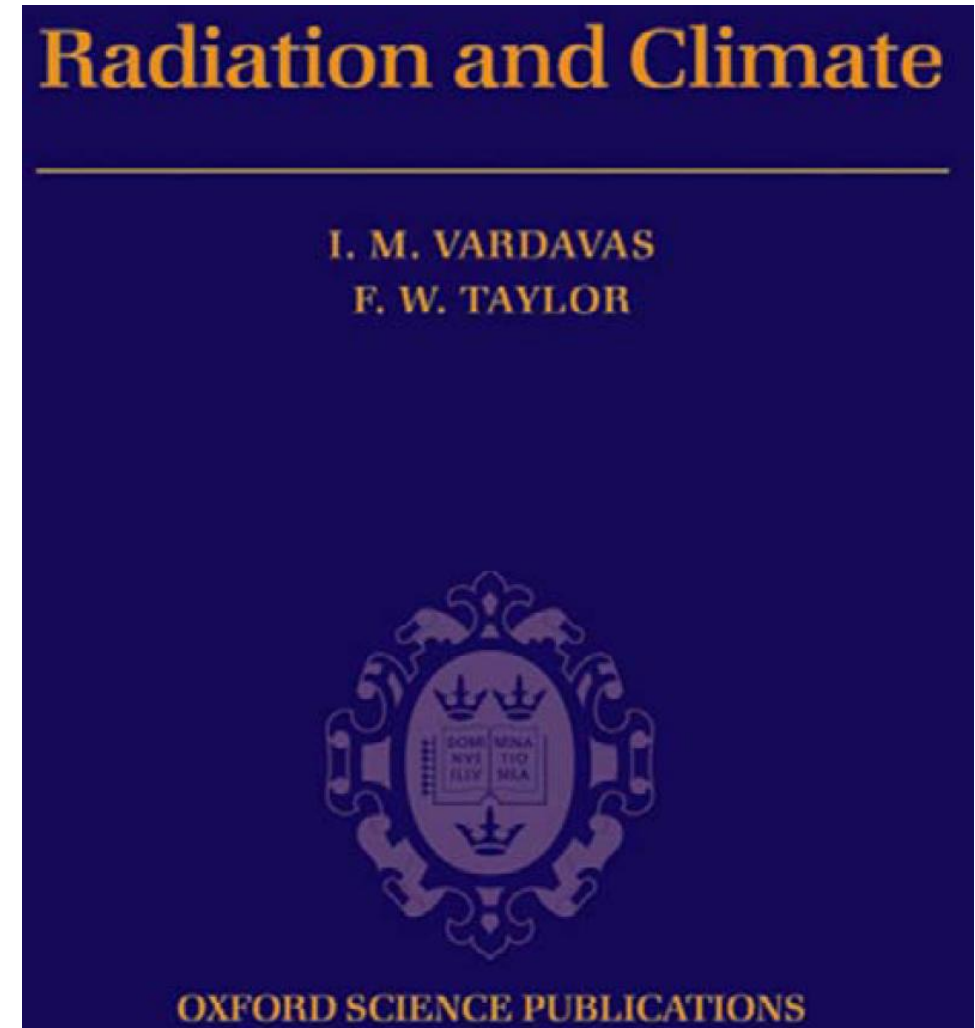


FIG. 2.11. Representative vertical temperature profiles calculated assuming (top curve) convective equilibrium in a moist atmosphere, (middle) convective equilibrium in a dry atmosphere, and (bottom) radiative equilibrium. (See Manabe and Wetherald 1967)



the stability of the atmosphere against convection. An atmosphere in radiative equilibrium (see Fig. 2.11) produces essentially a discontinuity (of about 20 K) between the Earth's surface temperature and the near-surface atmospheric temperature. This is a consequence of having a non-ideal blackbody atmospheric layer overlaying a blackbody surface. We can make an estimate of this discontinuity by considering the simple case of a grey atmosphere in radiative equilibrium (see §3.5.10). In the two-stream approximation the mean intensity is given by $J = (I^+ + I^-)/2$ and the net upwelling flux, f , is constant in radiative equilibrium and given by $f = \pi(I^+ - I^-)$. Thus the mean intensity can be expressed as $J = I^+ - f/2\pi$. At the Earth's surface, with temperature T_s , $I^+ = B(T_s)$, where $B(T_s) = \sigma T_s^4/\pi$, and we have seen that within the atmosphere, eqn (3.138),

$$J(\tau_s) = B(T(\tau_s)) = B(T_o) \left(1 + \frac{3}{2}\tau_s \right), \quad (11.7)$$

where $T(\tau_s)$ is the near-surface atmospheric temperature. Now $f/2\pi = B(T_o)$ where T_o is the atmospheric skin temperature, equal to $(1/2)^{1/4} T_\oplus$, where T_\oplus is the effective temperature of the Earth, so that the Earth's surface temperature can be calculated from

$$B(T_s) = B(T_o) \left(2 + \frac{3}{2}\tau_s \right). \quad (11.8)$$

If we set $\tau_s = 0.85$, for the total grey optical depth of the present atmosphere, and $T_\oplus = 255$ K then we obtain $T_o = 214$ K, $T_s = 288$ K and the near-surface air temperature is then $T(\tau_s) = 263$ K. We see that there is a discontinuity of 25 K

Radiation and Climate

464

8 Radiation and Climate

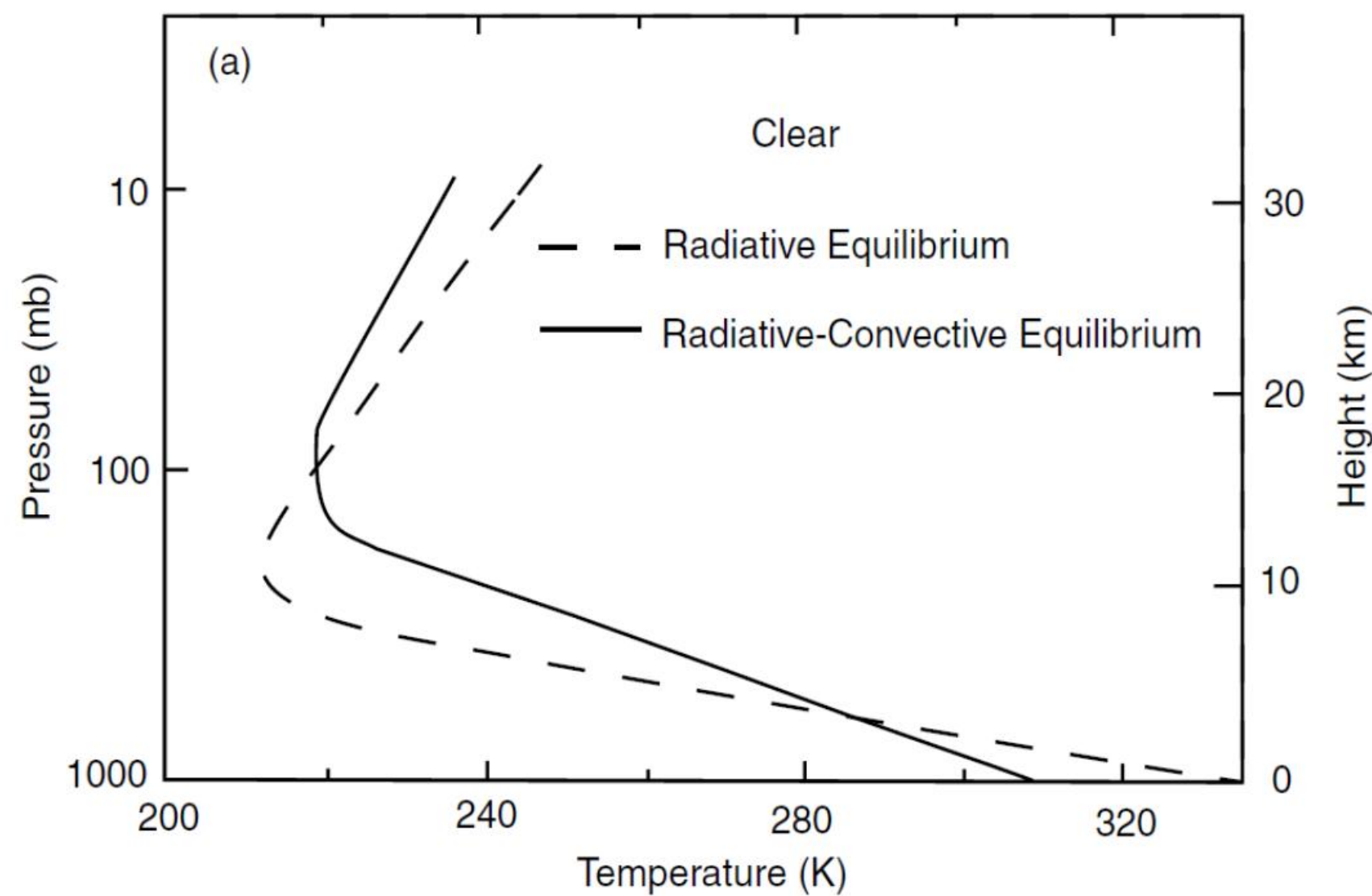
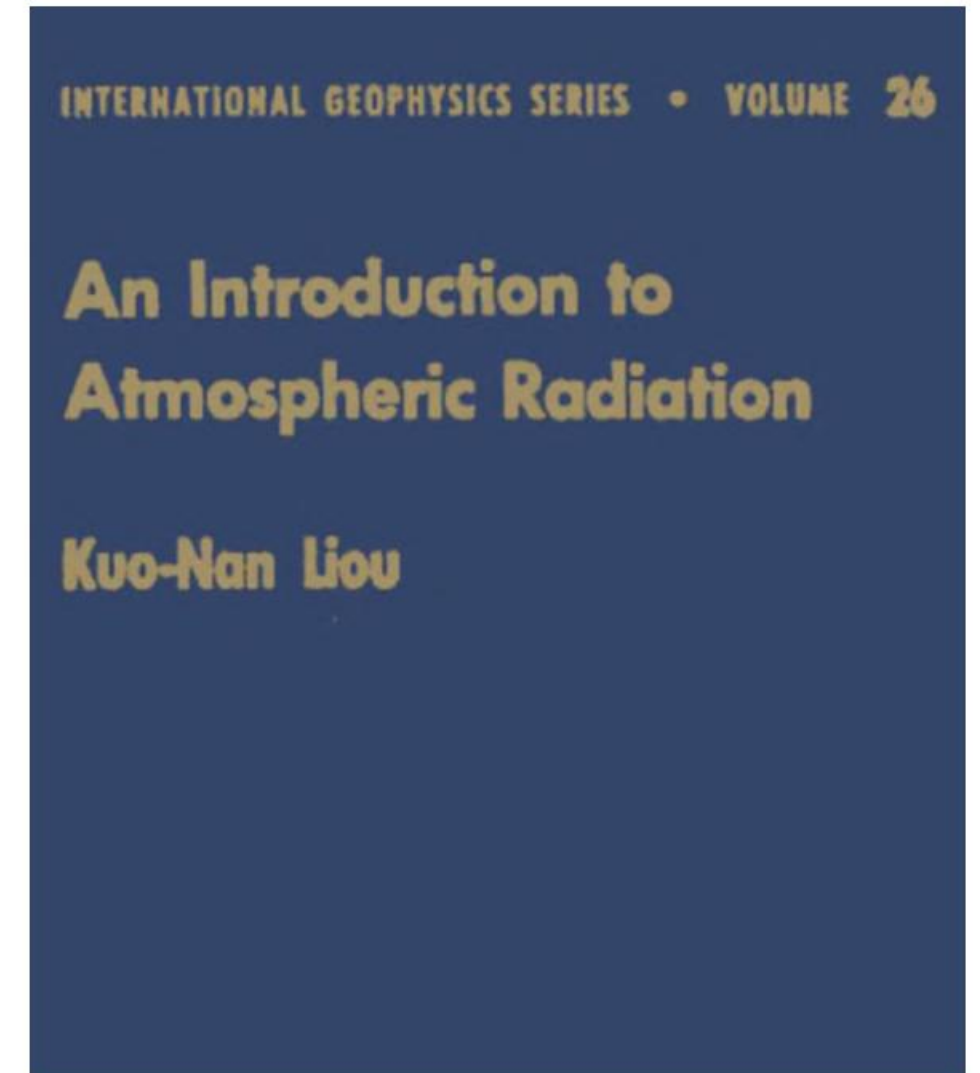


Figure 8.9 Vertical distributions of radiative and radiative–convective equilibrium temperatures in clear (a) and average cloud (b) conditions, simulated from a one-dimensional radiative–convective climate model.

Liou: An Introduction to Atmospheric Radiation
Academic Press (1980, 2002)



Visconti: Fundamentals of Physics and Chemistry of the Atmospheres — Springer (2001)

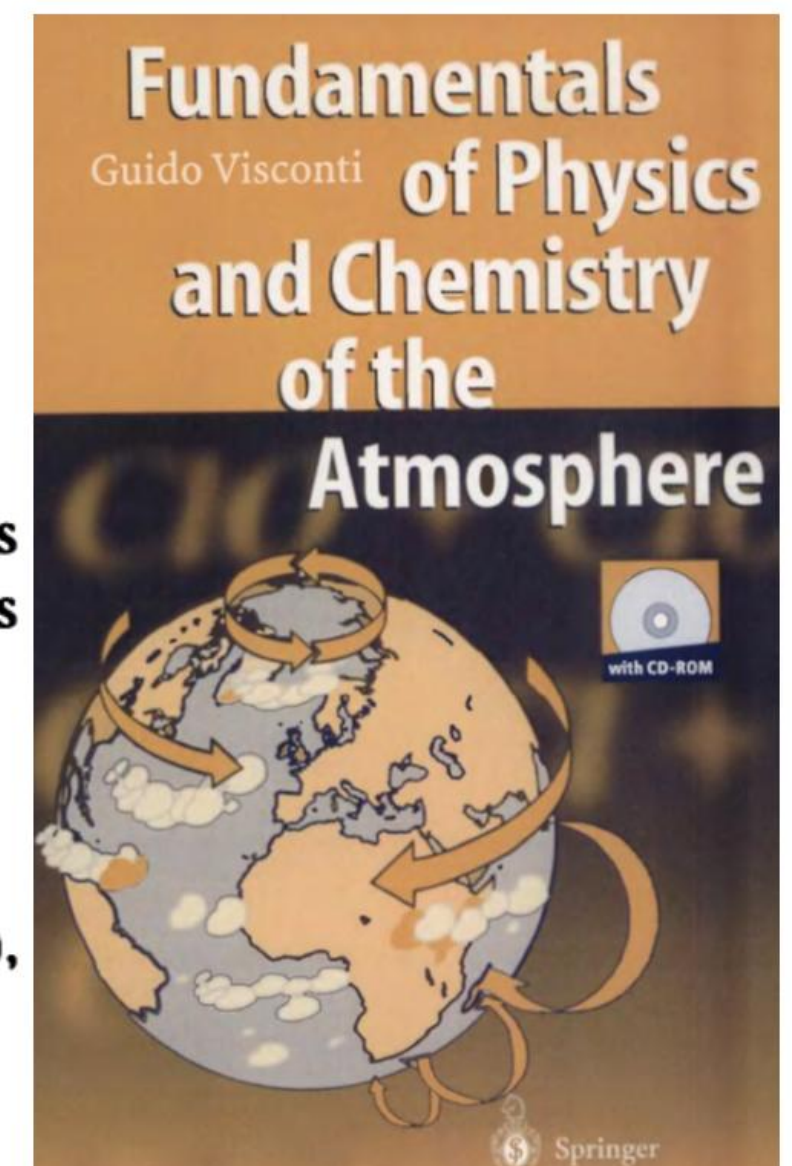
$$T_s^4 = \frac{T_e^4}{2} \left(\frac{3}{2} \tau + 1 \right) \quad (3.47)$$

where τ has been replaced by its effective value. An interesting consequence of this solution is to discover what happens at the surface, where the optical thickness is τ^* and the temperature is T_s ; we have

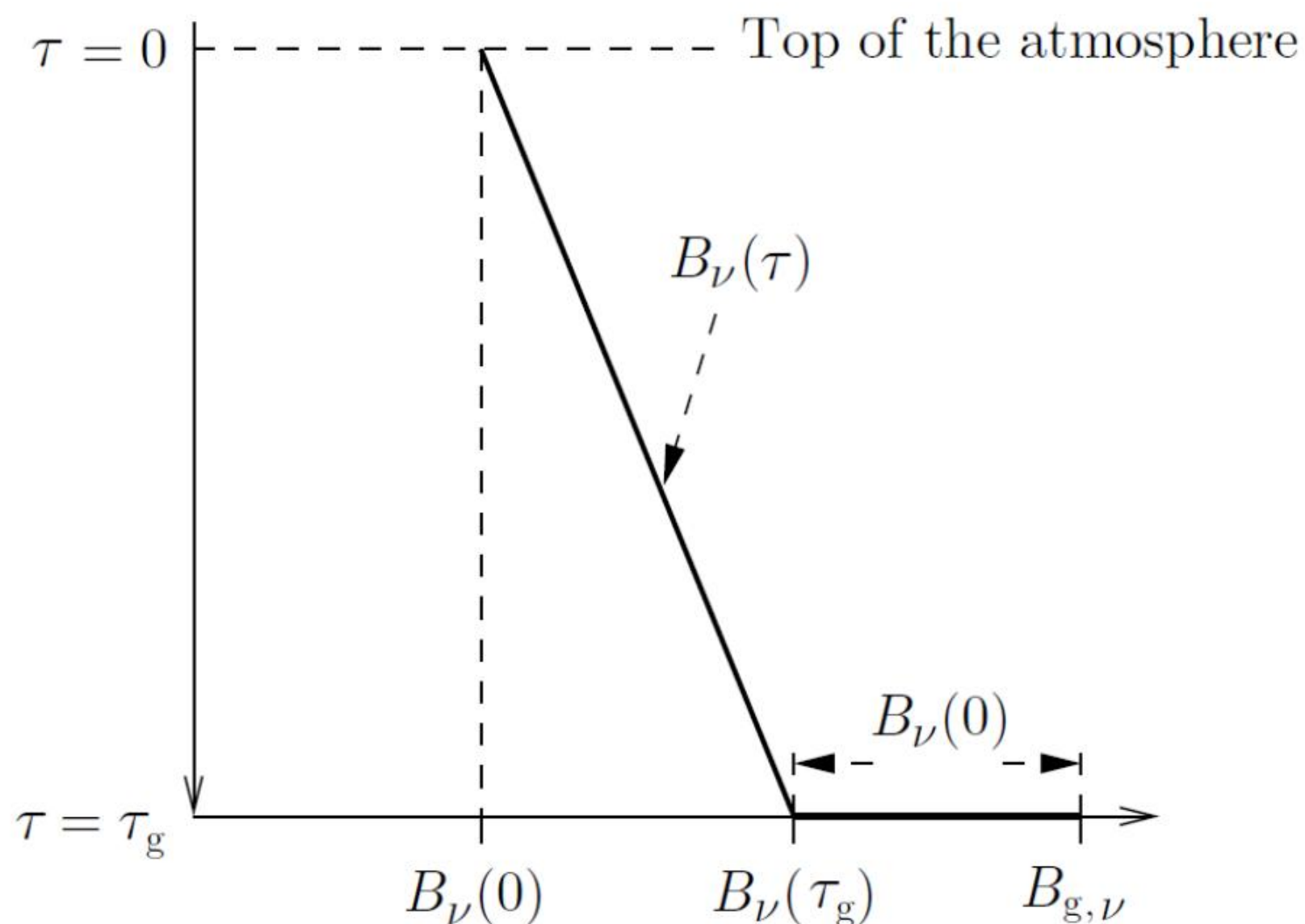
$$F^\uparrow(\tau^*) = \sigma T_s^4 = \frac{1}{2} \sigma T_e^4 \left(\frac{3}{2} \tau^* + 2 \right) \quad (3.48)$$

The temperature at the bottom of the atmosphere at τ^* is given by Equation (3.47), so that we have a discontinuity between the air temperature and that of the surface

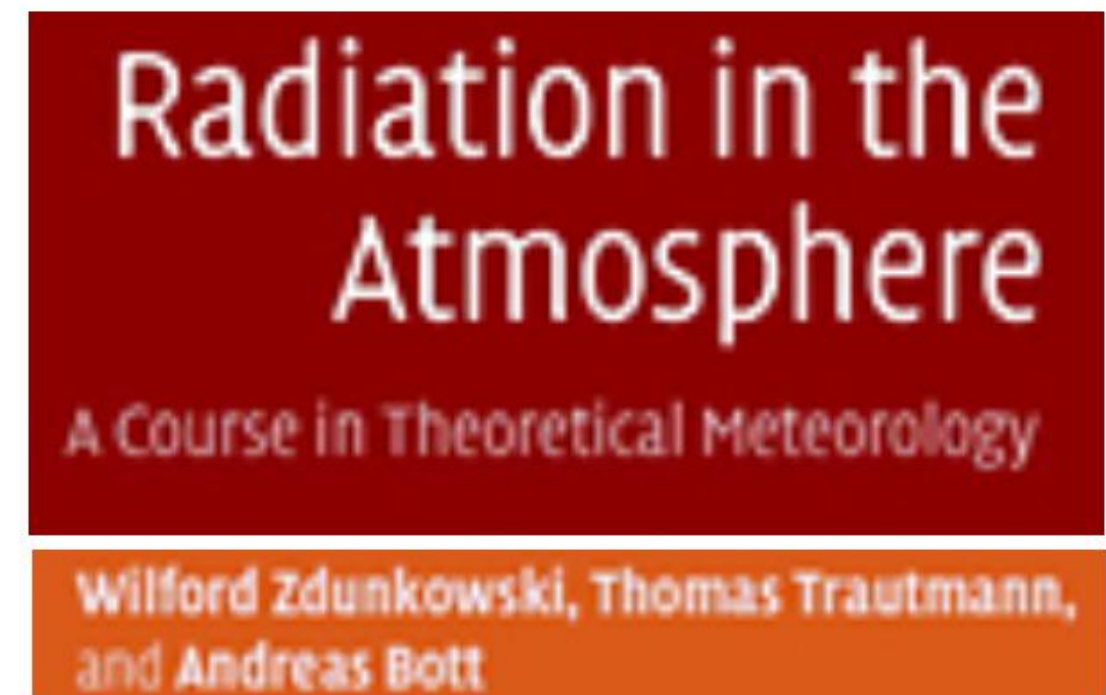
$$T_s^4 - T(\tau^*)^4 = T_e^4 / 2 \quad (3.49)$$



Two-stream methods for the solution of the RTE



Radiation in the Atmosphere
Zdunkowski, Trautmann and Bott
Cambridge (2008) Fig. 6.7

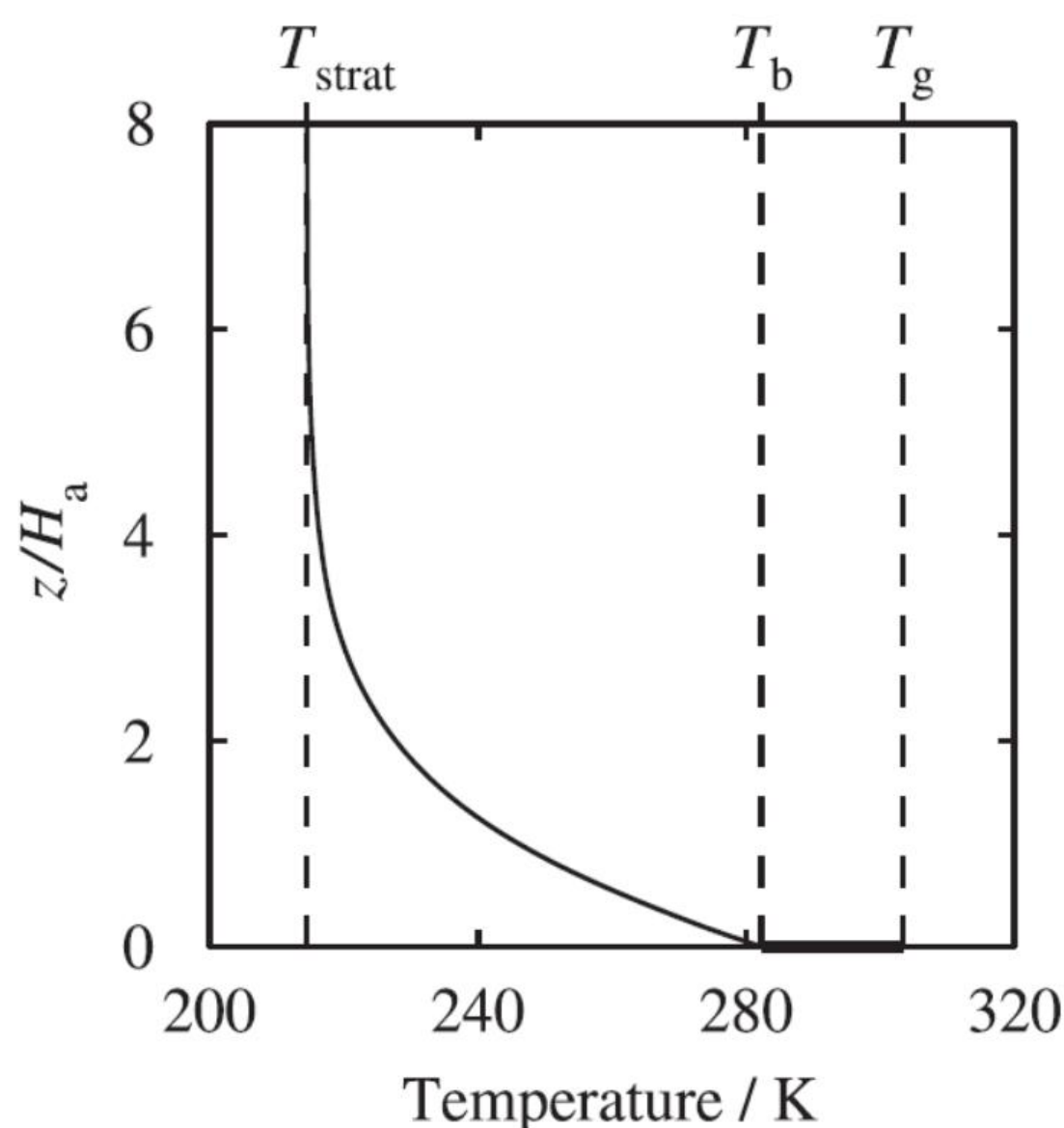


DISCONTINUITY = OLR/2, independent of τ

$$B_{g,\nu} = B_{\nu}(\tau_g) + \frac{1}{2\pi} E_{\text{net},\nu}$$

observe a discontinuity of the curve expressing a temperature jump ΔT_g between the surface temperature T_g and the lowest atmospheric layer $T(\tau_g)$, i.e.

$$\Delta T_g = T_g - T(\tau_g) > 0 \quad (6.155)$$



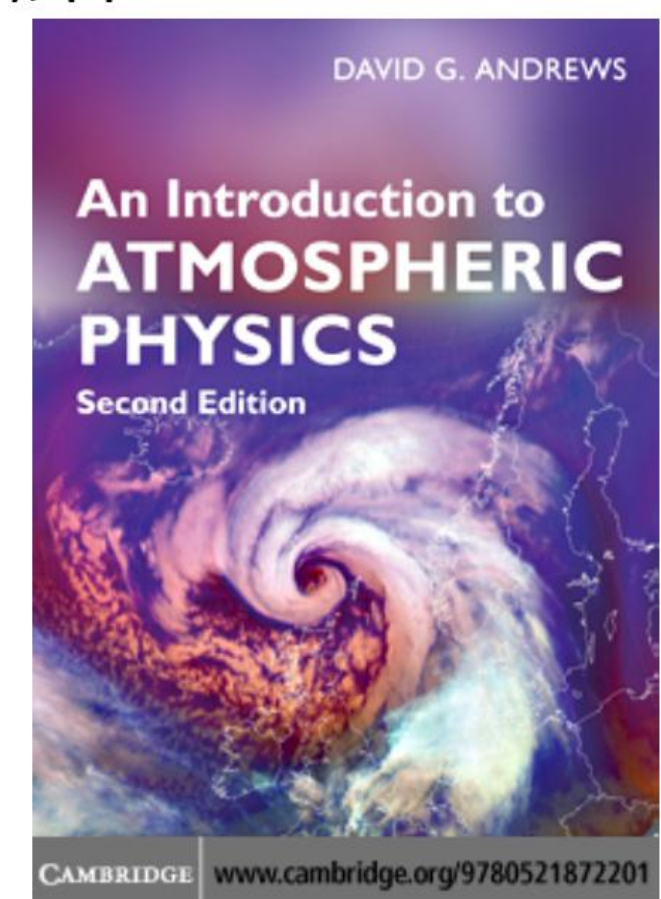
Andrews: An Introduction to Atmospheric Physics
Cambridge (2010), pp 85-86.

$$T_b \equiv T_e \left(\frac{1 + \chi_g^*}{2} \right)^{1/4}$$

$$T_g \equiv T_e \left(\frac{2 + \chi_g^*}{2} \right)^{1/4}$$

$$T_g^4 - T_b^4 = T_e^4/2$$

DISCONTINUITY = OLR/2 (independent of the optical depth)



discontinuity between the bottom of the atmosphere and the ground.

Inclusion of convection in the model removes the temperature discontinuity

Marshall and Plumb: Atmosphere, Ocean and Climate Dynamics

Elsevier Academic Press, 2008

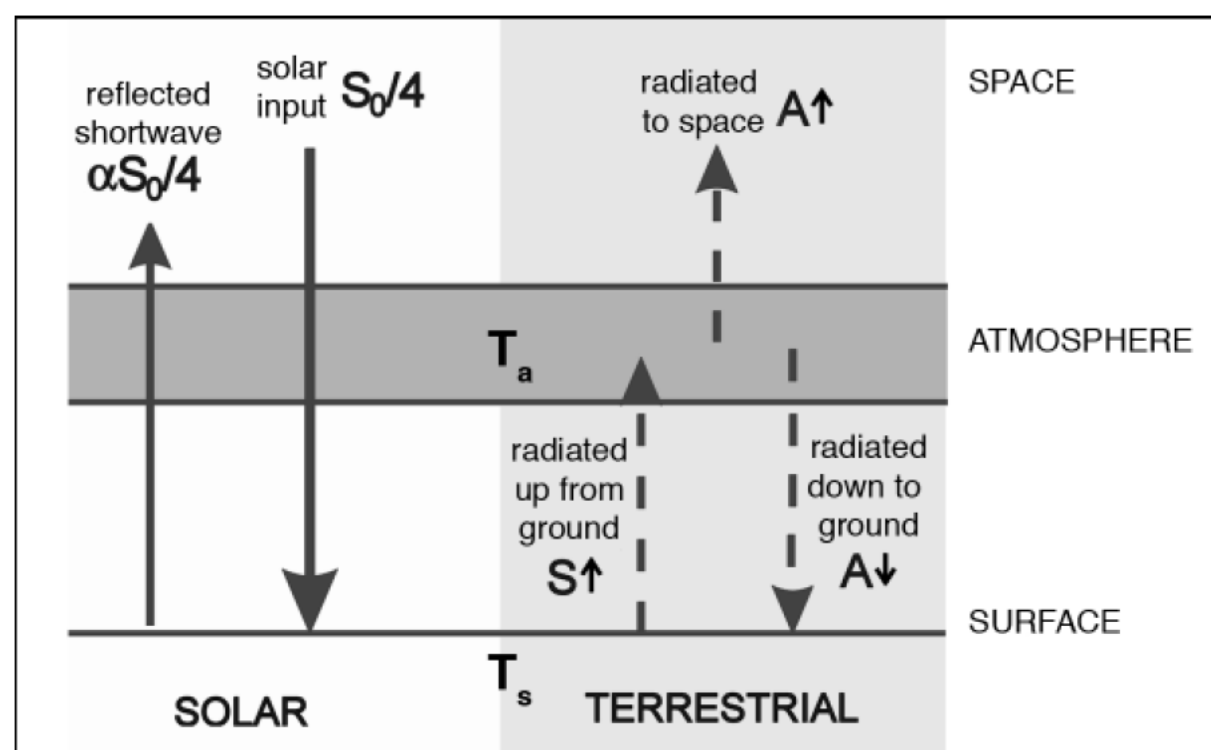
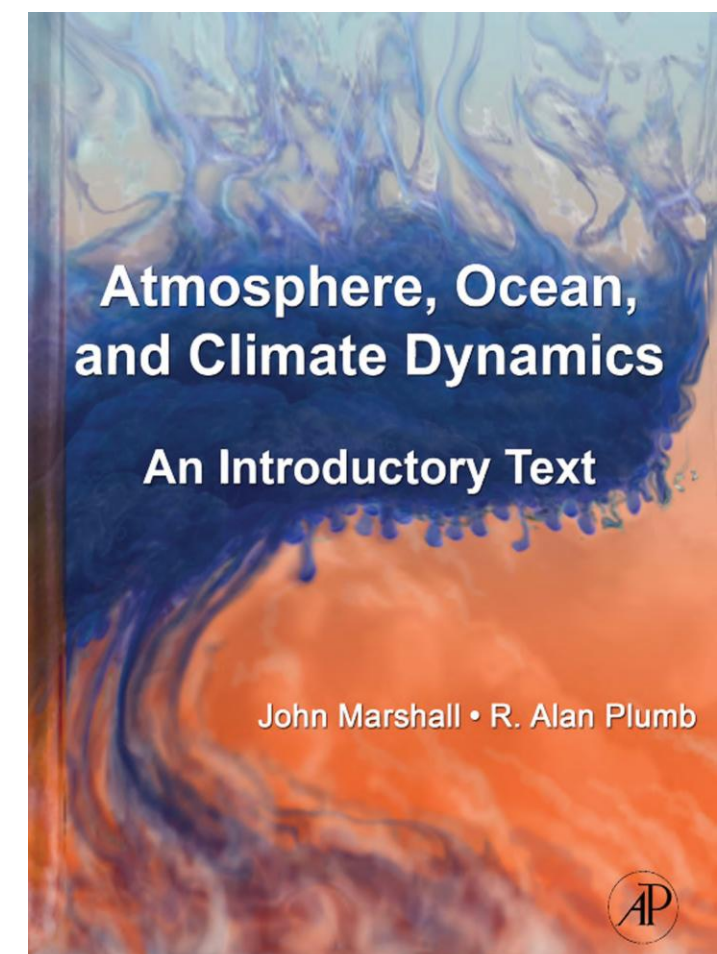


FIGURE 2.7. The simplest greenhouse model, comprising a surface at temperature T_s , and an atmospheric layer at temperature T_a , subject to incoming solar radiation $S_0/4$. The terrestrial radiation upwelling from the ground is assumed to be completely absorbed by the atmospheric layer.



“The resulting profile, which would be the actual mean atmospheric temperature profile if heat transport in the atmosphere occurred only through radiative transfer, is known as the radiative equilibrium temperature profile. It is shown in Fig. 2.11. In particular, note the presence of a *large temperature discontinuity at the surface in the radiative equilibrium profile*, which is not observed in practice.”

Problems: 4. “Consider the “two-slab” greenhouse model illustrated in Fig. 2.9, in which the atmosphere is represented by two perfectly absorbing layers of temperature T_a and T_b . Determine T_a , T_b , and the surface temperature T_s in terms of the emission temperature T_e .” (Eq. 2-16 and Fig. 2.12):

$$2T_n^4 = T_{n+1}^4 + T_{n-1}^4, \quad (2-16) \quad \text{and} \quad T_s = (N + 1)^{1/4} T_e,$$

Pierrehumbert: Principles of Planetary Climate

Cambridge University Press, 2010

“If we assume the planet to be in radiative equilibrium with the absorbed solar radiation $(1 - \alpha)S$, where α is the albedo of the ground, then $OLR = (1 - \alpha)S$ and the radiative energy budget of the ground is

$$\sigma T_g^4 = (1 - \alpha)S + I_-(0) = (1 - \alpha)S \cdot \left(1 + \frac{1}{2}\tau_\infty\right) \quad (4.44)$$

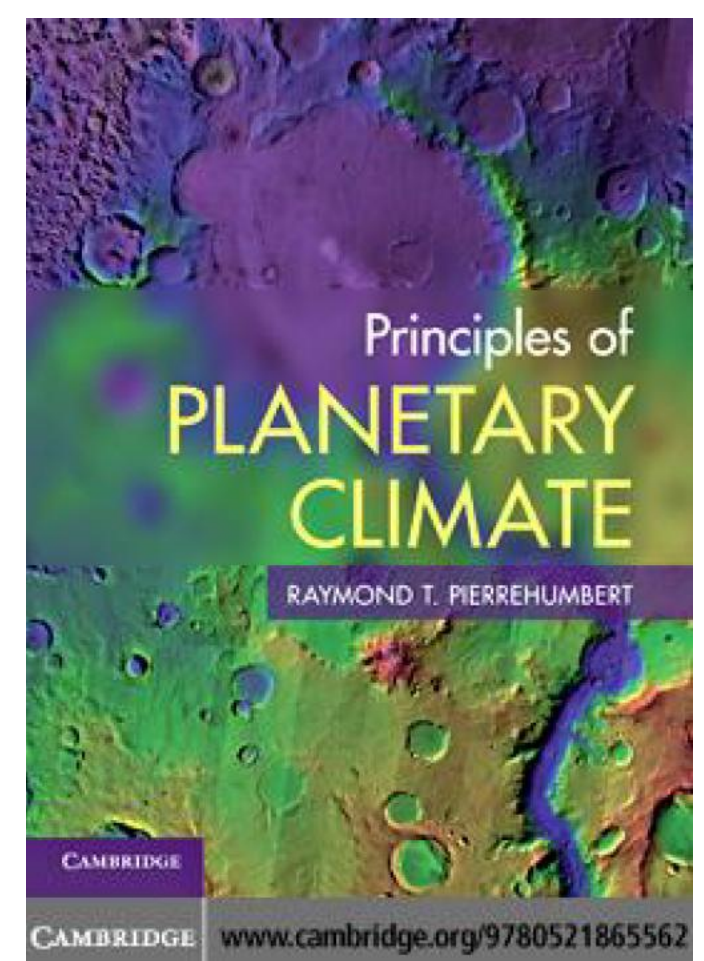
Let’s now compare the surface temperature with the temperature of the air in immediate contact with the surface. From Eq. (4.42) we find that the low-level air temperature is determined by

$$\sigma T(0)^4 = (1 - \alpha)S \cdot \left(\frac{1}{2} + \frac{1}{2}\tau_\infty\right).$$

Taking the ratio,

$$\frac{T(0)}{T_g} = \left(\frac{\frac{1}{2} + \frac{1}{2}\tau_\infty}{1 + \frac{1}{2}\tau_\infty}\right)^{1/4}. \quad (4.45)$$

Thus, the surface is always warmer than the overlying air in immediate contact with it.



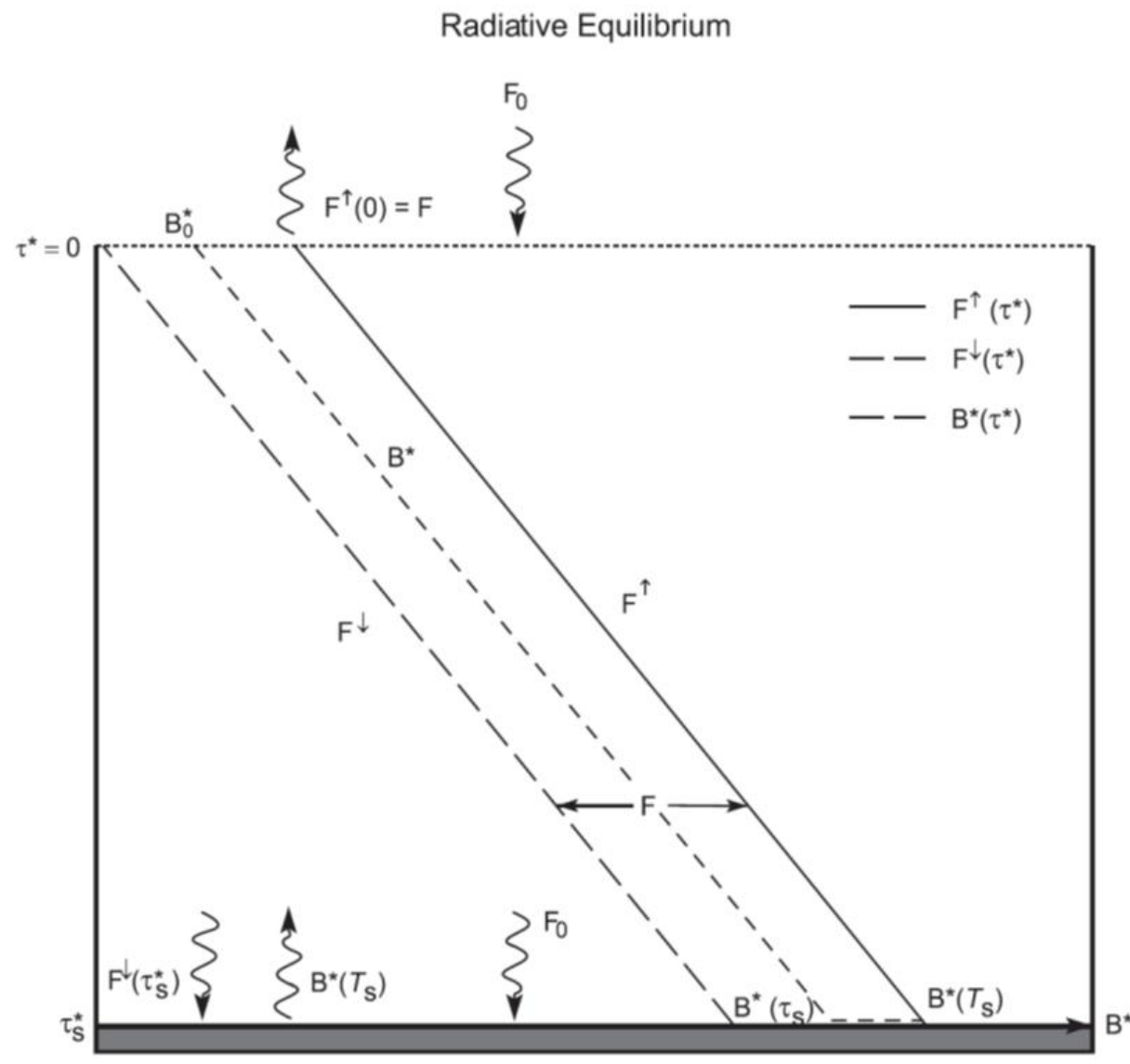
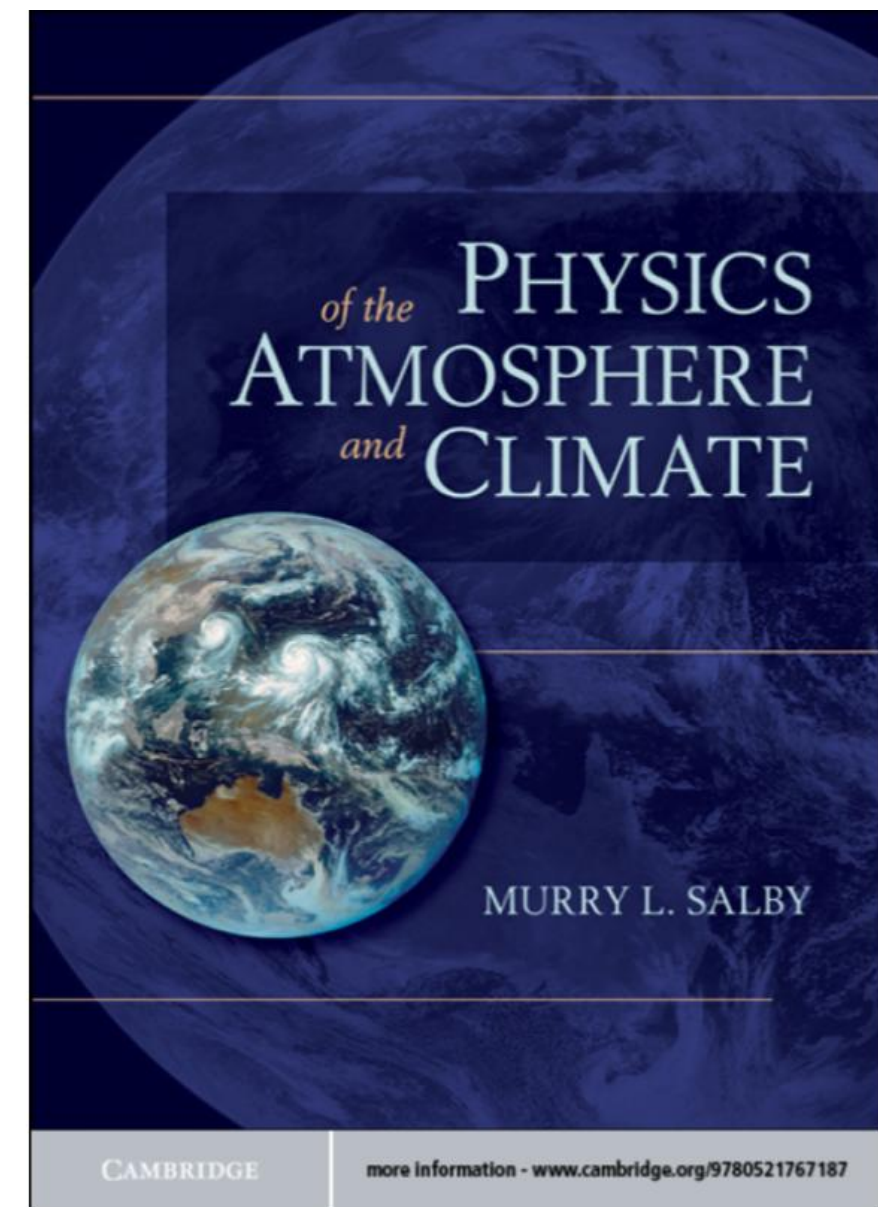


Figure 8.20 Upwelling and downwelling LW fluxes and LW emission in a gray atmosphere that is in radiative equilibrium with an incident SW flux F_0 and a black underlying surface. Note: the emission profile is discontinuous at the surface.



M. Salby: Physics of the Atmosphere and Climate
Cambridge, 2012

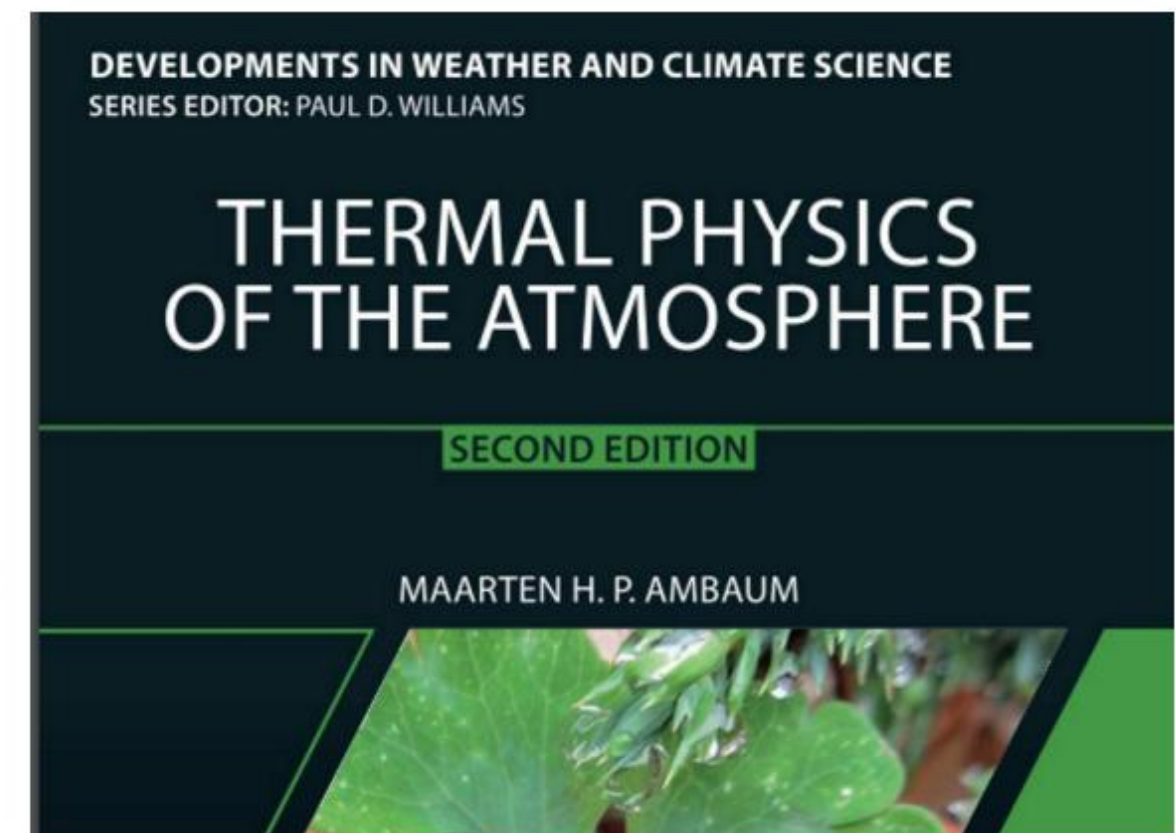
$$B^*(T_s) = B^*(\tau_s^*) + \frac{F_0}{2}. \quad (8.67)$$

According to (8.67), the temperature predicted by radiative equilibrium is discontinuous at the surface, the ground being warmer than the overlying air.



RMetS
Royal Meteorological Society

Copyright © 2021 Royal Meteorological Society.



These two budget equations can be combined by eliminating $L_{\downarrow 0}$ to find

$$\blacktriangleright \quad \sigma T_E^4 = \sigma T_S^4 + S_{n0}/2. \quad (10.56)$$

So we find that under radiative equilibrium the surface temperature is higher than the temperature of the adjoining atmosphere. This temperature discontinuity is unstable in practice and there will be turbulent heat exchange which will remove the temperature discontinuity. This instability of the radiative state is a driver of surface layer turbulence: the radiation will force the lower part of the boundary layer, the surface layer, towards instability and this tendency is compensated by turbulent fluxes near the surface.

University lecture notes with TRE Eq. (1)

Graeme L. Stephens: Radiative Transfer Notes AT 622.

Colorado State University, Fort Collins, CO

(“These notes are the sole intellectual property of Graeme L. Stephens”)

[G. L. Stephens: Radiative Transfer Notes AT 622 Colorado State Univ. \(1992-2013\)](#)

Example 6.3: Skin temperatures and temperature discontinuities

The solutions represented by Eqns. (6.10a) and (6.10b) provide rather interesting insights into the temperature profiles that are predicted by these equations. One of the results of this model is an estimate of the 'skin' temperature, which we think of as a measure of the stratospheric temperature. We obtain this using Eqn. (6.10a) with $\tilde{\tau} = 0$

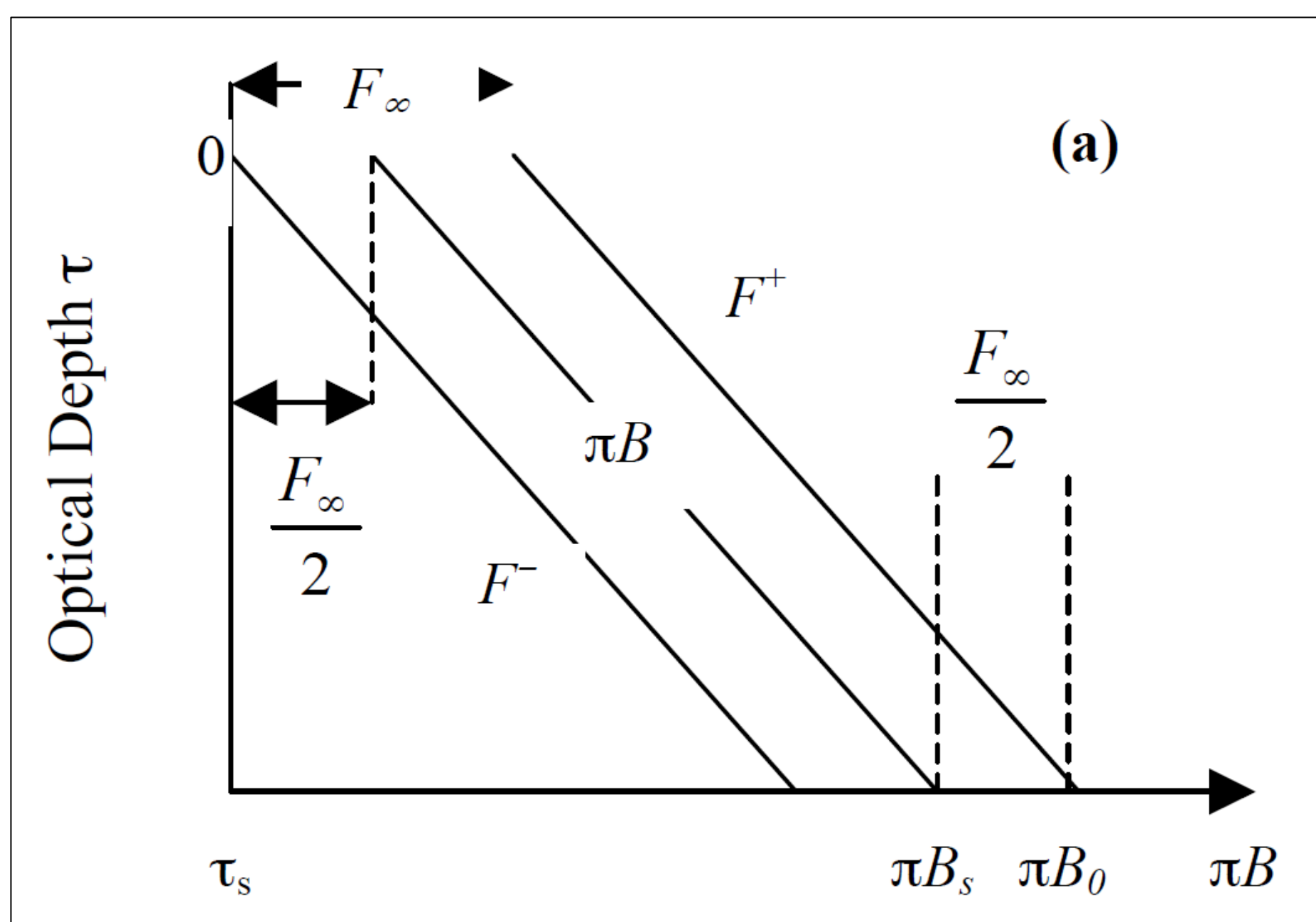
$$\sigma T^4(\tilde{\tau} = 0) = \frac{F_{\infty}}{2}$$

and with $F_{\infty} \approx 235 \text{ Wm}^{-2}$, it follows that this temperature is $T_{skin} = [117.5/5.68 \times 10^{-8}]^{0.25} = 213 \text{ K}$.

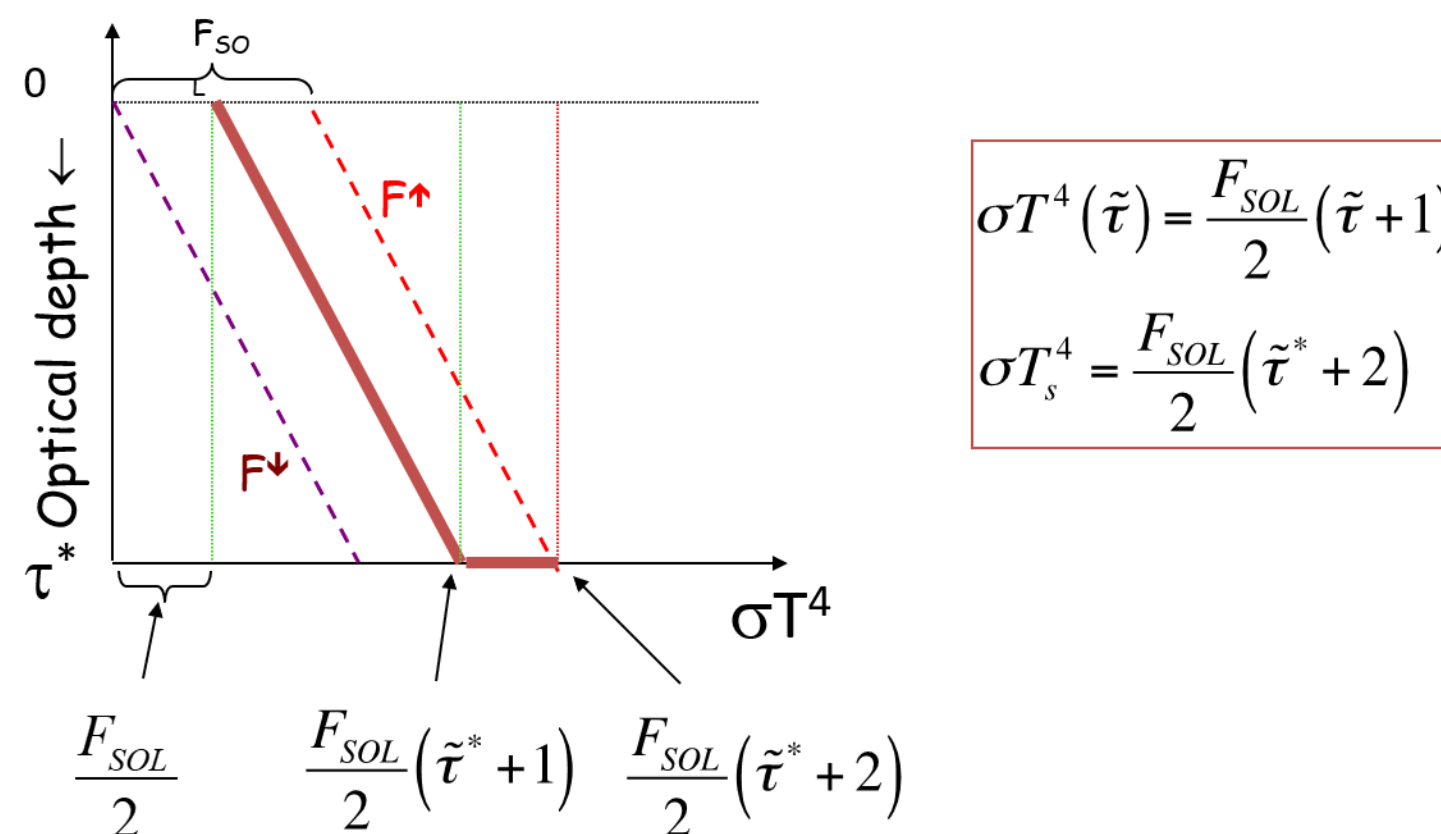
The solutions in Eqns. (6.10a) and (6.10b) predict a discontinuity between the surface temperature T_s and the air temperature just above the ground $T(\tilde{\tau}_s)$. Differencing these equations and with $\tilde{\tau} = \tilde{\tau}_s$,

$$\sigma T_s^4 - \sigma T^4(\tilde{\tau}_s) = \frac{F_{\infty}}{2}.$$

“This radiative equilibrium profile is unstable w.r.t. vertical motion and is destroyed by convection”



Chris O'Dell, Colorado State University (2013)



Kerry Emanuel: Elements of Radiation Transfer

GFD / MIT / Woods Hole, June 16, 2014

https://gfd.whoi.edu/wp-content/uploads/sites/18/2018/03/Lecture_1_Emanuel_218144.pdf

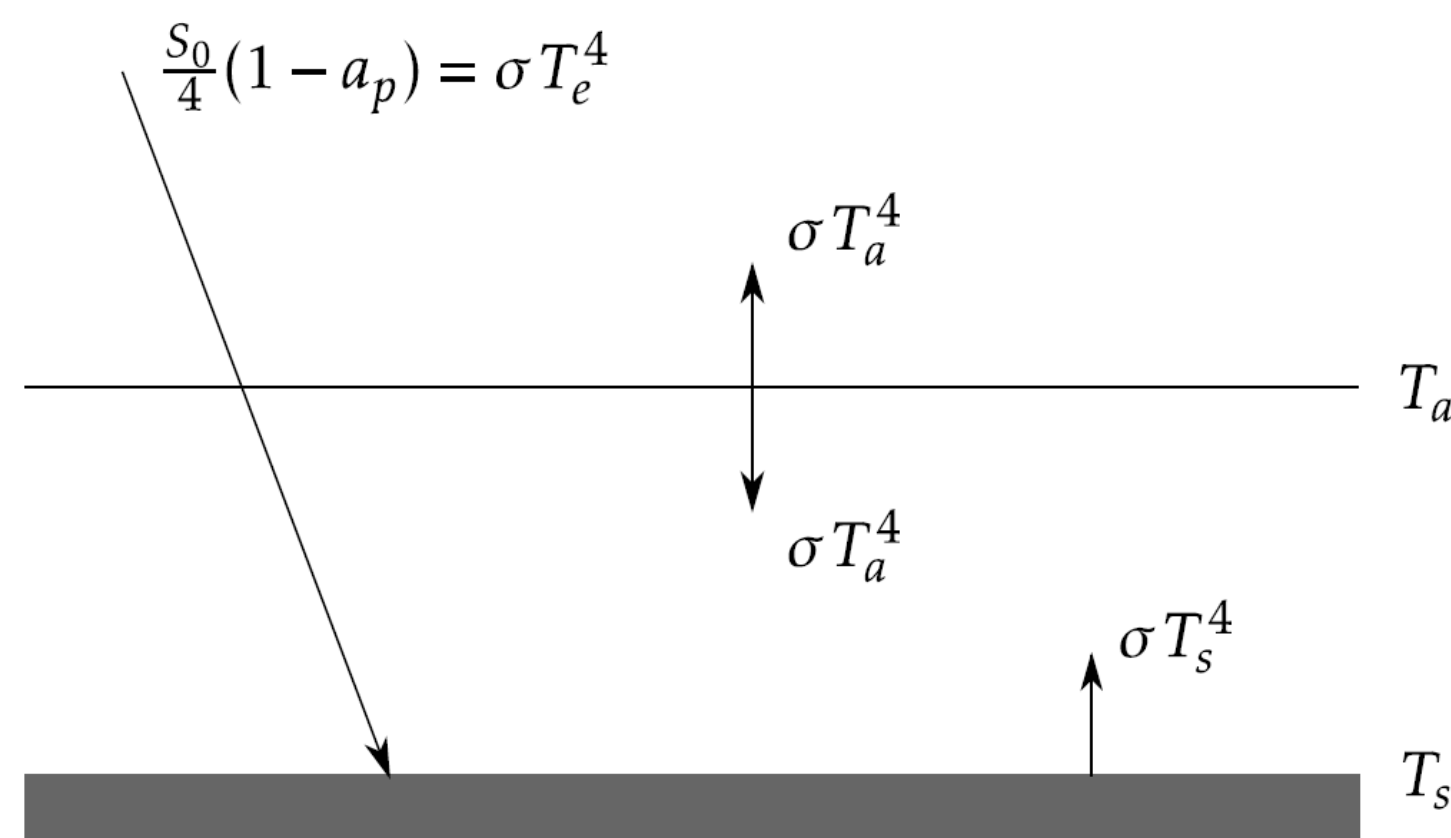


Figure 7: Radiative fluxes in a model with an atmosphere that consists of a single layer that is completely transparent to solar radiation and completely opaque to terrestrial radiation

$$\sigma T_e^4 = \sigma T_a^4, \sigma T_s^4 = 2\sigma T_a^4 = 2\sigma T_e^4 \text{ (This is our Eq. 2)}$$

Consider adding a thin layer of gas just above the surface. Let its temperature be T_{sa} and its emissivity ϵ tend to zero. The balance of this layer is then

$$\epsilon\sigma T_s^4 + \epsilon\sigma T_a^4 = 2\epsilon\sigma T_{sa}^4 \Rightarrow \sigma T_s^4 + \sigma T_a^4 = 2\sigma T_{sa}^4$$

“This layer therefore does not have the same temperature as the surface. This result is independent of ϵ so long as it is sufficiently small, and illustrates that a discontinuous emissivity entails a discontinuity in temperature. In radiative equilibrium, the surface atmospheric temperature is generally different from the temperature of the surface. Radiation drives the system into thermodynamic disequilibrium, which in reality is counteracted by heat diffusion or fluid motion.”

It follows that

$$\sigma T_s^4 - \sigma T_{sa}^4 = \sigma T_e^4/2 \text{ which is our Eq. (1). It also follows that } \sigma T_s^4 = (3/2) \sigma T_e^4$$

Manchester University (UK)

Consider the boundary conditions at the surface. We must balance the upward flux of radiation emitted by the Earth at a temperature T_s , $B(T_s)$, with the downwelling short and longwave radiation.

$$\pi B(T_s) = F_s + F^\downarrow(\chi_s)$$

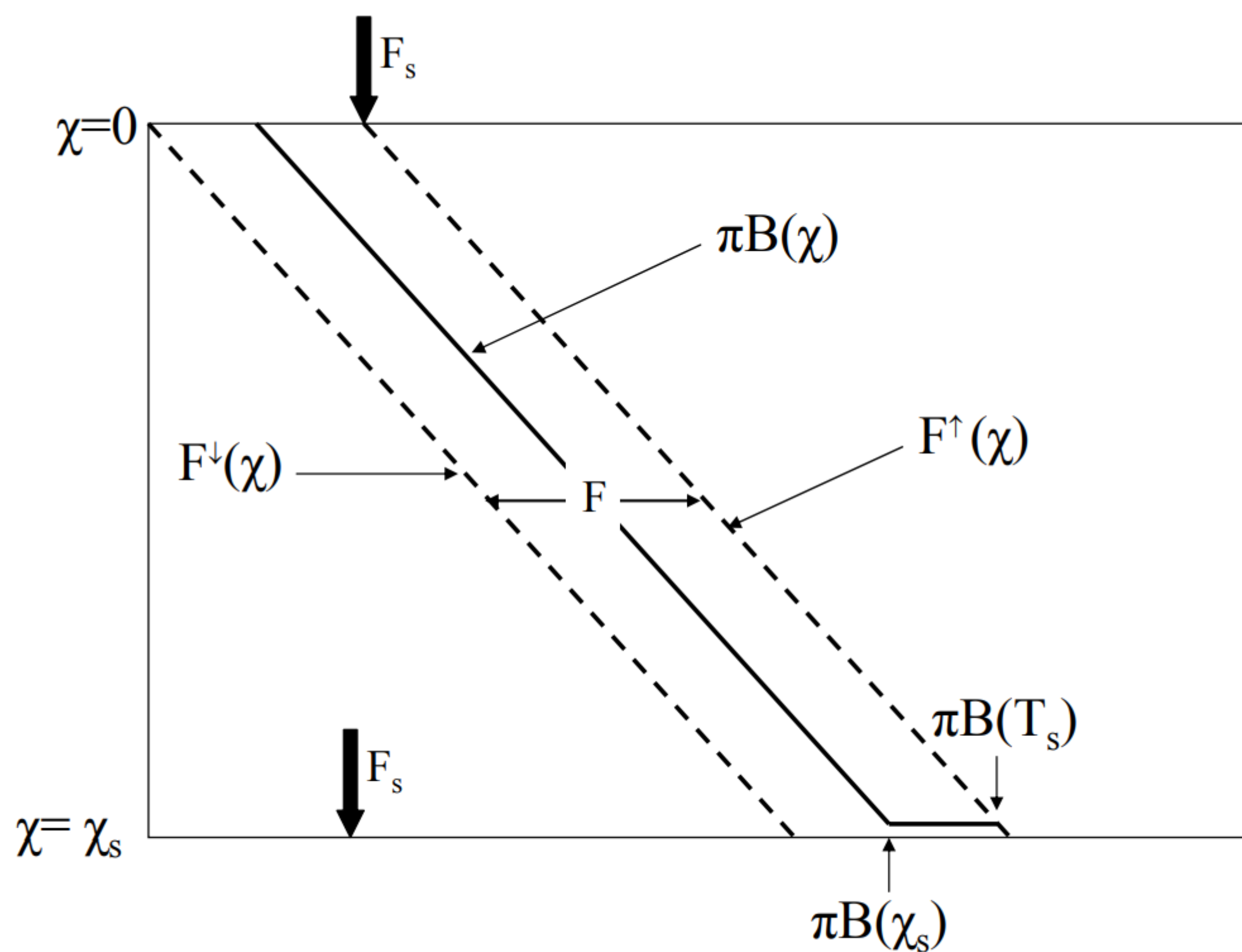
where χ_s is the optical depth of the lowest layer of the atmosphere. However,

$$\bar{F} - F = 2F^\downarrow = 2\pi B - F_s$$

which when evaluated at the surface gives

$$\pi B(T_s) = \pi B(\chi_s) + F_s/2.$$

This expression implies that there is a temperature discontinuity between the surface and the cooler lowest layer of the atmosphere.



P607 Climate and Energy Lecture 3

(Dr Hugh Coe, University of Manchester, UK 2008)

惑星大気学_放射(2022).docx

惑星大気学_放射
(2022-05-02)

(3.10)(3.11)より

$$\underbrace{B^*(T_s)}_{\text{地表面}} = \underbrace{B^*(\tau_s^*)}_{\text{大気下端}} + \frac{F^0}{2}$$

放射平衡では大気下端の温度と地表面温度は不連続になる。($B^* = \sigma T^4$ に注意)

From (3.10)(3.11)

$$\underbrace{B^*(T_s)}_{\text{surface}} = \underbrace{B^*(\tau_s^*)}_{\text{bottom of atmosphere}} + \frac{F^0}{2}$$

A temperature discontinuity exists at the surface. (Note that $B^* = \sigma T^4$)

(Planetary atmospheric science_radiation, Takeshi Imamura)

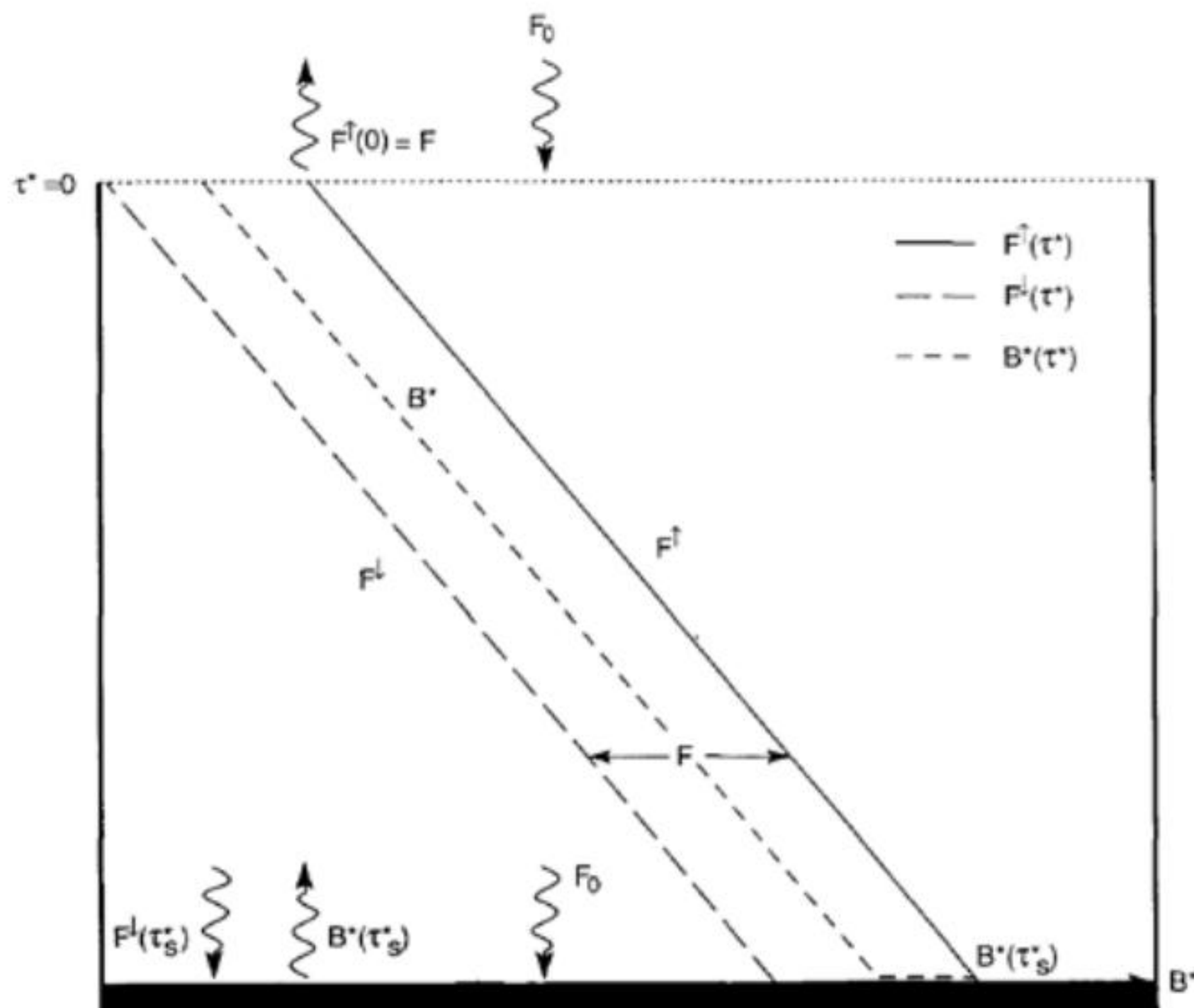


Figure 8.20 Upwelling and downwelling fluxes and emission in a gray atmosphere that is in radiative equilibrium with an incident SW flux F_0 and a black underlying surface. *Note:* the emission profile is discontinuous at the surface.

Toronto University

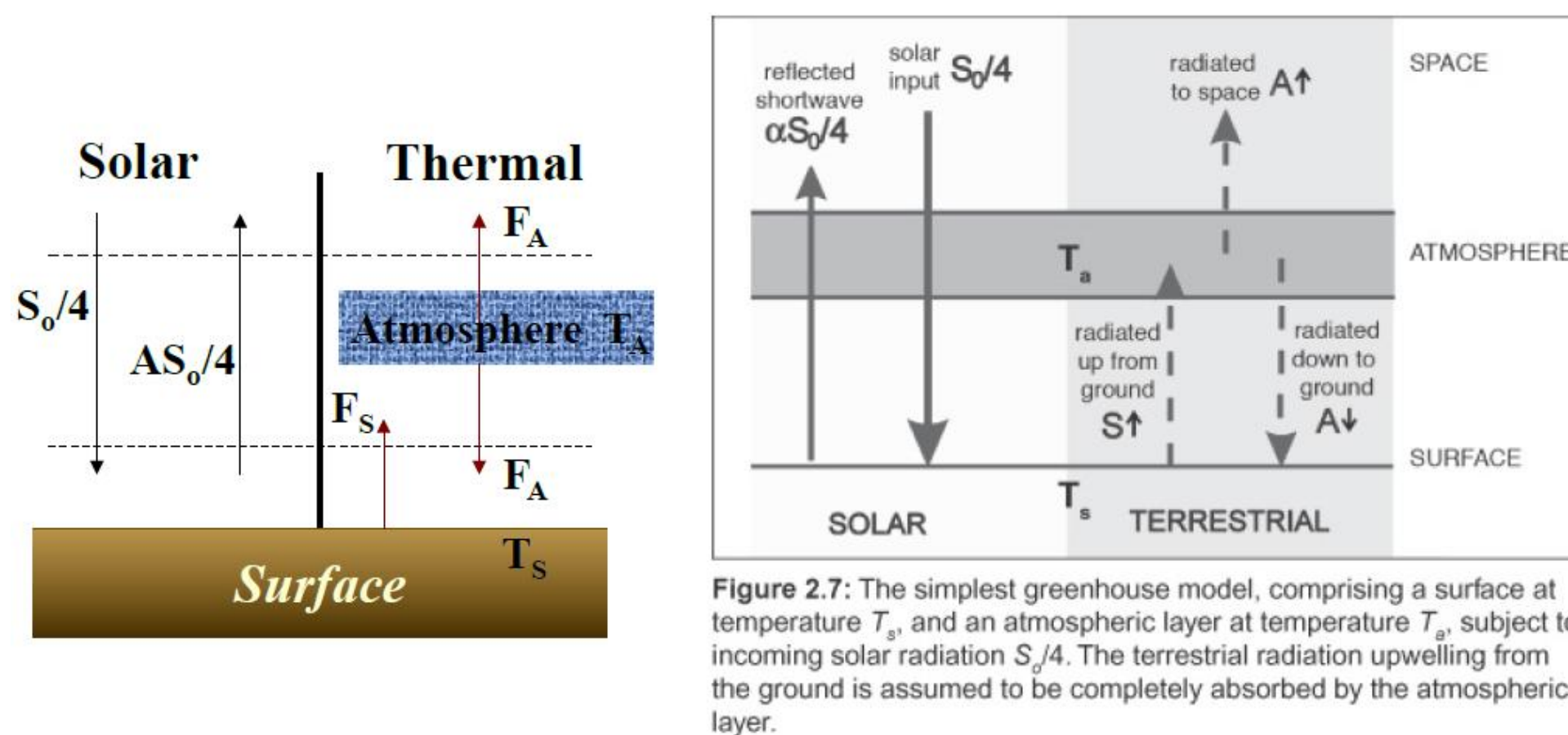
PHY2505S

Atmospheric Radiative Transfer and Remote Sounding

Lecture 6

- A Simple Greenhouse Model
- Terrestrial Fluxes: Schwarzschild's Equation Revisited
- The Two-Stream Model

Same Diagram, Slightly Different Symbols



Copyright © 2008, Elsevier Inc. All rights reserved.

A Simple Greenhouse Model - 3

- Writing down the equation for vertical energy transfer above the atmosphere and stating that the atmosphere/planet system is in radiative equilibrium:

$$S_0/4 = \alpha S_0/4 + F_A$$

Planetary albedo points to $\alpha S_0/4$.
Average solar flux density points to $S_0/4$.
IR flux density emitted by the atmosphere points to F_A .

- Below the atmosphere:

$$S_0/4 + F_A = \alpha S_0/4 + F_s$$

$$(S_0/4 + F_A) + F_A = \alpha S_0/4 + F_s$$

$$F_s = 2F_A$$

$$\sigma T_s^4 = 2\sigma T_e^4$$

“We will use “Schwarzchild’s Equation for Fluxes” in our simple greenhouse atmospheric model.”

Two-Stream Model Solution - 1

- We have thus solved for the upward and downward flux densities:

$$F_{\text{up}} = \sigma T_e^4 (\chi^* + 2) / 2$$

$$F_{\text{down}} = \sigma T_e^4 \chi^* / 2$$

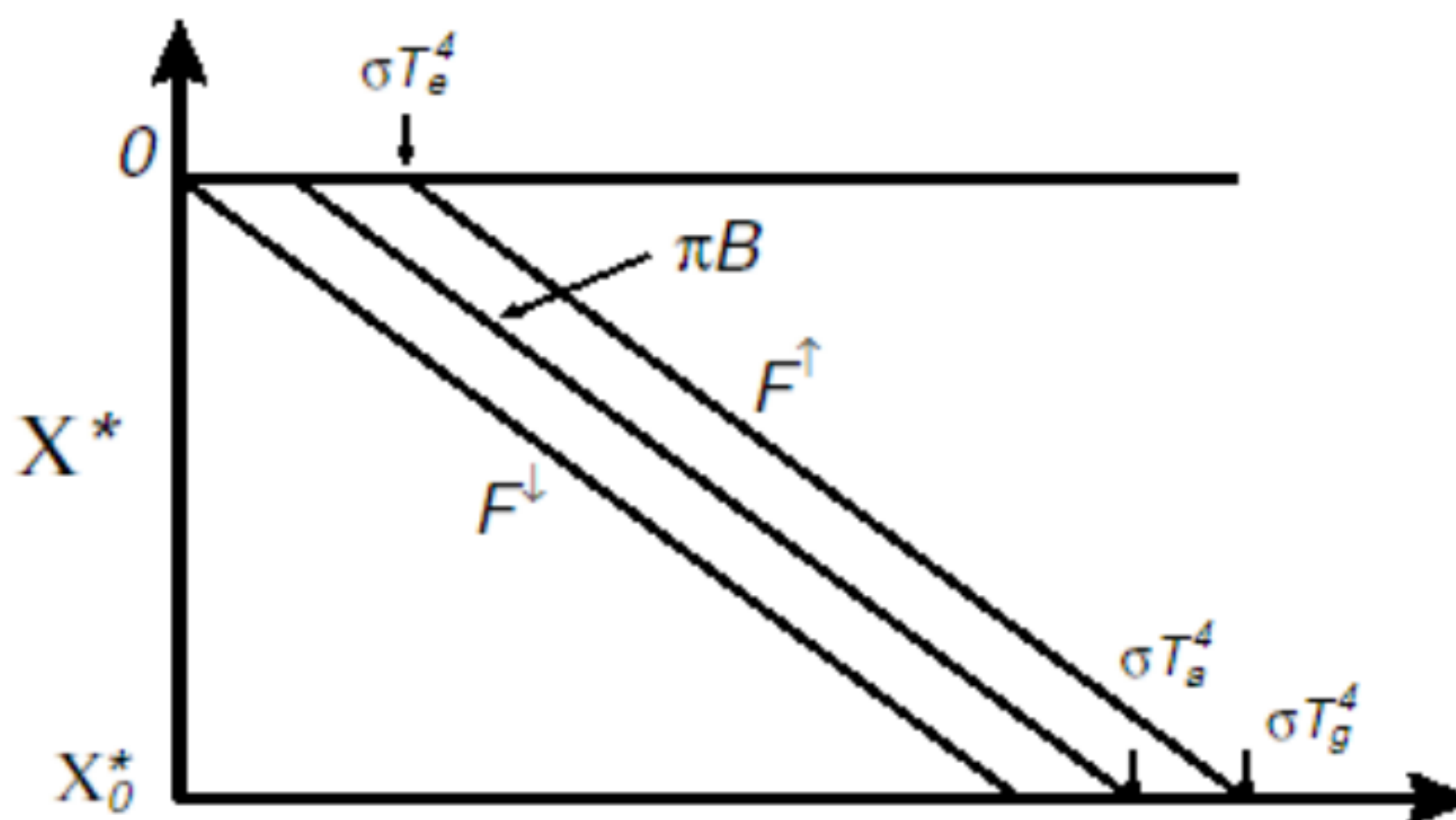
- Finally, we can use the original equations to solve for:

$$\pi B = \sigma T_a^4 = \frac{\sigma T_e^4 (\chi^* + 1)}{2}$$

where T_a is the atmospheric temperature.

- These three solutions can be plotted against χ^* .
 - Gives three parallel lines that show how the flux densities and the blackbody function vary with χ^* and hence with altitude.

Two-Stream Model Solution - 3



- If the central line represents the atmospheric temperature and the line for F_{up} must match the ground temperature, then there is a temperature discontinuity at the ground.

Southampton University / Tyndall Centre (UK)

In order to determine the temperature at the ground surface (T_g) for this purely radiative equilibrium, we need to consider the upward flux of infra-red radiation, since

$$[F_{up}]_{z=0} = \sigma T_g^4 \quad (13)$$

Since $F_{up} = (F_{tot} + F_{net})/2 = (F_{tot} + F_0)/2$, we find using equation (10) that

$$F_{up} = \{F_0 (\tau + 1) + F_0\}/2 = F_0 (1 + \tau/2) \quad (14)$$

Finally therefore, we also deduce that

$$F_{dn} = F_{up} - F_{net} = F_{up} - F_0 = F_0 (\tau/2) \quad (15)$$

Thus in the special case of pure radiative equilibrium, F_{net} is constant and equal to F_0 , and both F_{up} and F_{dn} increase linearly with optical thickness. This is illustrated in Figure 2 (see also [Salby, 1992 #3107][Houghton, 1997 #3186]).

However, it is very important to notice that the (ground) surface temperature is set by F_{up} through equation (13), i.e.

$$\sigma T_g^4 = [F_{up}]_{z=0} = F_0 (1 + \tau/2) \quad (16)$$

whereas the air temperature just above the ground is set by F_{tot} through equation (11) so that

$$\sigma T_0^4 = B(\tau) = F_0 (\tau + 1)/2 \quad (17)$$

ground surface temperature derived above exceeds that of the overlying air in this model, by an amount corresponding to an extra heat flux of $F_0/2$. This calculated ground-air temperature discontinuity may be substantial (10 or 20 °K, or more). It only occurs because we have assumed that the only heat fluxes are those due to radiation, so there is no conduction and no turbulent convection. In the real atmosphere these would operate together, as conduction will transfer heat into the air near the ground, creating an unstable

Final TP Profile

Expressions for intensity:

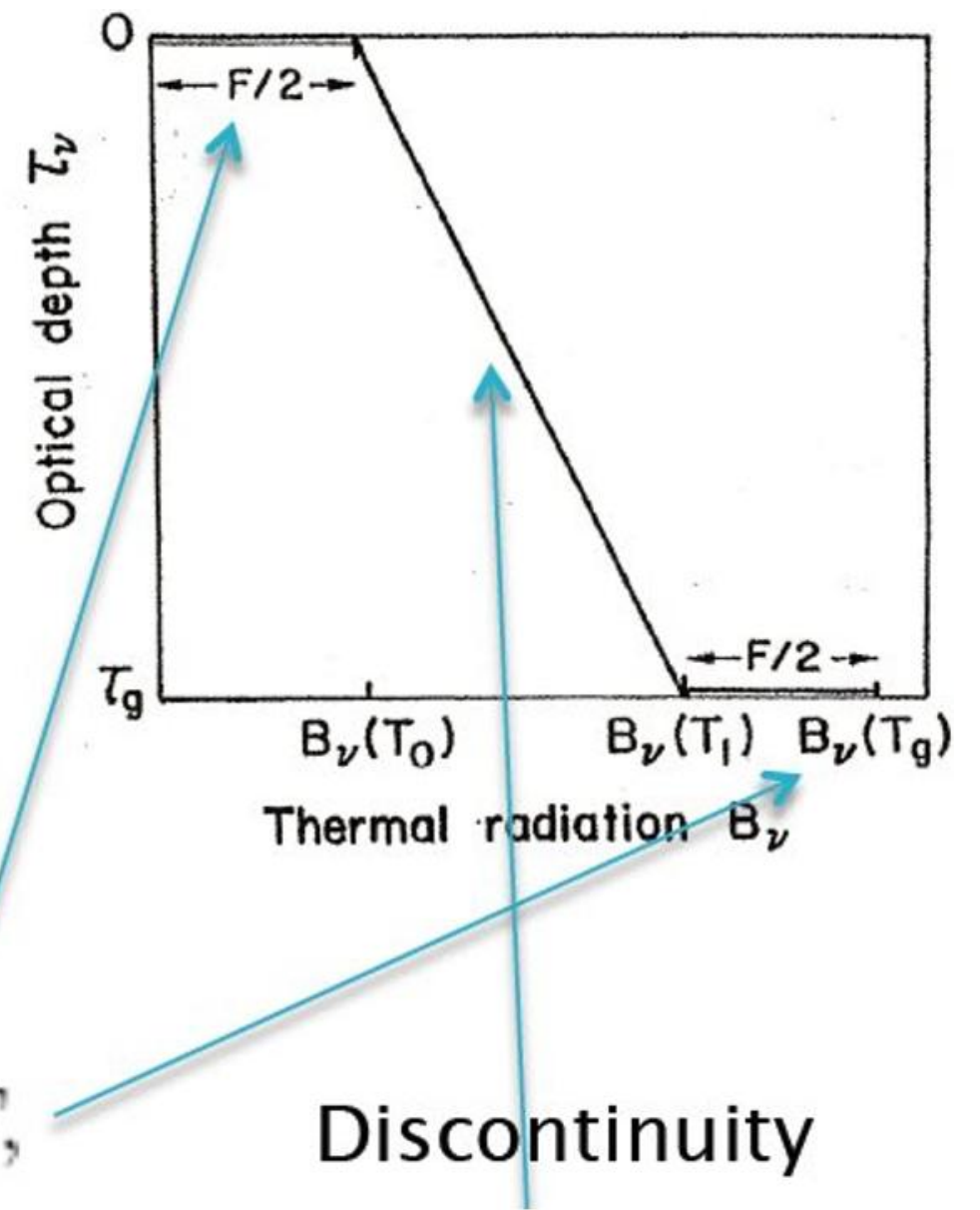
$$I^+ = B(T) + \frac{1}{2\pi}F$$

$$I^- = B(T) - \frac{1}{2\pi}F$$

Boundary Conditions:

At the Ground:

$$I_g^+ = B(T_g) = B(T_1) + \frac{1}{2\pi}F,$$



* * *

Harvard (2018)

We have got the temperature structure in the atmosphere as a function of τ . Now consider energy balance at the surface (looks familiar?),

$$B(T_s) = F_0 + F^\downarrow(\tau_s)$$

From their definitions, we have

$$F^\downarrow = \frac{1}{2}(\bar{F} - F)$$

As the net flux F is constant and equal to F_0 , and use Eq. (14), we have:

$$B(T_s) = B(\tau_s) + \frac{F_0}{2}$$

Note the jump at the surface.

Everybody knows everything

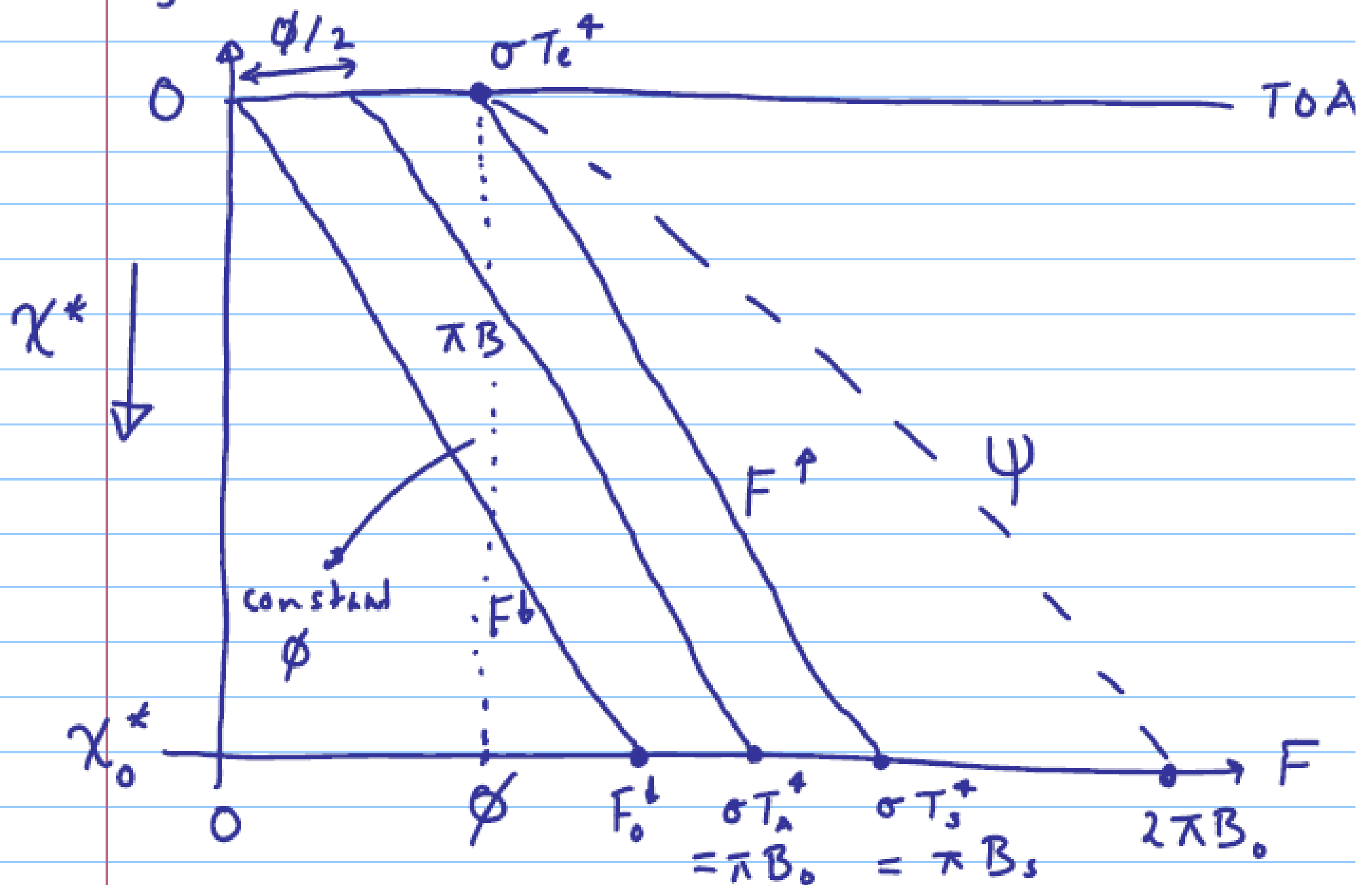
$$\phi = F^{\uparrow} - F^{\downarrow} = \sigma T_e^4$$

$$F^{\uparrow} = \frac{\phi}{2} (\chi^* + 2)$$

$$F^{\downarrow} = \frac{\phi}{2} \chi^*$$

$$\pi B = \frac{\phi}{2} (\chi^* + 1)$$

Let's plot these with χ^* on the y axis.



TRE Equation (1) is there everywhere:

Ambaum, M. (2021): Thermal physics of the atmosphere. Royal Meteorological Society. (Eq. 10.56)
Andrews, D. (2010): An introduction to atmospheric physics. Cambridge University Press (pp. 85-86)
Chamberlain, J. (1978): Theory of planetary atmospheres. Academic Press (Eq. 1.2.29 and Fig. 1.4.) (2nd edition: 1987)
Goody, R. (1964) Atmospheric radiation: Theoretical basis. Oxford University Press (Eq. 2.115) (2nd edition 1989, Eq. 2.146)
Hartmann, D. (1994) Global physical climatology. Academic Press. (Eqs. 3.48-3.54). (2nd edition: 2016)
Houghton, J. (1977) The physics of atmospheres. Cambridge University Press (Eq. 2.13). (2nd edition: 1986, 3rd edition: 2002)
Pierrehumbert, R. (2008): Principles of planetary climate. Cambridge University Press (Eq. 4.45)
Salby, M. (1996): Fundamentals of atmospheric physics. Academic Press. (Eq. 8.67)
Salby, M. (2012): Physics of the atmosphere and climate. Cambridge University Press (Eq. 8.67)
Vardavas, I. and Taylor, F. (2007): Radiation and Climate. Oxford University Press. (Eqs. 11.7-11.8)
Visconti, G. (2001): Fundamentals of physics and chemistry of the atmospheres. Springer Verlag (Eq. 3.49)
Zdunkowski, Trautmann and Bott (2008): Radiation in the atmosphere. Cambridge University Press (Fig. 6.7)

University Lecture Notes: Arizona, Columbia, Harvard, Manchester UK, MIT, Southampton UK Tyndall Centre, Tokyo, Toronto ...

Except:

The Charney Report (1979)
The Villach Statement (1980) (UNEP/WMO/ICSU/WCRP)
Theory of Climate (1983) (Academic Press)
Climate Change 1990 – The IPCC Scientific Assessment. Cambridge University Press
Climate Change 1992 – The Supplementary Report. Cambridge University Press
Climate Change 1995 – The Science of Climate Change. Cambridge University Press
Climate Change 2001 – The Physical Science Basis. Cambridge University Press
Climate Change 2007 – The Physical Science Basis. Cambridge University Press
Climate Change 2013 – The Physical Science Basis. Cambridge University Press
Climate Change 2021 – The Physical Science Basis. Cambridge University Press

Missing from essential journal articles:

Mamane and Möller (1961)
Manabe and Strickler (1964)
Manabe and Wetherald (1967)
Manabe and Wetherald (1975)
Ramanathan and Coakley (1976)
Ramanathan, Lian and Cess (1979)
Raval and Ramanathan (1989)

...

TRE basics: The four equations

Schwarzschild, K. (1906)

Ueber das Gleichgewicht der Sonnenatmosphäre, Eq. (11)

E emission of a layer, A upward beam, B downward beam, A_0 emerging flux at TOA, τ optical depth:

$$E = \frac{A_0}{2} (1 + \bar{\tau}), \quad A = \frac{A_0}{2} (2 + \bar{\tau}), \quad B = \frac{A_0}{2} \bar{\tau}. \quad (11)$$

Eq. (1) $A - E = \Delta A = A_0/2$ Net radiation at the surface, independent of τ

Eq. (1) SFC Net = $A - E = A_0/2$ (clear-sky, net)

Eq. (2) SFC Tot = $A = 2A_0$ (clear-sky, total at $\tau = 2$)

Separating atmospheric radiation transfer from the longwave cloud effect (LWCRE):

Eq. (3) SFC Net = $A - E = (A_0 - L)/2$ (all-sky, net, incl LWCRE)

Eq. (4) SFC Tot = $A = 2A_0 + L$ (all-sky, total at $\tau = 2$ incl LWCRE)

Eq. (1) From Schwarzschild (1906, Eq. 11), net, clear-sky:

$$A - E = \Delta A = A_0/2$$

Eq. (2) From Schwarzschild (1906, Eq. 11) at $\tau = 2$, total, clear-sky:

$$A = 2A_0$$

Eq. (3) From Schwarzschild (1906, Eq. 11), including LWCRE, net, all-sky:

$$A - E = \Delta A = (A_0 - L)/2$$

Eq. (4) From Schwarzschild (1906, Eq. 11) at $\tau = 2$, including LWCRE, total, all-sky:

$$A = 2A_0 + L$$

Eq. (1) Houghton (1977, 1986, 2002, Eq. 2.13), net, clear-sky:

$$B_g - B_0 = \phi/2\pi$$

Eq. (2) Houghton (1977, 1986, 2002, Eq. 2.15) at $\chi_0^* = 2$, total, clear-sky:

$$B_g = 2\phi/\pi$$

Eq. (3) Houghton (1977, 1986, 2002, Eq. 2.13), including LWCRE, net, all-sky:

$$B_g - B_0 = (\phi - L)/2\pi$$

Eq. (4) Houghton (1977, 1986, 2002, Eq. 2.15) at $\chi_0^* = 2$, including LWCRE, total, all-sky:

$$B_g = (2\phi + L)/\pi$$

Early verification of Eqs. (1) and (2)

CERES_EBAF-Surface_Ed2.8 Data Quality Summary (March 27, 2015)

Table 4-1. Global annual mean fluxes using data from March 2000 through February 2010 (W m⁻²).

	Flux Component	Ed3A SYN1deg -Month	EBAF- Surface Ed2.6r	EBAF- Surface Ed2.7	EBAF- Surface Ed2.8	EBAF- TOA Ed2.8
TOA	Incoming solar	339.9	339.9	339.9	339.8	339.8
	LW (all-sky)	237.3	239.7	239.6	239.6	239.6
	SW (all-sky)	98.5	99.6	99.6	99.6	99.6
	Net (all-sky)	4.06	0.64	0.69	0.63	0.59
	LW (clear-sky)	263.7	265.8	265.7	265.7	265.8
	SW (clear-sky)	52.5	52.5	52.6	52.6	52.6
	Net (clear-sky)	23.6	21.6	21.6	21.6	21.5
Surface	LW down (all-sky)	341.8	343.7	345.1	345.1	
	LW up (all-sky)	397.6	398.1	398.1	398.0	
	SW down (all-sky)	187.2	186.7	186.5	186.4	
	SW up (all-sky)	23.3	24.1	24.1	24.1	
	Net (all-sky)	108.1	108.3	109.4	109.4	
	LW down (clear-sky)	313.5	314.1	315.8	316.0	
	LW up (clear-sky)	396.6	398.3	398.4	398.0	
	SW down (clear-sky)	242.4	243.4	244.1	243.9	
	SW up (clear-sky)	28.7	29.6	29.7	29.7	
	Net (clear-sky)	130.6	129.6	131.8	132.2	

Eq. (1) R_N = Surface (SW down – SW up + LW down – LW up) (clear) = TOA LW (clear) / 2
 $243.9 - 29.7 + 316.0 - 398.0 = 265.7 / 2 - 0.65 \text{ Wm}^{-2}$

Eq. (2) R_T = Surface (SW down – SW up + LW down) (clear) = 2 × TOA LW (clear)
 $243.9 - 29.7 + 316.0 = 2 \times 265.7 - 1.2 \text{ Wm}^{-2}$

and Surface LW up = (3/2) TOA LW (clear) $398.0 = (3/2) \times 265.7 - 0.55 \text{ Wm}^{-2}$.

F. Rose et al. (16 May, 2017) CERES 27th STM (Langley Research Center)

Clear Sky	Ed2.8	Eq. (1) SFC (SW dn – SW up + LW dn – LW up) (clear) = TOA LW (clear) / 2 $244.06 - 29.74 + 316.27 - 398.40 = 265.59 / 2 - 0.60 \text{ Wm}^{-2}$
TOA SW Insolation	339.87	
TOA SW Up	52.50	Eq. (1) SFC (SW dn – SW up + LW dn) (clear) = 2 × TOA LW (clear) $244.06 - 29.74 + 316.27 = 2 \times 265.59 - 0.59 \text{ Wm}^{-2}$
TOA LW Up	265.59	
SFC SW Down	244.06	and SFC LW up (clear) = (3/2) TOA LW (clear) $398.40 = (3/2) 265.59 - 0.015 \text{ Wm}^{-2}$
SFC SW Up	29.74	
SFC LW Down	316.27	
SFC LW Up	398.40	

Verification of the four equations

CERES EBAF Ed4.1 Version 3, 22 years (April 2000 – March 2022) (Wm⁻²)

Eq. (1)	SFC SW down – SW up + LW down – LW up (clear)	= TOA LW (clear)/2	
	240.8680 – 29.0724 + 317.4049 – 398.5211	= 266.0122 /2	– 2.3267
Eq. (2)	SFC SW down – SW up + LW down (clear)	= 2 × TOA LW (clear)	
	240.8680 – 29.0724 + 317.4049	= 2 × 266.0122	– 2.8238
Eq. (3)	SFC SW down – SW up + LW down – LW up (all)	= [TOA LW (all) – LWCRE]/2	
	186.8544 – 23.1629 + 345.0108 – 398.7550	= (240.2450 – 25.7672)/2	+ 2.7083
Eq. (4)	SFC SW down – SW up + LW down (all)	= 2 × TOA LW (all) + LWCRE	
	186.8544 – 23.1629 + 345.0108	= 2 × 240.2450 + 25.7672	+ 2.4450
Mean			0.0007

CERES EBAF Ed4.1 Version 3, 22 years (April 2000 – March 2022) (Wm⁻²)
CERES EBAF Ed4.2 Version 4, 22 years (April 2000 – March 2022) (Wm⁻²)
CERES EBAF Ed4.2 Version 4, 24 years (April 2000 – March 2024) (Wm⁻²)

Eq. (1)	SFC SW down – SW up + LW down – LW up (clear)	= TOA LW (clear)/2	
	240.8680 – 29.0724 + 317.4049 – 398.5211	= 266.0122 /2	– 2.3267
	241.0969 – 29.7521 + 317.8744 – 398.5890	= 265.9594 /2	– 2.3495
	241.0514 – 29.7043 + 318.0984 – 398.7742	= 265.9748 /2	– 2.3161
Eq. (2)	SFC SW down – SW up + LW down (clear)	= 2 × TOA LW (clear)	
	240.8680 – 29.0724 + 317.4049	= 2 × 266.0122	– 2.8238
	241.0969 – 29.7521 + 317.8744	= 2 × 265.9594	– 2.6996
	241.0514 – 29.7043 + 318.0984	= 2 × 265.9748	– 2.5042
Eq. (3)	SFC SW down – SW up + LW down – LW up (all)	= [TOA LW (all) – LWCRE]/2	
	186.8544 – 23.1629 + 345.0108 – 398.7550	= (240.2450 – 25.7672)/2	+ 2.7083
	187.1451 – 23.4950 + 346.1057 – 398.4220	= (240.3317 – 25.6277)/2	+ 3.9818
	187.1756 – 23.4607 + 346.3158 – 398.6162	= (240.3894 – 25.5854)/2	+ 4.0126
Eq. (4)	SFC SW down – SW up + LW down (all)	= 2 × TOA LW (all) + LWCRE	
	186.8544 – 23.1629 + 345.0108	= 2 × 240.2450 + 25.7672	+ 2.4450
	187.1451 – 23.4950 + 346.1057	= 2 × 240.3317 + 25.6277	+ 3.4647
	187.1756 – 23.4607 + 346.3158	= 2 × 240.3894 + 25.5854	+ 3.6665
Mean			0.0007
			0.5994
			0.7147

Mean annual bias of the four equations [-0.82, 1.41]

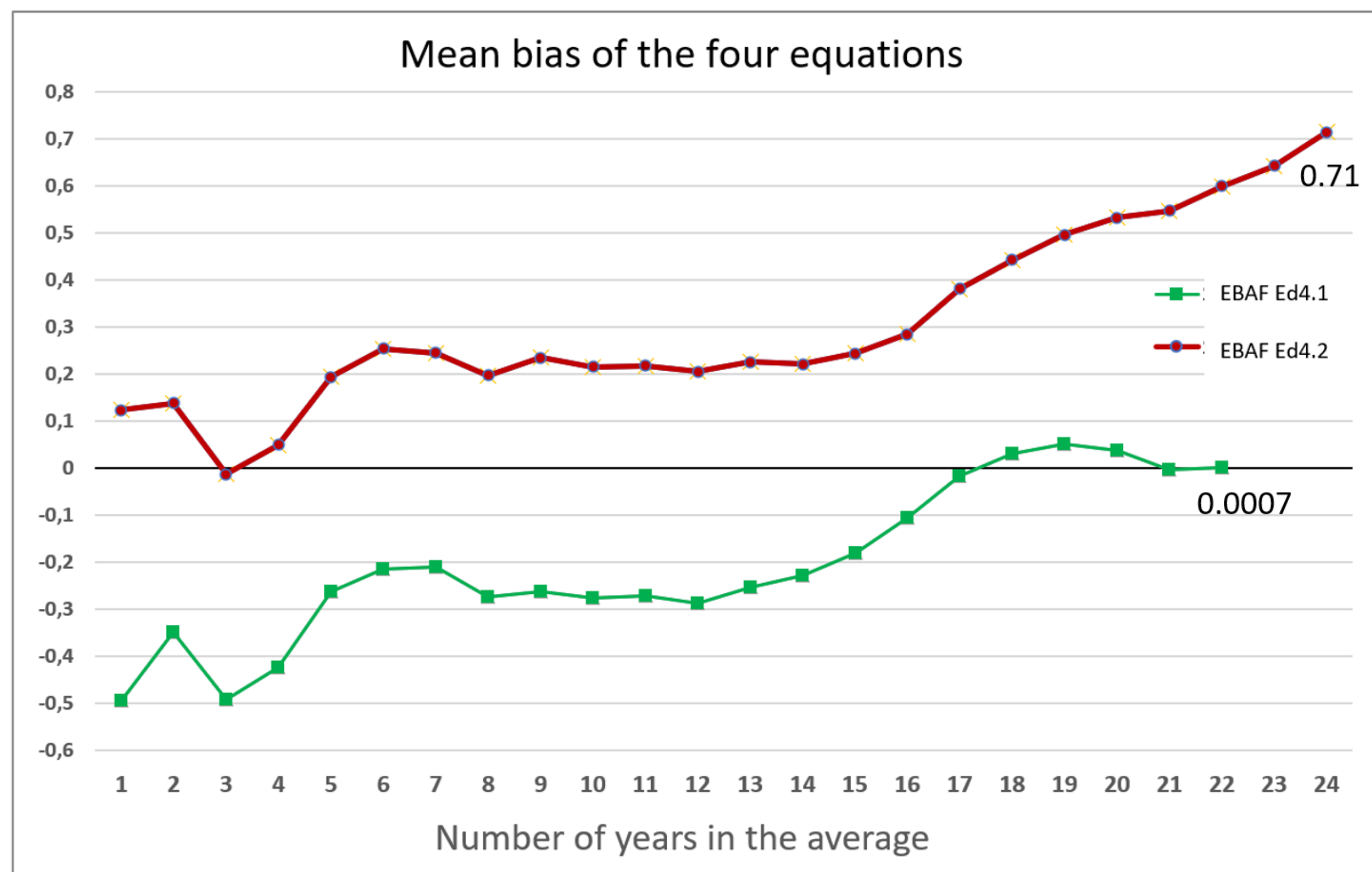
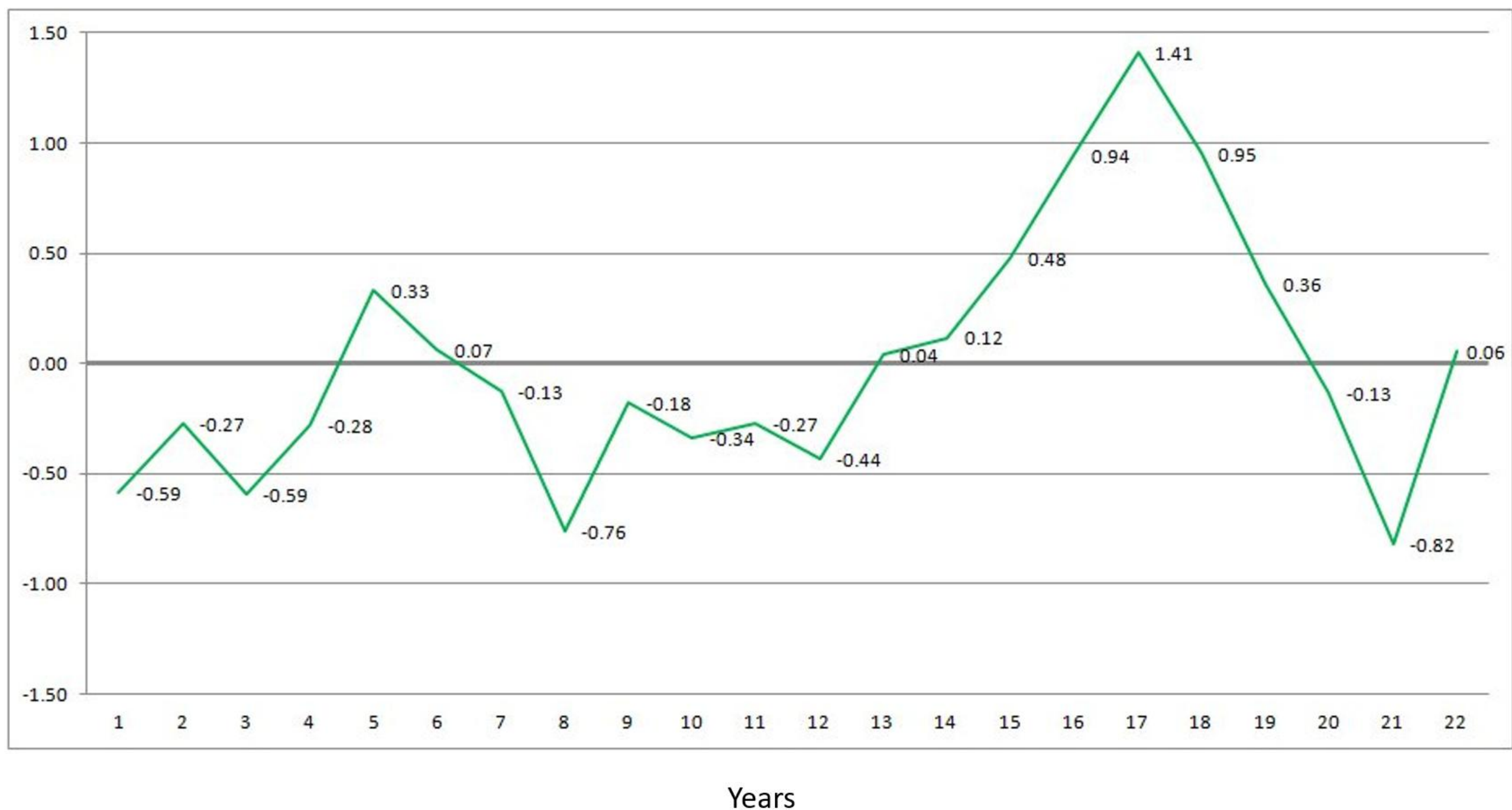


Fig. 6 Annual mean bias of the four equations (above) and mean bias as a function of the number of years (below)

The simplest greenhouse geometry

Four equations, coupling surface fluxes to TOA fluxes, without referring to GHG-s

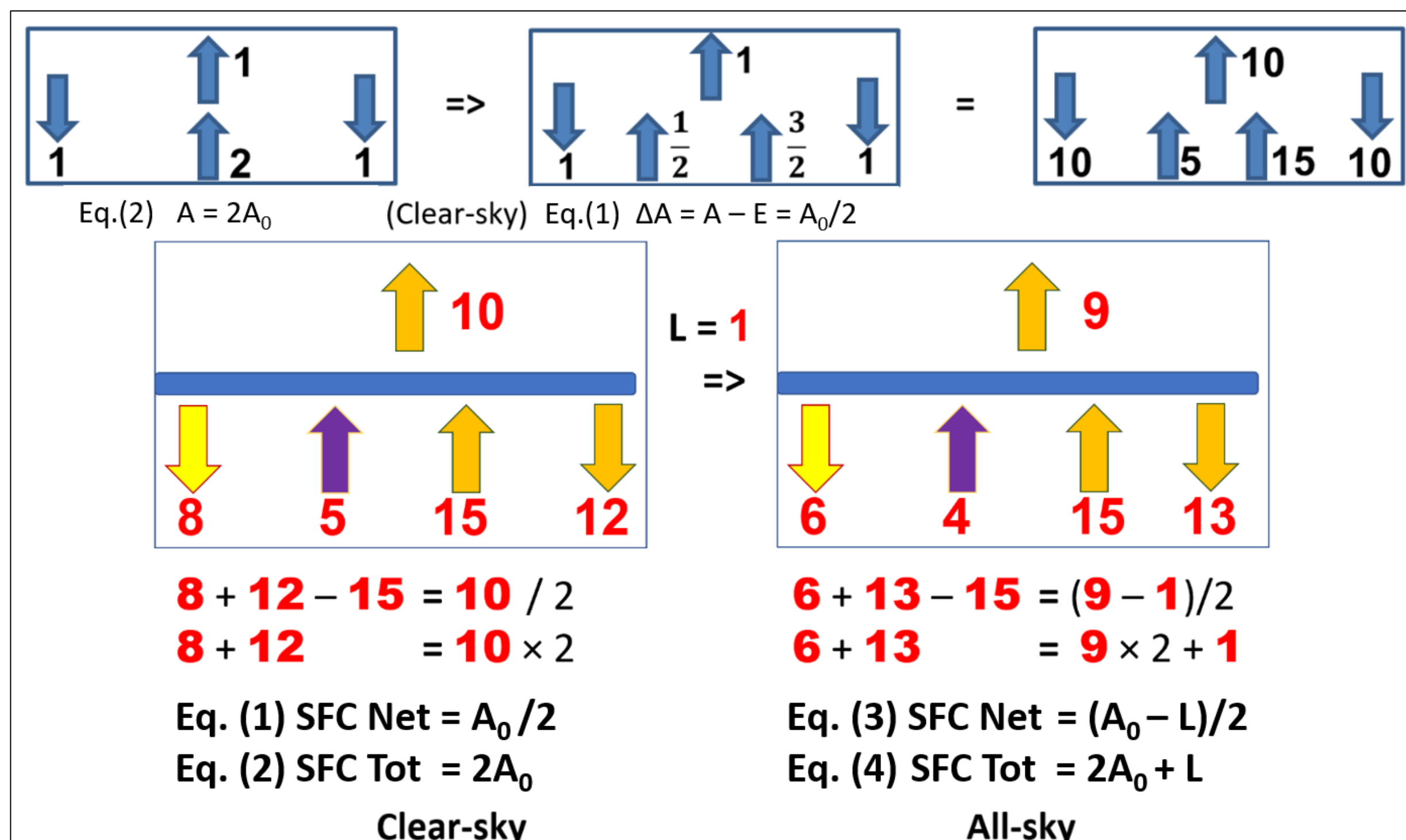


Fig. 5 Theoretical background for the reference estimate. Upper left panel: The simplest greenhouse geometry represents Eq. (2). Upper middle panel: The constraint on the net radiation at the surface (Eq.1) included. Upper right panel: since the unit is not specified yet, multiply it by 10. Lower left panel: The clear-sky structure in red units, with **1** unit = L , representing LWCRE. Lower right panel: The all-sky structure. Integer solution and the four equations are indicated.

The flux components with LWCRE = 1

TOA LW	clear-sky = 10	TOA LW	all-sky = 9
SFC LW up	clear-sky = 15	SFC LW up	all-sky = 15
SFC LW down	clear-sky = 12	SFC LW down	all-sky = 13
SFC LW net	clear-sky = -3	SFC LW net	all-sky = -2
SFC SW net	clear-sky = 8	SFC SW net	all-sky = 6
SFC SW+LW net	clear-sky = 5	SFC SW+LW net	all-sky = 4
SFC SW+LW total	clear-sky = 20	SFC SW+LW total	all-sky = 19
G greenhouse effect	clear-sky = 5	G greenhouse effect	all-sky = 6
SWCRE (surface)	= -2	LWCRE (surface. TOA)	= 1

TRE as a completed, coherent set of the integer solution. LWCRE = **1** = 26.68 Wm^{-2} corresponds to TSI = **51** units = 1360.68 Wm^{-2} c.f. the most accurate value is $1360.8 \pm 0.5 \text{ Wm}^{-2}$ (Kopp and Lean 2011) if spherical weighting is applied; with geometric weighting factor of 4.0034, as in CERES EBAF, TSI = 1361.84 Wm^{-2} .

241		95,353	239,685	54,535	265,303	-40,818	25,618	-15,200	337,434	190,746	239,062	24,855	30,177	343,153	317,451	400,769	400,410	
242		95,447	241,783	54,721	267,445	-40,726	25,662	-15,064	332,585	186,328	235,238	24,873	31,085	347,424	321,464	405,103	404,095	
243		94,748	243,653	52,368	268,842	-42,380	25,190	-17,190	329,614	179,961	230,369	21,661	27,821	351,881	326,080	408,133	407,299	
244		93,229	244,372	49,661	269,916	-43,569	25,544	-18,025	329,266	177,576	228,671	18,938	24,551	354,238	328,435	408,966	408,587	
245		91,200	244,796	48,524	270,265	-42,677	25,469	-17,208	331,600	180,825	230,967	18,070	23,493	353,598	327,599	408,248	407,728	
246		93,522	243,406	50,144	268,342	-43,378	24,936	-18,443	336,209	184,379	235,043	19,457	24,764	349,969	323,257	405,377	405,008	
247		99,960	240,666	53,206	266,197	-46,753	25,531	-21,222	342,033	188,506	243,908	23,298	28,984	344,441	316,277	399,994	399,627	
248		105,153	239,328	56,926	264,350	-48,227	25,021	-23,206	347,485	193,210	251,215	27,127	33,319	339,377	310,844	395,008	394,438	
249		107,742	237,758	57,036	262,951	-50,706	25,193	-25,513	350,953	193,344	253,883	27,058	33,152	335,309	307,389	390,669	390,449	
250		105,590	237,448	55,347	263,216	-50,243	25,768	-24,475	351,193	193,375	252,863	24,786	30,641	333,255	306,333	389,512	389,499	
251		100,909	238,551	54,053	263,572	-46,856	25,021	-21,835	348,320	193,167	249,184	23,027	29,049	334,525	308,038	390,523	390,833	
252		97,347	238,327	53,761	263,778	-43,586	25,450	-18,136	343,350	192,217	244,177	23,100	28,775	337,431	311,242	394,143	394,461	
253		96,018	238,578	54,536	264,364	-41,482	25,786	-15,696	337,529	190,544	239,745	24,841	30,368	341,326	315,414	399,249	399,052	
254		96,465	240,493	54,783	266,702	-41,683	26,210	-15,473	332,568	185,198	235,392	24,634	31,124	346,845	320,182	404,380	403,388	
255		94,443	242,463	52,122	268,077	-42,322	25,614	-16,708	329,597	180,391	230,664	21,678	27,871	351,224	325,245	407,640	406,783	
256		93,235	244,019	50,193	269,585	-43,042	25,566	-17,476	329,253	177,040	227,387	18,976	24,485	354,971	329,091	409,170	408,753	
257		91,248	244,527	49,343	269,337	-41,906	24,809	-17,096	331,630	180,035	228,828	17,951	23,211	354,051	327,911	408,525	408,038	
258		93,310	242,530	49,731	267,824	-43,580	25,295	-18,285	336,223	184,936	235,997	19,395	24,734	350,749	323,572	405,223	404,610	
259		98,633	240,874	52,761	265,929	-45,871	25,055	-20,816	342,035	189,649	244,424	22,766	28,571	345,043	317,252	400,266	399,765	
260		104,357	238,192	55,983	263,800	-48,374	25,608	-22,766	347,511	193,334	251,464	26,307	32,442	339,903	311,451	395,210	394,979	
261		107,262	237,329	56,519	262,954	-50,743	25,624	-25,119	350,948	193,126	253,603	26,343	32,380	336,003	308,218	390,950	390,797	
262		104,735	237,315	55,233	262,965	-49,501	25,650	-23,851	351,238	193,858	252,529	24,629	30,463	333,918	307,249	389,882	389,981	
263		100,422	238,699	54,249	263,628	-46,172	24,929	-21,243	348,479	193,638	248,699	23,076	28,839	335,035	308,781	391,151	391,254	
264	month	97,714	238,489	54,196	264,088	-43,509	25,599	-17,910	343,513	191,770	243,601	23,128	28,777	338,861	312,673	394,885	394,891	
265	name	sw_all	lw_all	sw_clr	lw_clr	cre_sw	cre_lw	cre_net	solar	sw_dn_all	sw_dn_cl	sw_up_all	sw_up_cl	lw_dn_all	lw_dn_cl	lw_up_all	lw_up_cl	
266	mean	98,96	240,25	53,72	266,01	-45,24	25,77	-19,48	340,02	186,85	240,87	23,16	29,07	345,01	317,40	398,75	398,52	
267	N	15/4	36/4	8/4	40/4	-7/4	1	-3/4	51/4	7	9	1	1	13	12	15	15	
268	N × unit	100,05	240,12	53,36	266,8	-46,69	26,68	-20,01	340,17	186,76	240,13	26,68	26,68	346,84	320,16	400,2	400,2	
269	diff	-1,09	0,13	0,36	-0,79	1,45	-0,91	0,53	-0,15	0,09	0,74	-3,52	2,39	-1,83	-2,76	-1,45	-1,68	
270		TOA max diff -1.09 Wm ⁻² sw all								Surface max diff 3,52 Wm ⁻² sw up all								
271																		
272		ΔEq1= -2,3267			ΔEq2= -2,8238													
273		ΔEq3= 2,7083			ΔEq4= 2,4451			mean = 0,00070			g(clear)= 0,333			g(all)= 0,398				

CERES EBAF Ed4.1 data table, 22 full running years (264 monthly means) (only the last 24 months are displayed); The largest differences at TOA and at SFC; the four equations and their mean bias; and the greenhouse factors.

The all-sky integer structure and Eqs. (3) and (4) on Hartmann (2016)

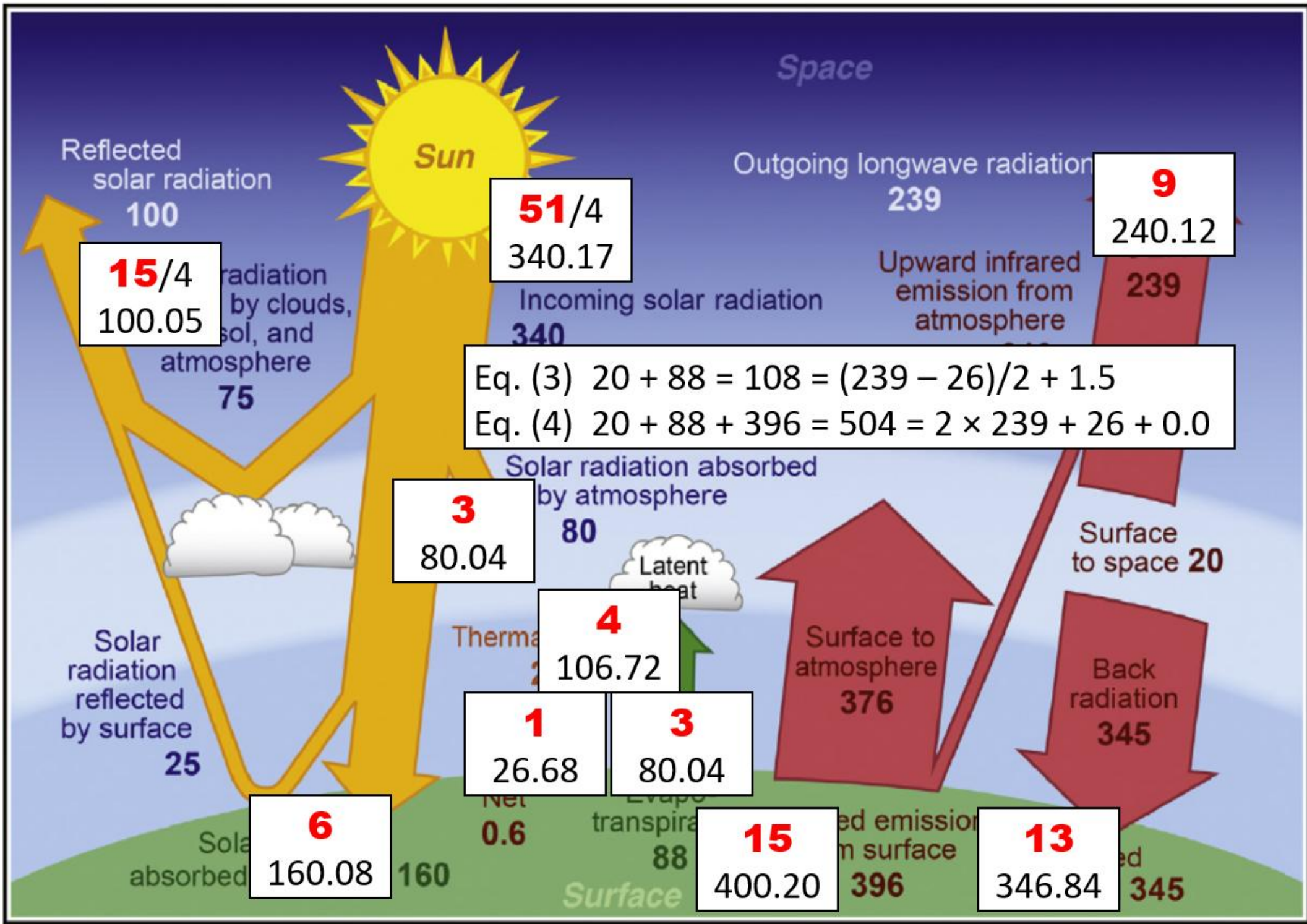


FIGURE 2.4 Global and annual average radiative and nonradiative energy-flow diagram for Earth and its atmosphere. Units are Wm^{-2} .

Figure 2.4 of D. Hartmann (IPCC AR5 2013 WGI Chapter 2 Coordinating Lead Author) Global Physical Climatology, 2nd Ed. (2016). With LWCRE = 26 Wm^{-2} of the book, Eq. (3) differs by 1.5 Wm^{-2} ; Eq. (4) is exact.

The all-sky integer structure on Stephens et al. (2012)

An update on Earth's energy balance in light of the latest global observations Nature Geosci 2012

Graeme L. Stephens^{1*}, Juilin Li¹, Martin Wild², Carol Anne Clayson³, Norman Loeb⁴, Seiji Kato⁴, Tristan L'Ecuyer⁵, Paul W. Stackhouse Jr⁴, Matthew Lebsock¹ and Timothy Andrews⁶

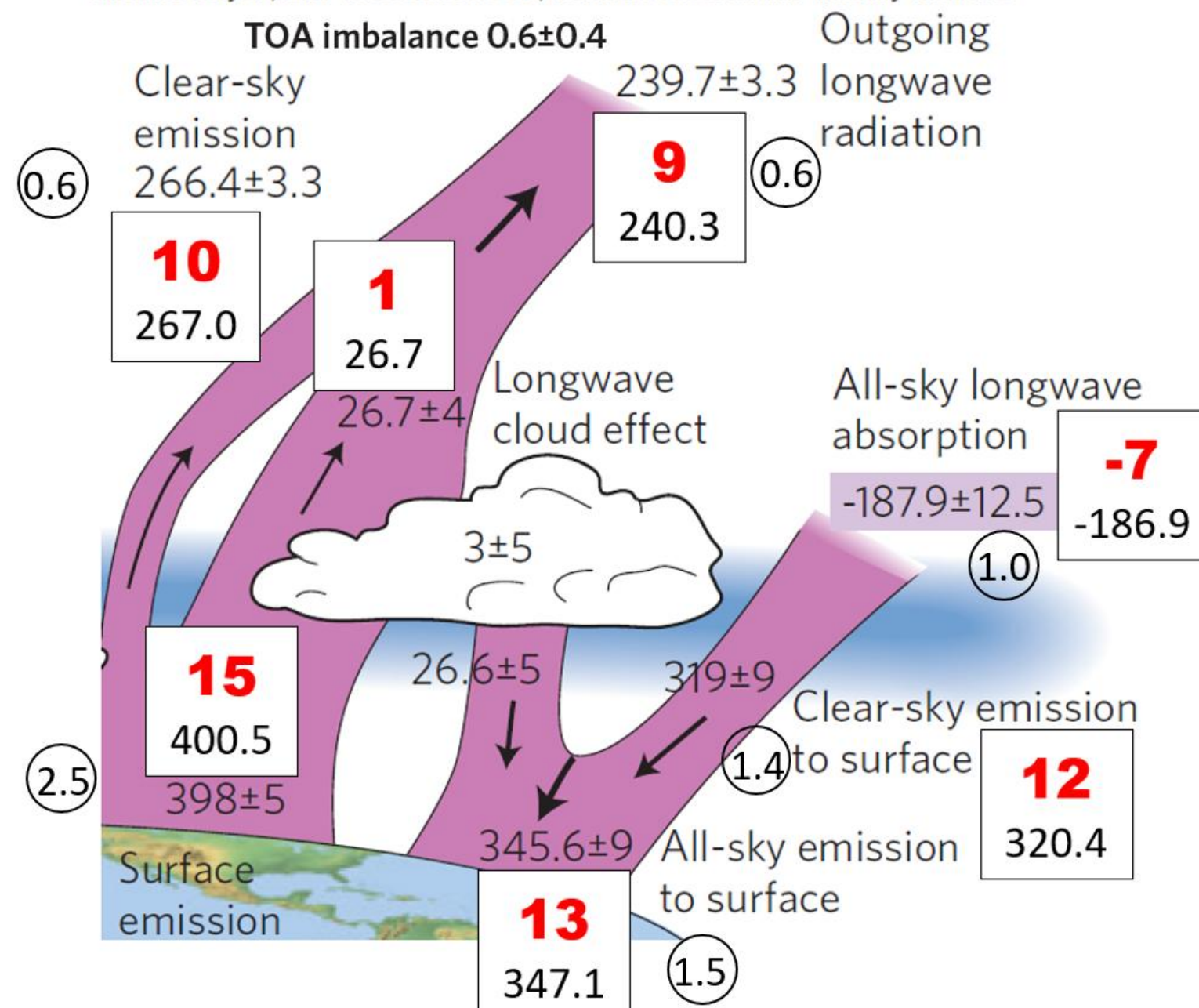


Fig. 7a Theoretical reference estimate projected on the LW part of the updated energy balance of Stephens et al. (2012) with unit flux LWCRE at TOA = 26.7 Wm^{-2} . Deviation from the integer position at TOA equals the TOA imbalance (0.6 Wm^{-2}); the largest difference at the surface is 2.5 Wm^{-2} , still within the noted range of uncertainty.

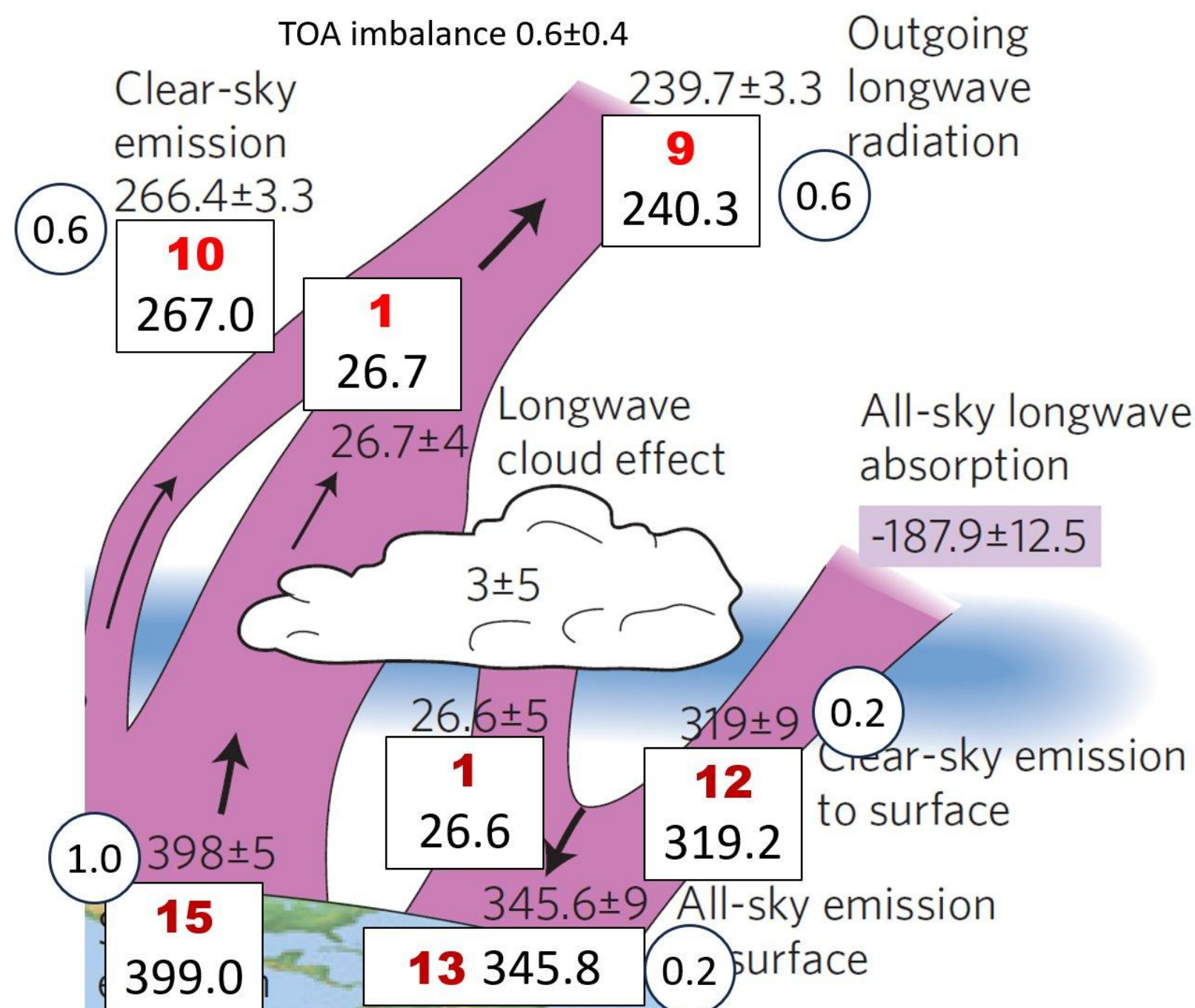


Fig. 7b When LWCRE at the surface is used as unit for the surface fluxes (shown in purple with 26.6 Wm^{-2}), the difference from the integer positions for the downward emissions drop to 0.2 Wm^{-2} .

A short video explaining this figure is available here:

<https://earthenergyflows.com/Stephens2012-iPoster-1080.mp4>

All-sky equations on Stephens et al. (2023)

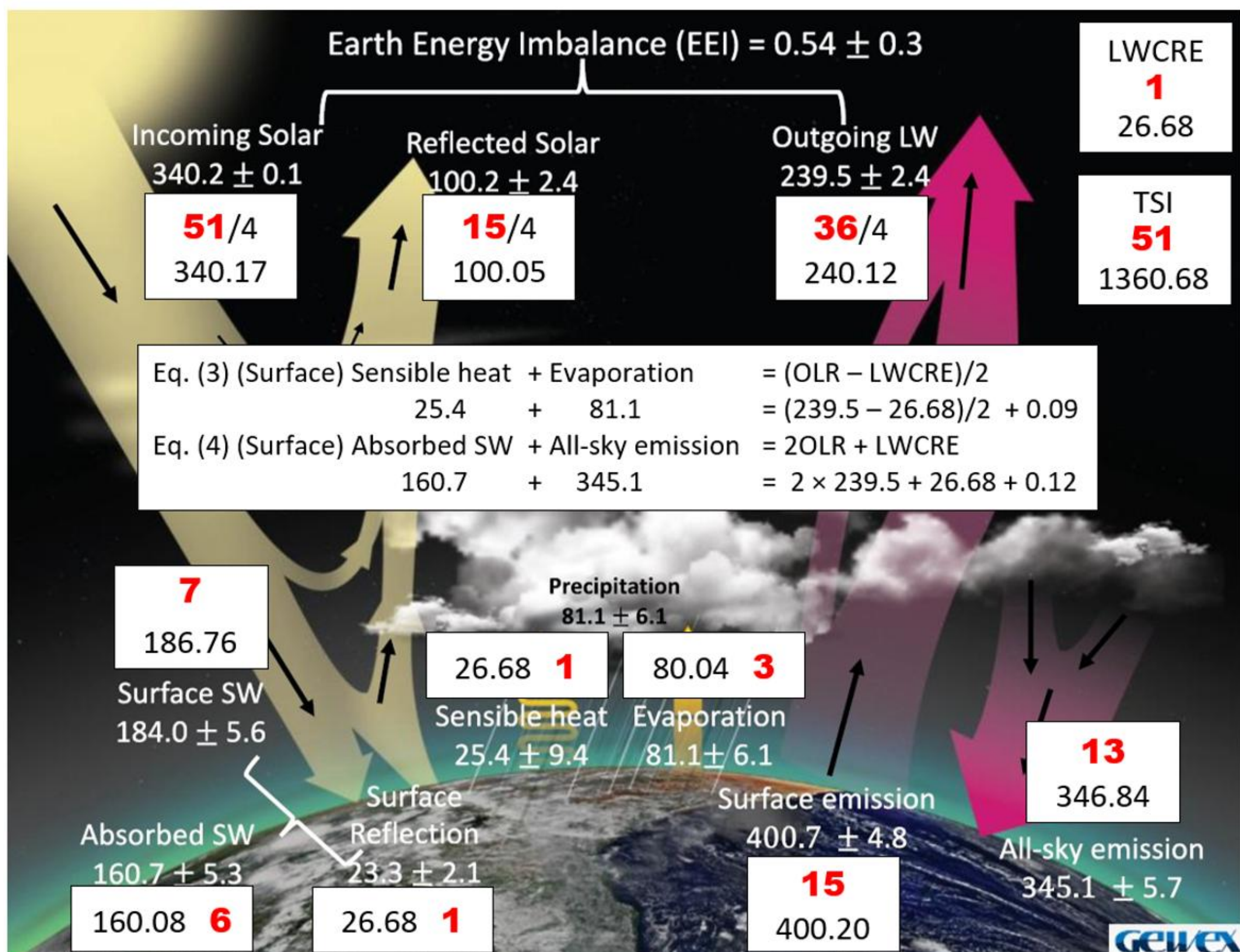


Fig. 8 Theoretical reference estimate projected on 30 years of GEWEX data (Stephens et al. 2023, BAMS). The two all-sky equations are satisfied in the magnitude of 0.1 Wm^{-2} . The value of LWCRE is the theoretical (1 units = 26.68 Wm^{-2}); compare to that of 26.7 Wm^{-2} of Stephens, Li, Wild, Clayson, Loeb, Kato, L’Ecuyer, Stackhouse et al. (2012). The largest difference from integer position at TOA is 0.62 Wm^{-2} (Outgoing LW), in the magnitude of EEI.

“The CERES flying on the Terra and Aqua satellites confirm that Earth’s albedo is $29.4\% (\pm 0.3\%)$ ” [Ackerman, L’Ecuyer, Loeb et al. 2019, AMS Met Monographs, Chapter 4]. With Incoming Solar of the GEWEX estimate, $TSI = 340.2 \text{ Wm}^{-2}$, the corresponding Reflected Solar Radiation is $0.294 \times 340.2 = 100.02 \text{ Wm}^{-2}$; our theoretical reflected solar is $RSR = 15/51 \times 340.17 = 100.05 \text{ Wm}^{-2}$, since our TRE albedo is $\alpha_{TRE} = 15/51 = 0.294$. As $15/51 = 5/17$, OLR on the disk is 12; after spherical weighting $OLR = 3$, $ULW = 5$ and $G = 2$ in this ‘big unit’ (80.04 Wm^{-2}), with all-sky values of 240.12 Wm^{-2} , 400.20 Wm^{-2} and 160.08 Wm^{-2} , respectively.

It deserves to mention that the unique accuracy of separate components of the hydrological cycle (Sensible heat and Evaporation) in the GEWEX assessment is based on the NASA Energy and Water-cycle Study (NEWS) methodology (Rodell et al. 2015, L’Ecuyer et al. 2015).

With this exemplary accuracy, this estimate, published “officially” in the Bulletin of AMS, serves as a “benchmark” for any other global energy flow estimate, and justifies the saying of Dr Stephens: “Instead of the traditional paradigm of properties define processes, study how processes define property.”

An independent estimate: All-sky Equations on L’Ecuyer et al. (2015)

“Radiative Forcing of Climate”, Meteorological Monographs 2019

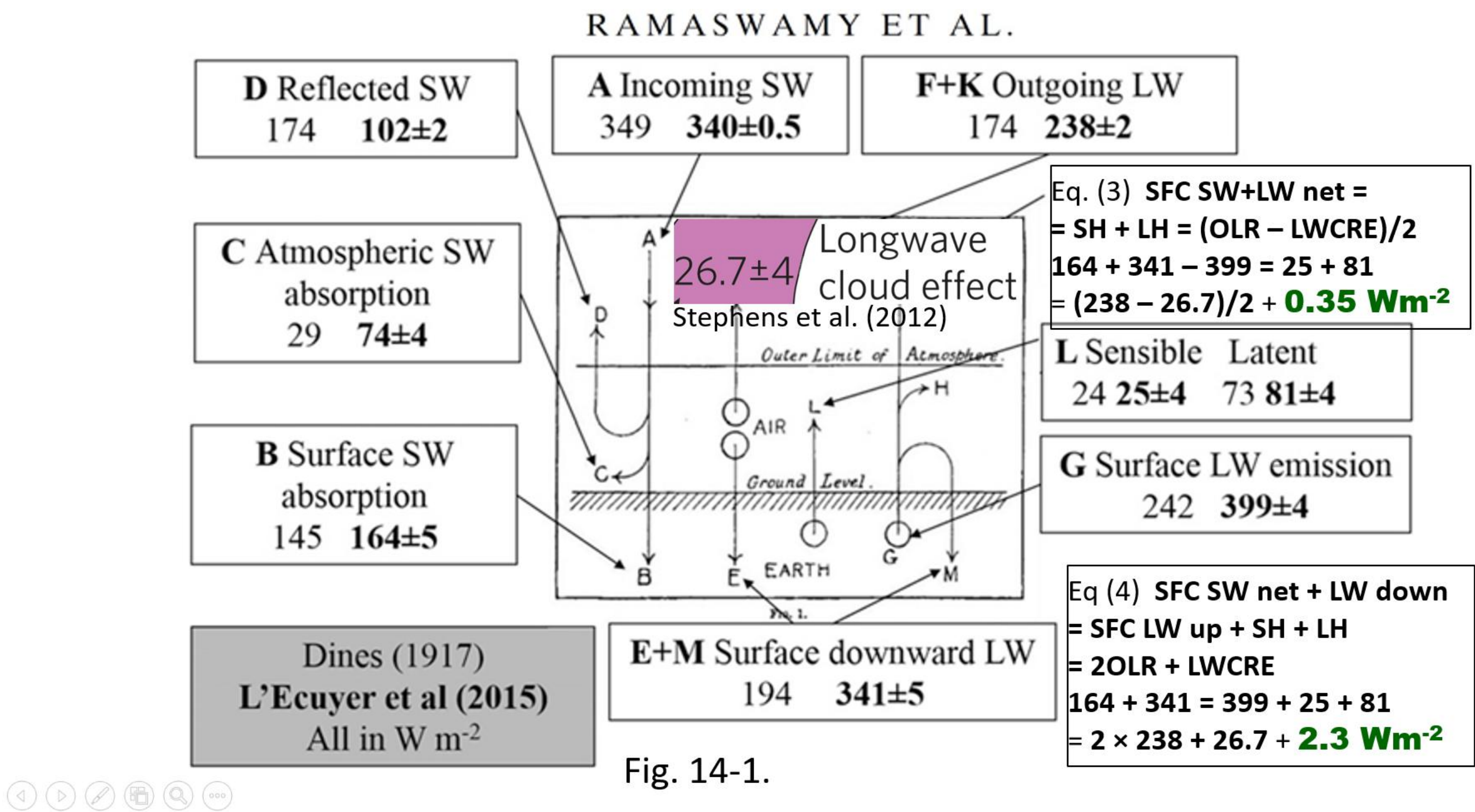


Fig. 9 Ramaswamy et al. (AMS, 2019) compare historical estimate of global energy budget to that of L’Ecuyer et al. (2015) (bold font). Longwave cloud effect is projected from Stephens et al. (2012) as 26,7 Wm⁻².
Eq. (3) is valid by a difference of 0.35 Wm⁻², Eq. (4) by 2.3 Wm⁻².

An independent estimate: Clear-sky Greenhouse Effect at GFDL DL

LWCRE (TRE) = **1** = 26.68 ± 0.01 Wm⁻²

G (clear, geo) = **15** – **10** = **5** = 133.40 ± 0.05 Wm⁻²

G (GFDL AM4) = 133.4 ± 0.6 Wm⁻²

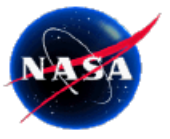
Quantifying the Drivers of the Clear Sky Greenhouse Effect, 2000–2016

Shiv Priyam Raghuraman✉, David Paynter, V. Ramaswamy (JGR 2019)

Table 2					
Global Mean and Time Mean G Comparison Between Observational, Reanalysis, and Modeling Data Sets Over March 2000 to August 2016					
Quantity	ERBE	CE 4.1 “c”	CE 4.1 “t”	ERA-Interim	GFDL AM4
G _{Oceans}	146 ± 7	131.3 ± 0.5	134.1 ± 0.5	134.8 ± 0.6	135.0 ± 0.5
G	–	129.7 ± 0.6	132.4 ± 0.6	133.1 ± 0.7	133.4 ± 0.6

A Case Study: Surface Solar Radiation (all-sky)

- Zagoni TRE integer position: **7** units = 186.76 Wm^{-2} (**1** unit = 26.68 Wm^{-2})
- Stackhouse et al. GEWEX SRB (EGU 2023) 186 Wm^{-2}
- Stackhouse, Cox, Mikovitz, Zhang (EGU 2020) 187.8, 185.8, 185.4, 187.1:



SRB (R4-IP) SW Global Annual Averages Fluxes for 2001-2007

Flux Component	Rel 3.0 (2001-2007)	Rel 4_IP (NEW algorithm, NEW inputs nnHIRS, HXS V01)	CERES Syn1Deg (Ed. 4A)	CERES EBAF (Ed 4.0)
Surface total down	187.8	185.8	185.4	187.1

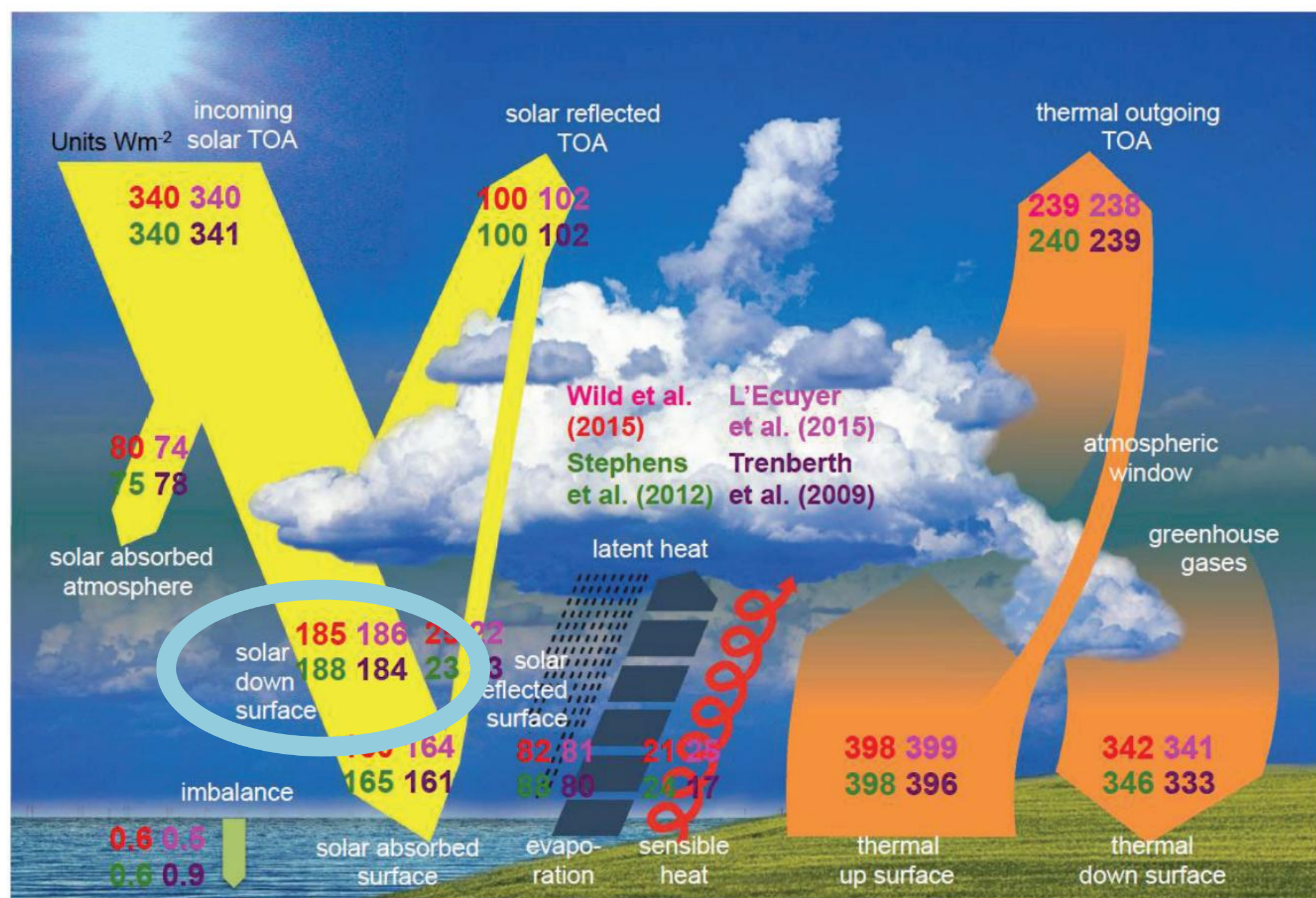
- Trentmann and Pfeifroth (EGU2023-2563):
Global surface irradiance (2000 to 2017): 187 W/m^2
- Kato et al. (2018) 187.1 (CERES EBAF Ed4); 186.6 (Ed2.8):

TABLE 5. Global annual mean irradiances (W m^{-2}) computed with Ed2.8 and Ed4 EBAF products from July 2005 through June 2015.

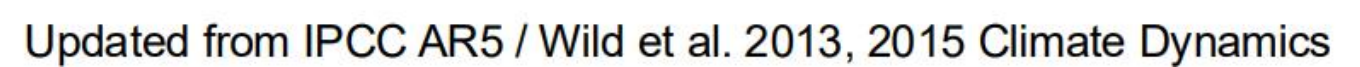
	Ed4	Ed2.8	Ed4 – Ed2.8
All-sky (Jul 2005–Jun 2015)			
TOA SW insolation	340.0	339.8	0.17
TOA SW up	99.1	99.6	–0.5
TOA LW up	240.0	239.5	0.5
SW down	187.1	186.6	0.53

1	23.6119	163.219	186.831
2	23.3151	162.957	186.273
3	23.3751	163.367	186.742
4	23.4779	163.474	186.952
5	23.2294	163.073	186.307
6	23.1536	163.565	186.715
7	23.0952	163.26	186.315
8	23.3998	163.52	186.815
9	23.3719	163.514	186.885
10	23.0131	162.615	185.628
11	23.0608	163.338	186.399
12	23.1055	163.538	186.643
13	23.3977	163.303	186.715
14	23.363	163.598	186.961
15	23.1144	163.788	186.902
16	22.684	164.215	186.899
17	22.8377	164.482	187.315
18	22.9748	164.252	187.227
19	22.8119	164.023	187.025
20	23.18	163.57	186.75

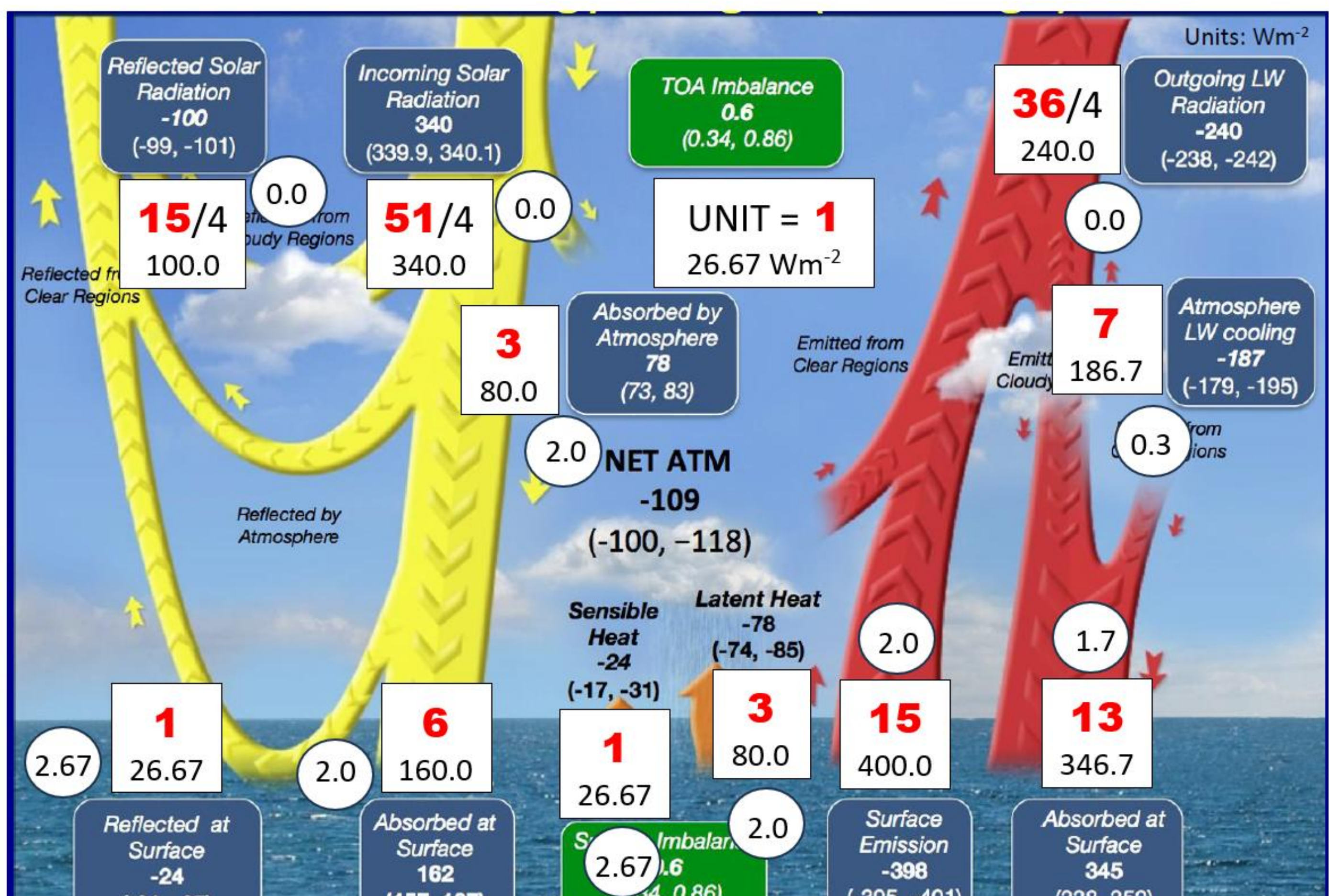
- Wild (2017, AIP):



-



- **Loeb** (2014, NASA LaRC, CERES): Solar down surface = 186 Wm^{-2}

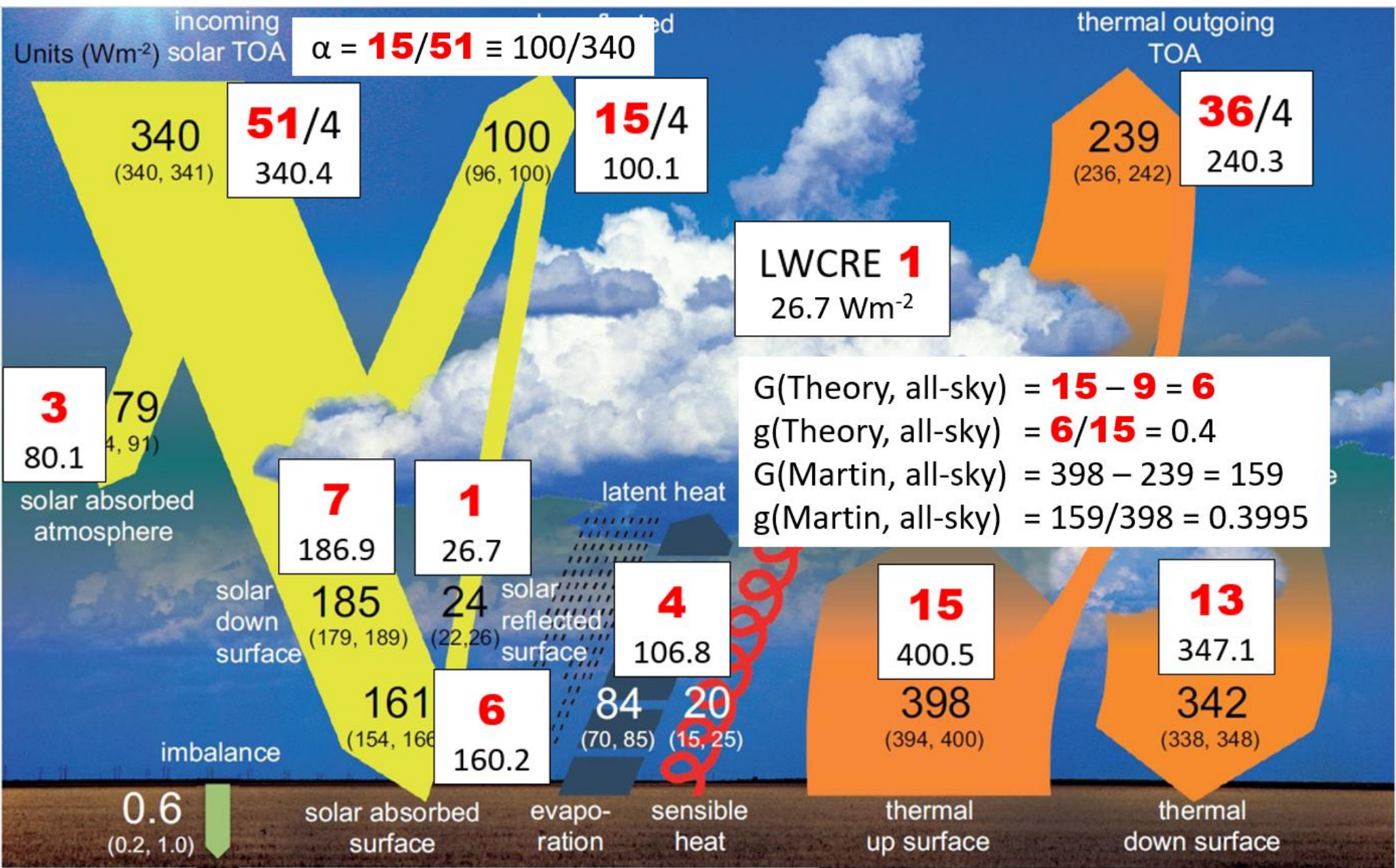


3

Attribution of global warming: greenhouse effect?

All-sky greenhouse factor, $g(\text{TRE}) = (15 - 9)/15 = 0.4$

All-sky greenhouse factor, $g(\text{IPCC}) = (398 - 239)/398 = 0.3995$



Clear-sky greenhouse factor, $g(\text{TRE}) = (15 - 10)/15 = 1/3$

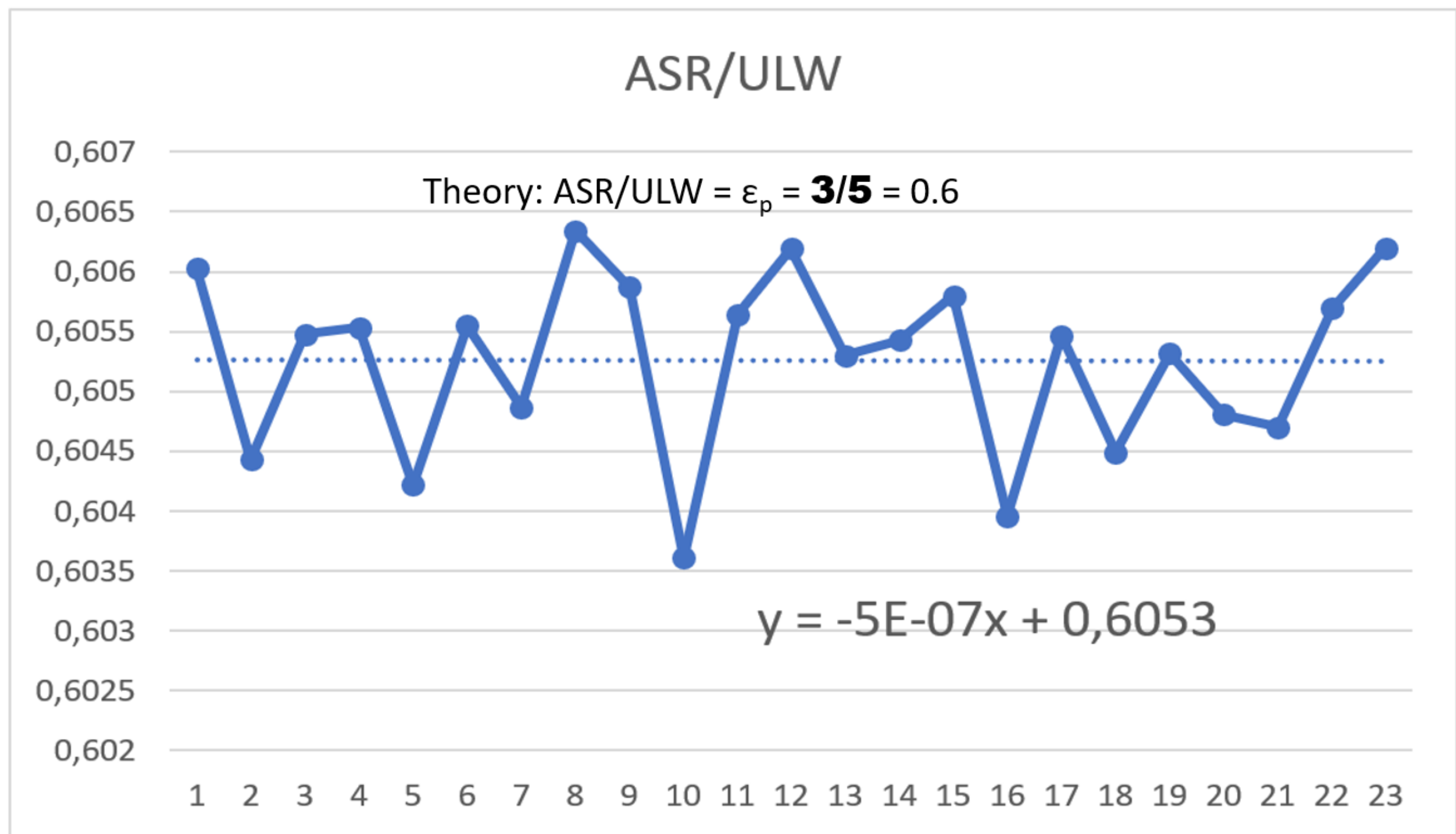
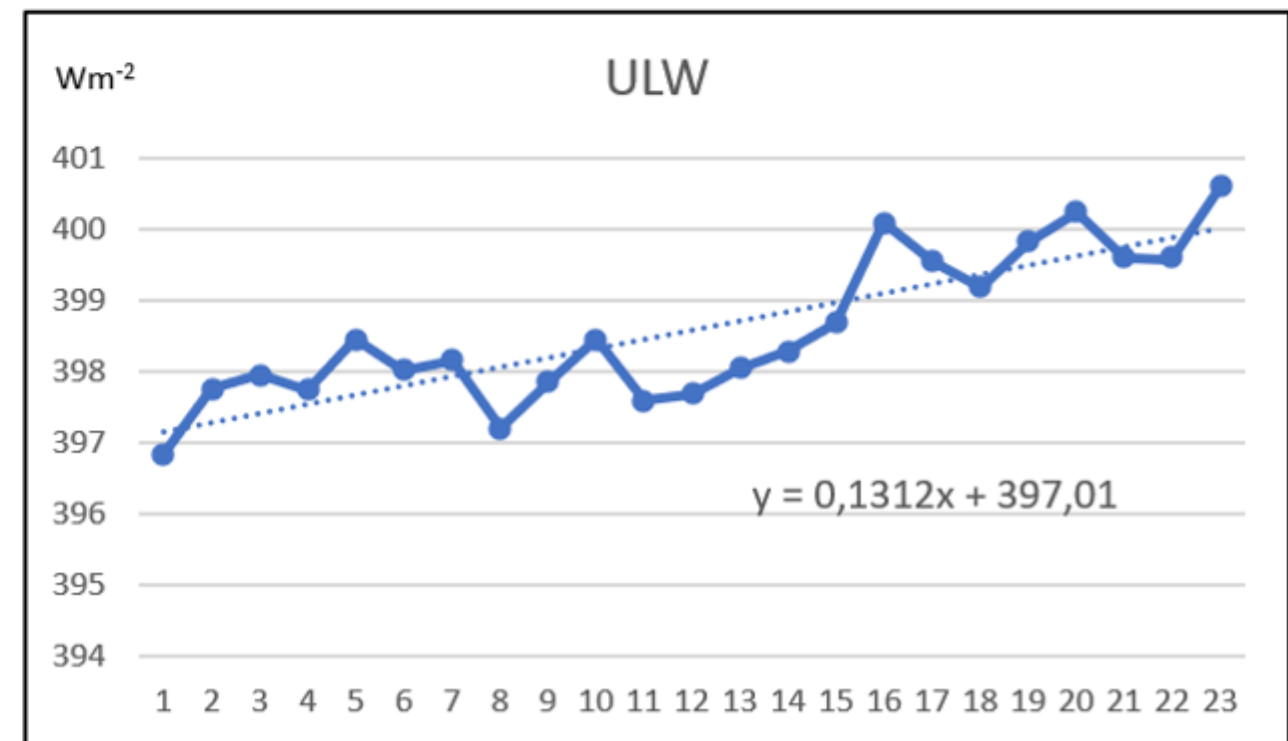
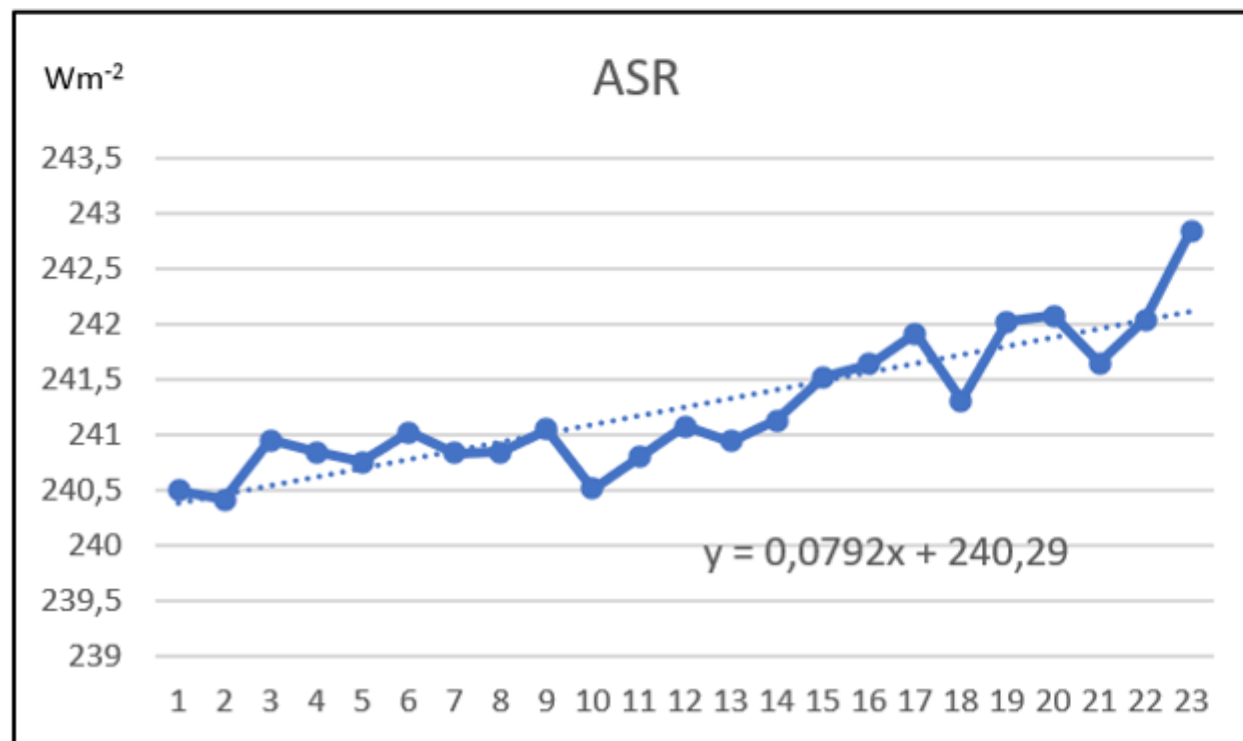
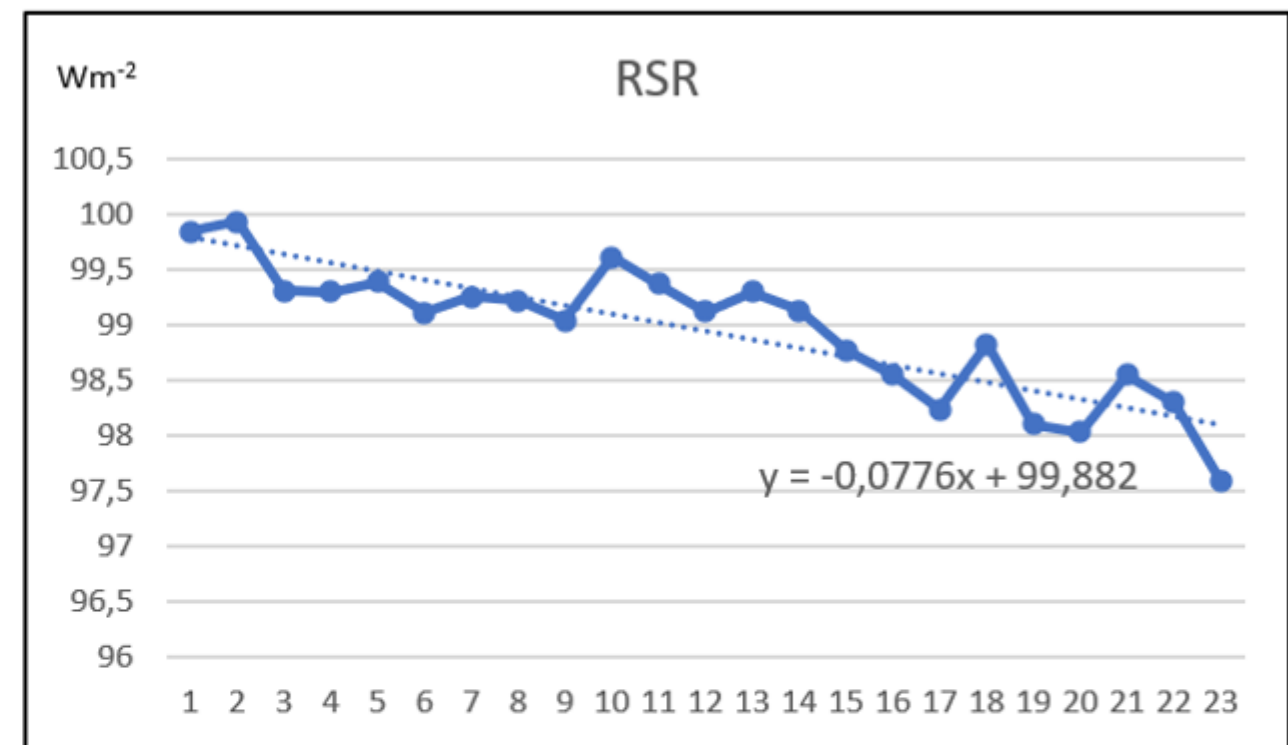
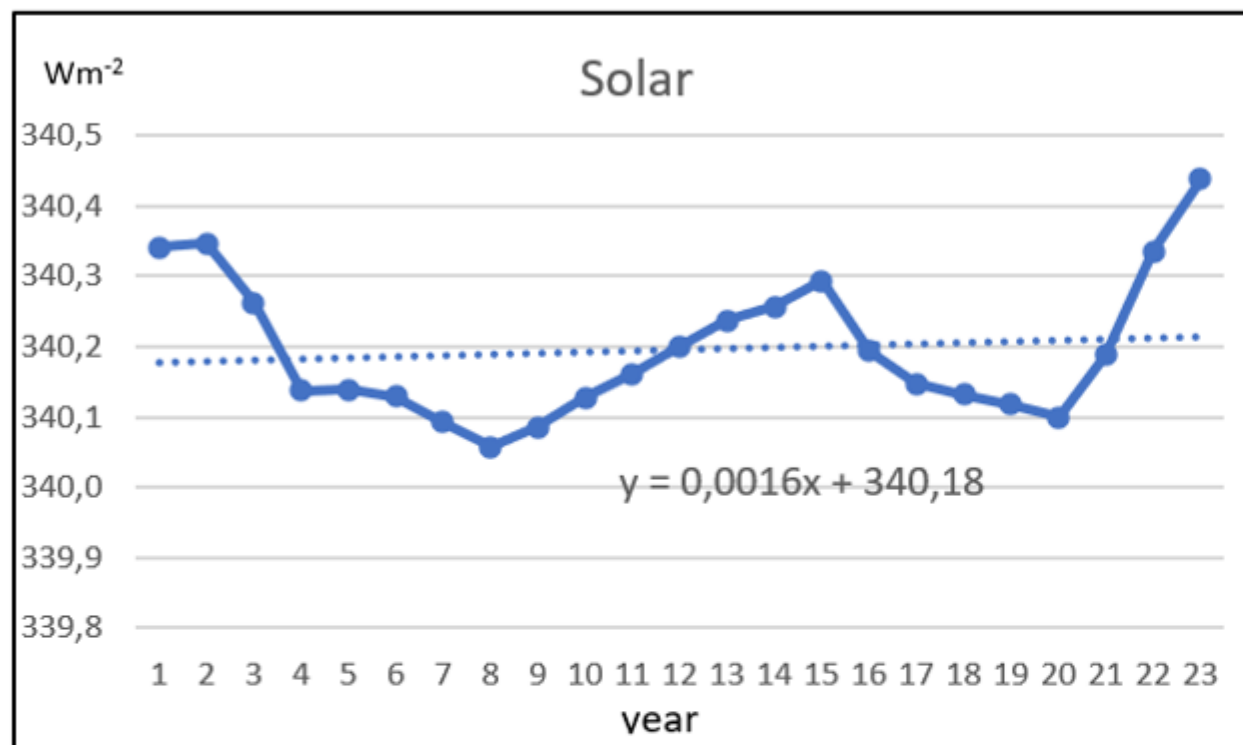
Clear-sky greenhouse factor, $g(\text{CERES}) = (398.92 - 265.98)/398.92 = 0.33325$

CERES EBAF Ed4.2.1, 24-yr mean (Oct 2000 – Sep 2024)

Clear-sky	N	Theory	CERES
Surface LW up	15	400.20	398.92
TOA LW up	10	266.80	265.98
G	5	133.40	132.94
g	5/15	1/3	0.33325
All-sky	N	Theory	CERES
Surface LW up	15	400.20	398.72
TOA LW up	9	240.12	240.42
G	6	160.08	158.30
g	6/15	0.4	0.397

What Are the Drivers of Global Warming?

Data: CERES EBAF Ed4.2 V2, release date 2 Jan 2024 (Oct 2000 – Sept 2023)



2017: Theoretical Reference Estimate introduced to the science community

NASA CERES Science Team Meeting, Goddard Space Flight Center, Washington

Patterns in the CERES Global Mean Data

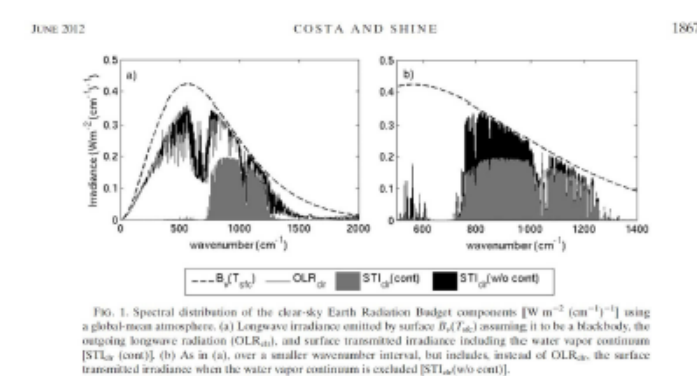


"To search for something – though it be mushrooms – or some pattern – is impossible, unless you look and try."
Dmitri Mendeleev

Pattern 3. Clear-sky integer ratios

Costa and Shine (2012) Line-By-Line

- ULW = 386 Wm⁻²
- OLR = 259 Wm⁻²
- ATM = 194 Wm⁻²
- G = 127 Wm⁻²
- STI = 65 Wm⁻²



	STI	G	ATM	OLR	ULW	2OLR
CS12 =	65	127	194	259	386	518
Pattern	65	130	195	260	390	520
Ratios	1	2	3	4	6	8
Diff	0	3	1	1	4	2 (Wm ⁻²)

Direct surface–TOA coupling puts the atmospheric processes into parenthesis.

All-sky and clear-sky integer positions and their values in Wm⁻²
(From the 2017 NASA CERES STM presentation)

EdMZ all-sky integer ratios

$$F = N \times \text{UNIT}$$

$$\text{UNIT} = \text{OLR}(\text{all-sky})/9$$

All-sky Flux	EdMZ	N
TOA SW In	340.04	
TOA SW Up	99.60	
TOA LW Up	240.14	9
SFC SW In	160.09	6
SFC LW Down	346.87	13
SFC (SW in + LW in)	506.96	19
SFC LW Up	400.23	15
SFC Net	106.73	4
G	160.09	6
SFC LWCRE	26.68	1
2 x TOA LW Up + LWCRE	506.96	19

EdMZ clear-sky and all-sky integer ratios

$$F = N \times \text{UNIT}, F = N \times \text{UNIT}$$

$$\text{UNIT} = \text{OLR}(\text{clear-sky})/4$$

Clear-sky Flux	EdMZ	N	N
TOA SW In	340.04		
TOA LW Up	266.82	4	10
ATM emitted Up	200.11	3	30/4
STI	66.7	1	10/4
SFC (SW + LW) In	533.65	8	20
SFC LW Up	400.23	6	15
SFC Net	133.42	2	5
G	133.42	2	5

Model data set: EdMZ All-sky pattern positions

All-sky	Ed2.8	Ed4.0	EdMZ
TOA SW In	339.87	340.04	340.04
TOA SW Up	99.62	99.23	99.60
TOA LW Up	239.60	240.14	240.14
SFC SW In	162.34	163.67	160.09
SFC LW Down	345.15	344.97	346.87
SFC (SW in + LW in)	507.49	508.64	506.96
SFC LW Up	398.27	398.34	400.23
SFC Net	109.22	110.30	106.73
G	158.67	158.20	160.09
SFC LWCRE	28.88	30.90	26.68

Model data set: EdMZ Clear-sky pattern positions

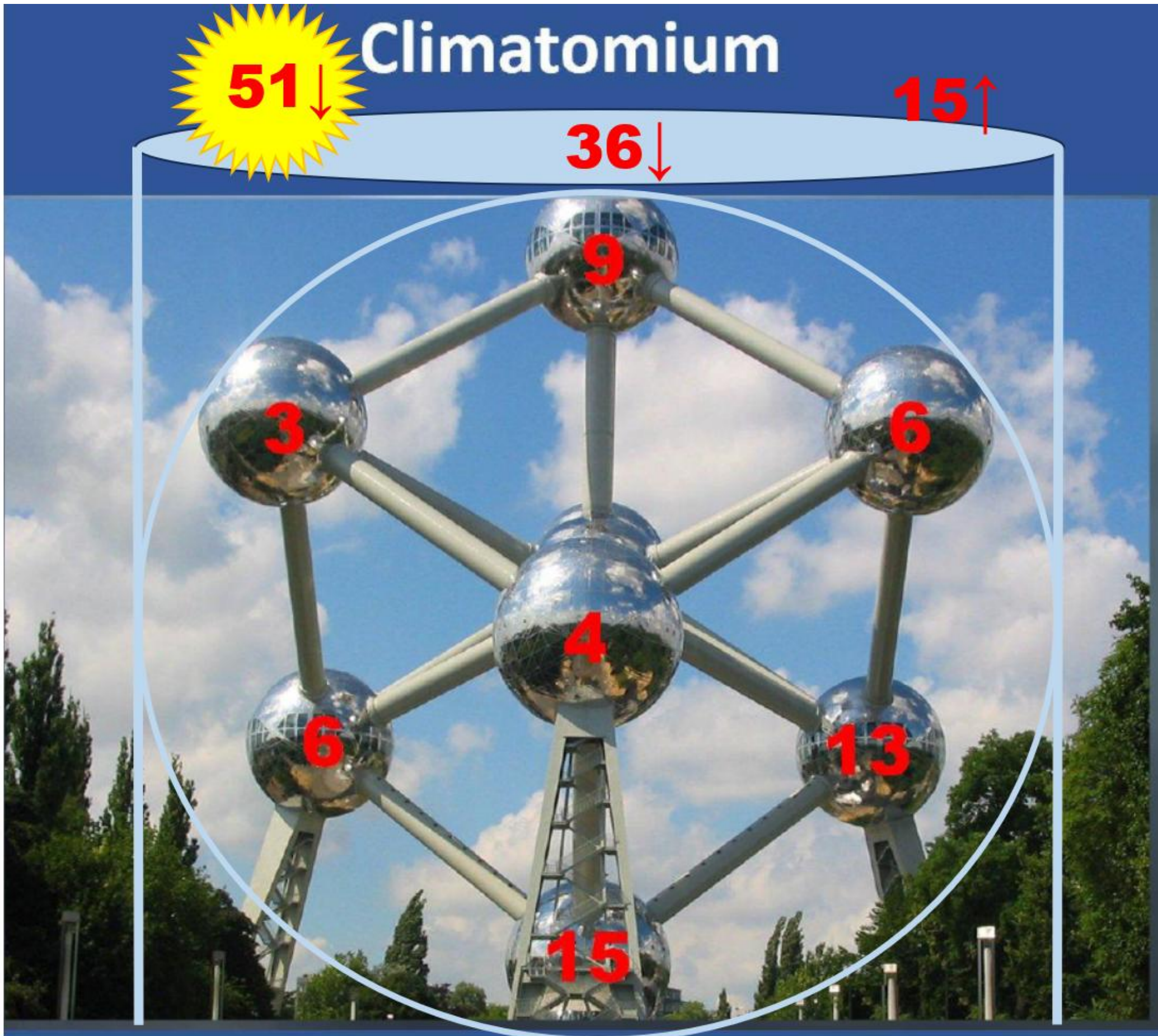
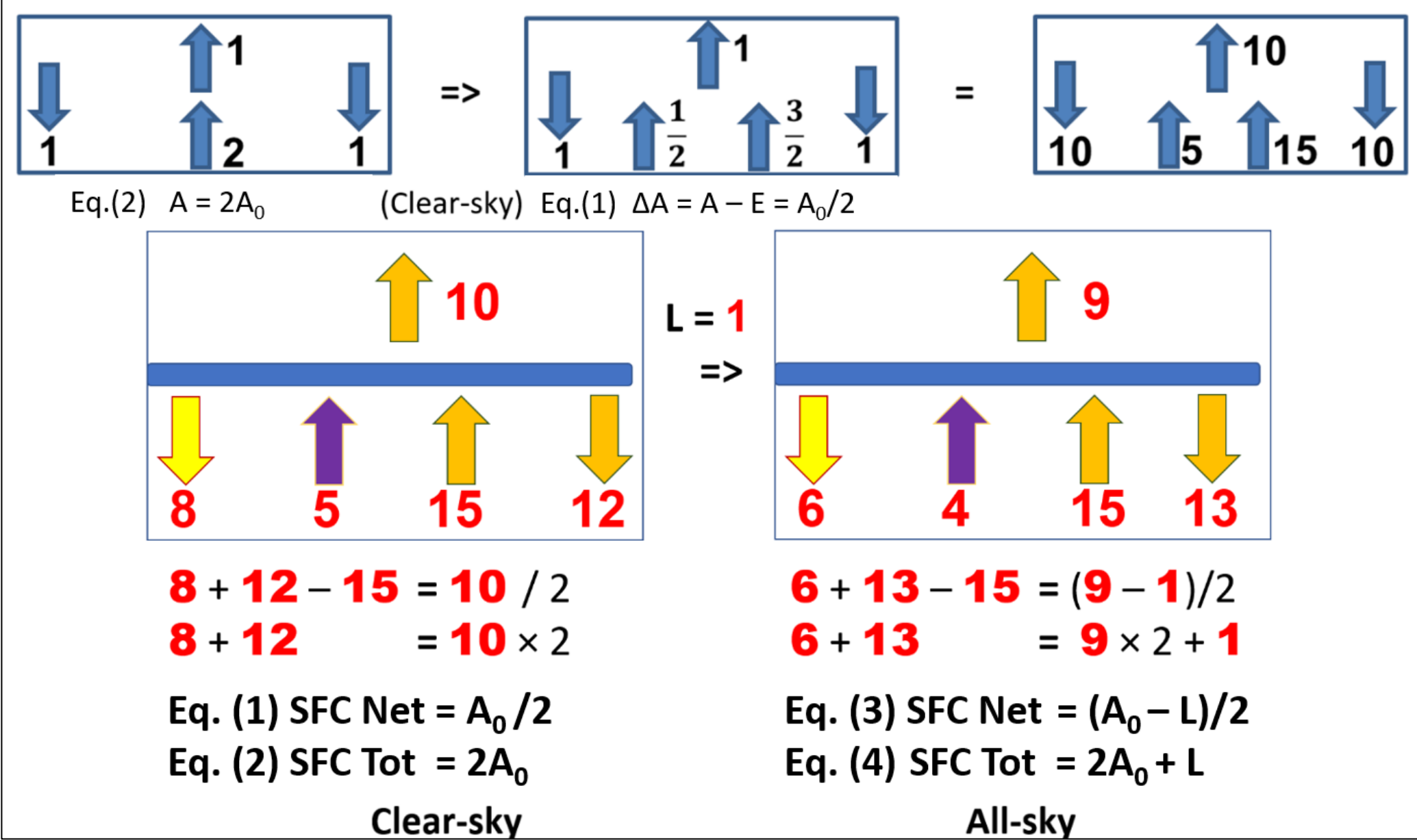
Clear-sky	Ed2.8	Ed4.0	EdMZ
TOA SW in	339.87	340.04	340.04
TOA LW up	265.59	268.13	266.82
SFC SW in	214.32	213.91	213.47
SFC LW down	316.27	314.07	320.18
SFC (SW + LW) in	530.59	527.98	533.65
SFC LW up	398.40	397.59	400.23
SFC Net	132.19	130.39	133.42
G	132.81	129.46	133.42
TOA LWCRE	25.99	27.99	26.68

CERES Science Team Meeting presentations are summarized at <https://earthenergybudget.com>

Homepage: <https://earthenergyflows.com>

Contact: miklos.zagoni@earthenergyflows.com

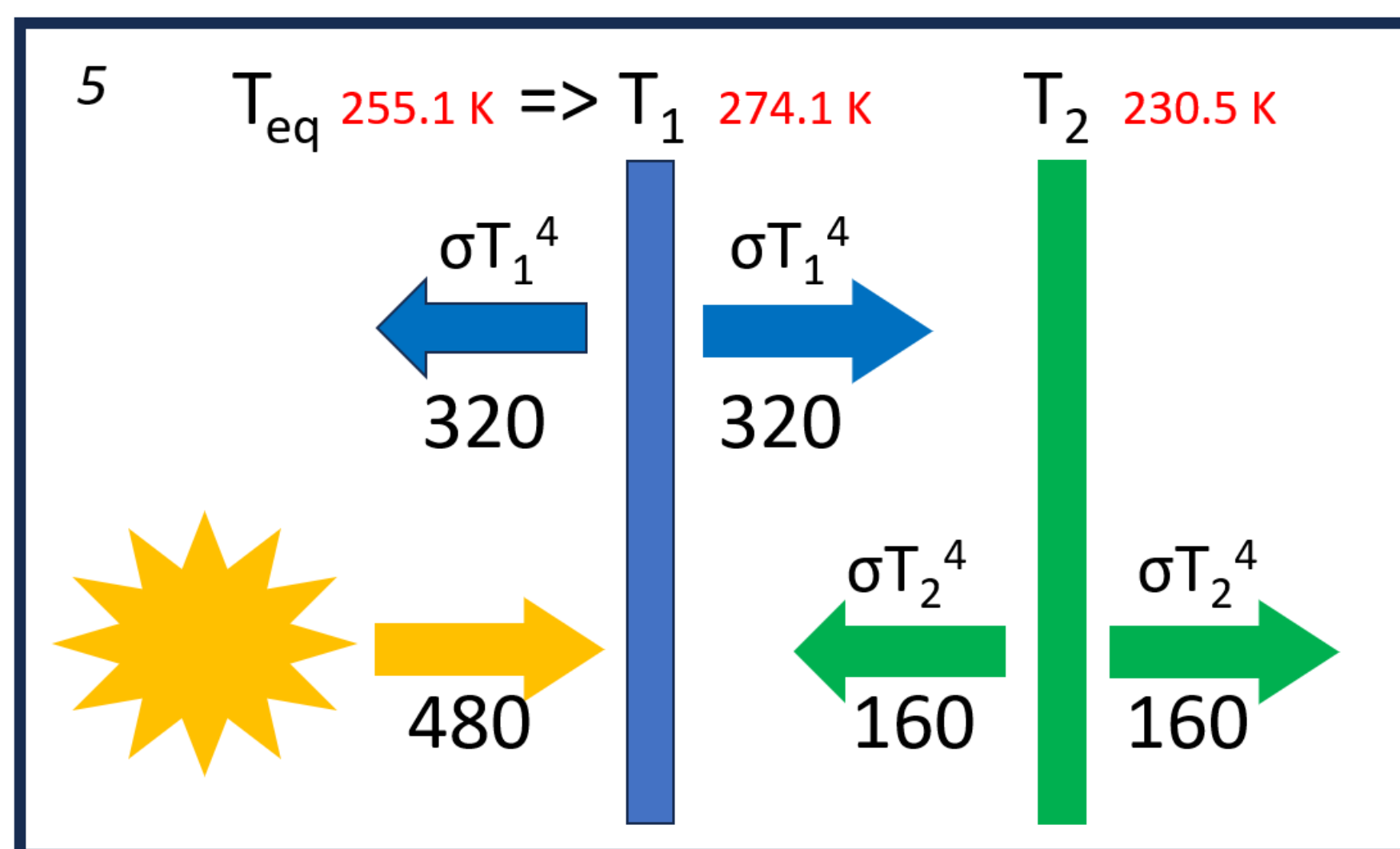
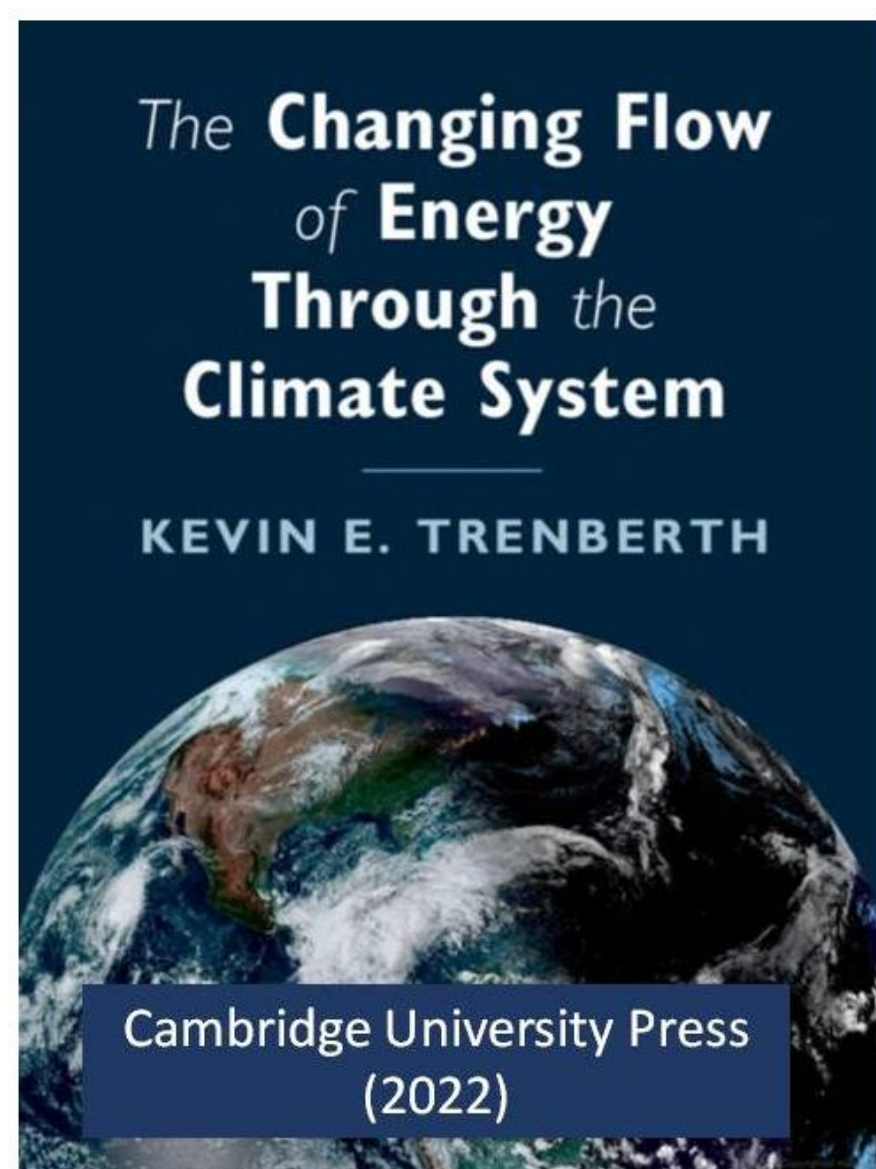
Geometric Summary



https://www.earthenergyflows.com/Zagoni-EGU2024-Trenberths-Greenhouse-Geometry_Full-v03-480.mp4 (Length 2:2:28)

The Physical Science Basis:

Trenberth's Greenhouse Geometry



Sidebar 3.2, Fig. 3.3. Panel 5: Two plates in space

In this book, there is a 2-page long sidebar: “How Does a Greenhouse Effect Work?”, where an idealized geometric model is depicted, consisting of two plates in space, without any reference to the atmospheric composition or the concentration of the greenhouse gases; and four equations are presented to describe the resulting energy flow system.

In this Brochure I showed, and in the video below I explain in more detail, that the radiative structure of this model is the same as that of the real Earth's clear-sky atmosphere, and the governing equations of that simple arrangement and the generated fundamental energy flow ratios are identical to the real Earth atmospheric clear-sky greenhouse effect.

Video presentation:

Trenberth's (2022) Greenhouse Geometry and its Representation on the Earth's Atmosphere Part I. The Physical Science Basis

Miklos Zagoni

Budapest, Hungary

miklos.zagoni@t-online.hu

Supplementary Video for a talk given at the

EGU General Assembly, 18 April 2024, Vienna, Austria

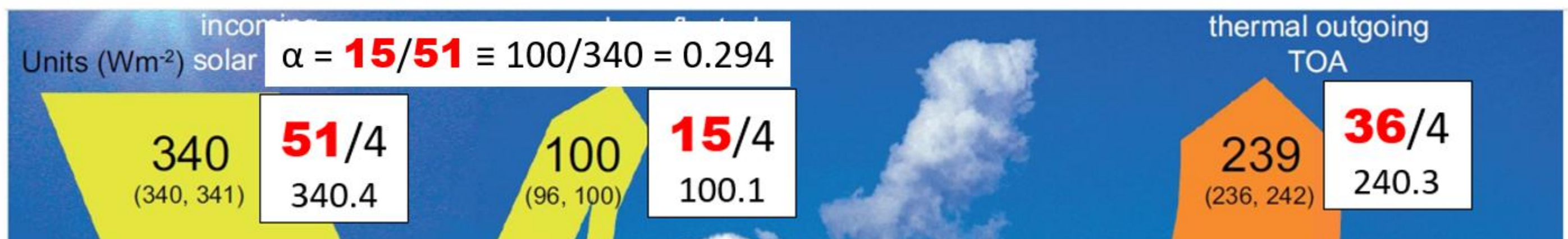
Session CL2.1 – Earth radiation budget, radiative forcing and climate change

Conveners Martin Wild, Jörg Trentmann, Paul Stackhouse

Updated 30 November 2024 (Length 1:16:08)

An Unresolved Mystery: Albedo / All-Sky

IPCC WGI AR6 (2021); Wild et al. (2013)



These integer ratios belong to the plane-parallel approximation of Schwarzschild's (1906, Equation 11).

Using the integral equation from Schwarzschild's (1914) with the same parameters, a solution might be:

$$\alpha_p = 1 - \int_{-45^\circ}^{45^\circ} \cos(x)/2 dx$$

$$= 1 - \sin 45^\circ = 1 - \sqrt{2}/2$$

$$= 0.292893$$

OBSERVATION:

CERES - EBAF Data
Time Range: January to December - CLIMATE YEAR
Time Resolution: CLIM
Valid Range: 0 - 800

Incoming Solar Flux (W m ⁻²)	TOA Shortwave Flux All-Sky (W m ⁻²)	Albedo
CLIM 1 350.69	106.26	0.30300265
CLIM 2 348.15	102.27	0.29375269
CLIM 3 343.98	99.31	0.28870865
CLIM 4 337.54	97.44	0.2886769
CLIM 5 332.3	97.45	0.2932591
CLIM 6 329.24	96.39	0.29276516
CLIM 7 328.89	93.93	0.28559701
CLIM 8 331.43	92.62	0.27945569
CLIM 9 336.78	94.79	0.28145971
CLIM 10 342.04	100.24	0.29306514
CLIM 11 347.05	106.18	0.30595015
CLIM 12 350.34	108.29	0.30909973
AVERAGE 339.8692	99.5975	0.29289938

In an assumed equilibrium (OLR = ASR), EBAF Ed4.2.1 CLIMATE YEAR data:

Solar = 340.163, TOA ASR (all-sky) = 240.196, TOA SW up (all-sky) = 99.967 [Wm⁻²] => $\alpha_p = 0.2939$.

Applying the geodetic weighting factor (4.0034) instead of the spherical (4) on the 15/51 = 5/17 = 0.2941 ratio, we have 0.2939.

An attempt of explanation is given in:

<https://www.earthenergyflows.com/Zagoni-EGU2024-Trenberths-Greenhouse-Geometry-Full-v03-480.mp4> esp. from 1:47:00

An Unresolved Mystery: Albedo / Clear-Sky

In the all-sky, TOA albedo was $\alpha = 15/51 = 5/17$. In this unit, TSI = **17** units = 1360.68 Wm^{-2} , and **1** = 80.04 Wm^{-2} .

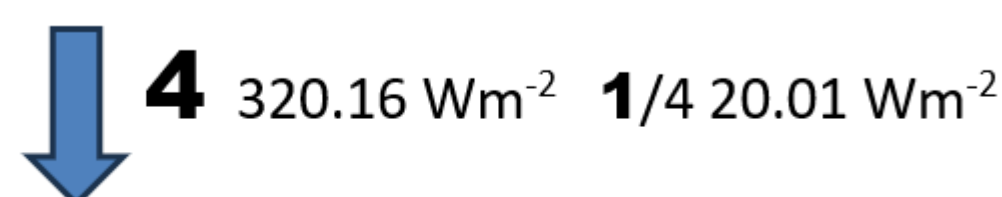
Now I DEFINE "clear-sky" via TOA net clear-sky imbalance as TOA net clear IMB = **1** quantum = 80.04 Wm^{-2} .

This is the extra energy absorbed in the clear-sky part, to be transported to the cloudy part.

Therefore, there remains **16** units to be processed in the clear-sky part on the disk.



After spherical weighting, we have **4** units for clear-sky incoming, and **1/4** units as clear-sky TOA imbalance:



But in the clear-sky, we have already two constraints.

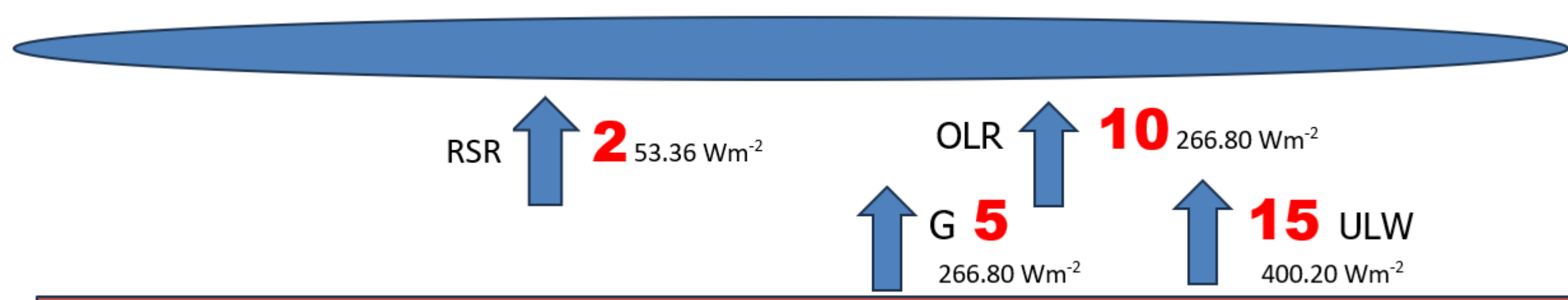
First, the clear-sky ratios must be $G : \text{TOA LW up} : \text{SFC LW up} = 1 : 2 : 3$.

Second, SFC LW up is the same as in the all-sky, **15** (red) units = 400.20 Wm^{-2} .

Hence, G must be **5** (red) units, and TOA LW up = **10** (red) units = 266.80 Wm^{-2} .

Thus, to satisfy all these three constraints, clear-sky ISR of **4** (black) quanta = **12** (red) units = 320.16 Wm^{-2} should be decreased to TOA LW up = **10** (red) units = 266.80 Wm^{-2} .

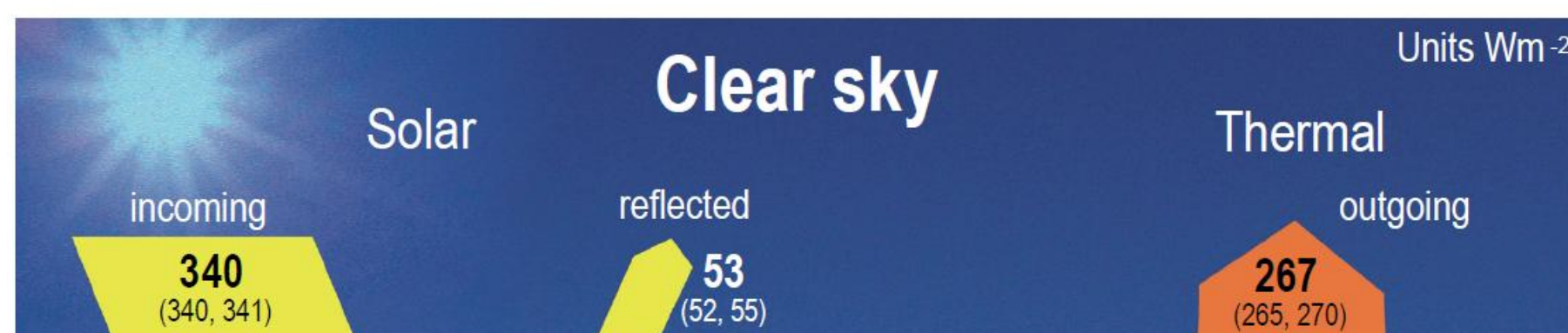
Therefore, the system has to get rid of **2** (red) units = 53.36 Wm^{-2} .



That's why my Theoretical Reference Estimate is

2 (red) units = 53.36 Wm^{-2} for TOA clear-sky reflection, and

1/4 (black) unit = **3/4** (red) = 20.01 Wm^{-2} for TOA clear-sky imbalance:



IPCC WGI AR6: reflected solar = 53, TOA IMB = $340 - 53 - 267 = 20$.

Alternative logics perhaps might lead to different integers,
but certainly not to slightly different values.

TOA Net Clear-Sky Imbalance = – TOA Net CRE

Above, we found that the integer position for the clear-sky TOA imbalance is **1** (black) quantum = **3** (red) units = 80.04 Wm^{-2} on the disk, that is, **3/4** (red) units = 20.01 Wm^{-2} after spherical weighting. Here I show that TOA net clear-sky imbalance is arithmetically identical to the negative of TOA NET CRE.

RSR = Reflected Solar Radiation at TOA, ISR = Incoming Solar Radiation at TOA, ASR = Absorbed Solar Radiation at TOA, and IMB for Earth Energy Imbalance, EEI:

$$\begin{aligned}
 \text{Net CRE TOA} &\equiv \text{SW CRE TOA} + \text{LW CRE TOA} = \text{RSR}(\text{clear}) - \text{RSR}(\text{all}) + \text{OLR}(\text{clear}) - \text{OLR}(\text{all}) = \\
 &= [\text{ISR} - \text{ASR}(\text{clear})] - [\text{ISR} - \text{ASR}(\text{all})] + \text{LWCRE} = \text{ASR}(\text{all}) - \text{ASR}(\text{clear}) + \text{OLR}(\text{clear}) - \text{OLR}(\text{all}) = \\
 &= \text{ASR}(\text{all}) - \text{OLR}(\text{all}) - [\text{ASR}(\text{clear}) - \text{OLR}(\text{clear})] = \text{TOA IMB (all)} - [\text{ASR}(\text{clear}) - \text{OLR}(\text{clear})] = \\
 &= \text{TOA IMB (all-sky)} - \text{TOA IMB (clear-sky)}.
 \end{aligned}$$

In equilibrium, TOA IMB (all-sky) = 0. That is, in principle, despite its name, **TOA Net CRE is a clear-sky phenomenon**. Its role in the climate system can be understood and its magnitude can be computed without any reference to clouds. It depends only on clear-sky values: Absorbed Solar Radiation in the clear-sky and Emitted Longwave Radiation in the clear-sky.

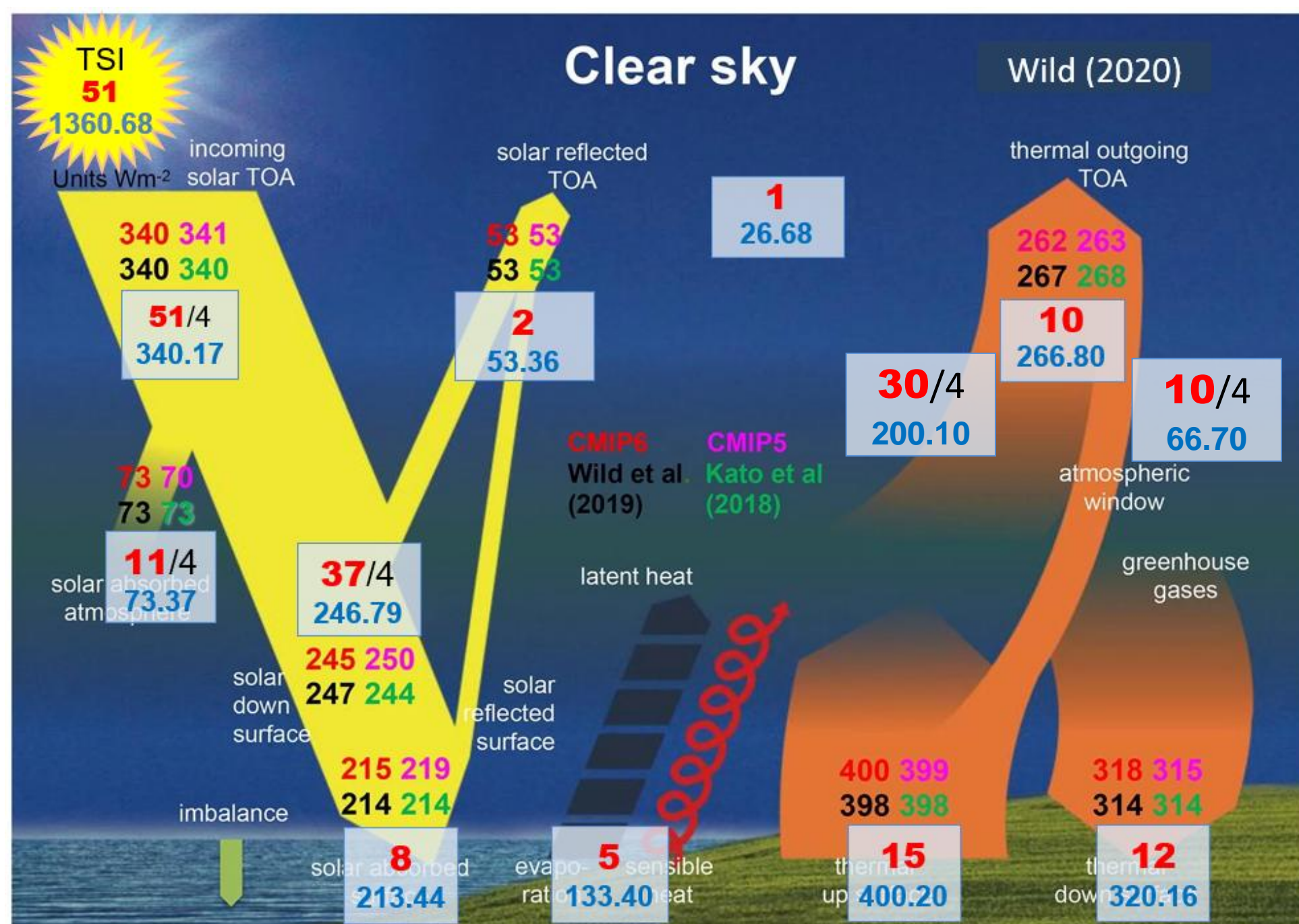
$$\begin{aligned}
 \text{TOA IMB (clear-sky)} &= \text{ASR} - \text{OLR} = \mathbf{43/4} - \mathbf{40/4} = \mathbf{3/4} = 20.01 \text{ Wm}^{-2} \\
 \text{Net CRE TOA} &= -\text{TOA IMB (clear-sky)} = \mathbf{-3/4} = -20.01 \text{ Wm}^{-2}
 \end{aligned}$$

Clear-Sky Atmospheric Window Radiation

An important, non-observable energy flow component at TOA is the atmospheric window radiation. This is the only element in Fig.1 (Wild 2020, Fig.13) which is indicated in the graphical arrangement but without an assigned value. Shown also in Li, Li, Wild and Jones (2024), without quantification.

Costa and Shine (2012) performed a detailed line-by-line computation in the clear-sky and found that in the annual global mean, $\text{WIN}(\text{clear-sky}) = 65 \text{ Wm}^{-2}$. This value is related to their model-OLR of 259 Wm^{-2} . Assuming proportionality, comparing it to our theoretical reference estimate of $\text{OLR}(\text{clear}) = 266.80 \text{ Wm}^{-2}$, the corresponding value would be $(266.8/259) \times 65 = 66.96 \text{ Wm}^{-2}$.

Notice that in the integer ratio system, 66.70 Wm^{-2} is an integer position, **10/4** units on the sphere, that is, **10** units on the disk. Thus, the system in clear-sky would look like this: Atmospheric window = **10/4**, Atmospheric upward emission = **30/4** = **15/2** = 200.1 Wm^{-2} .

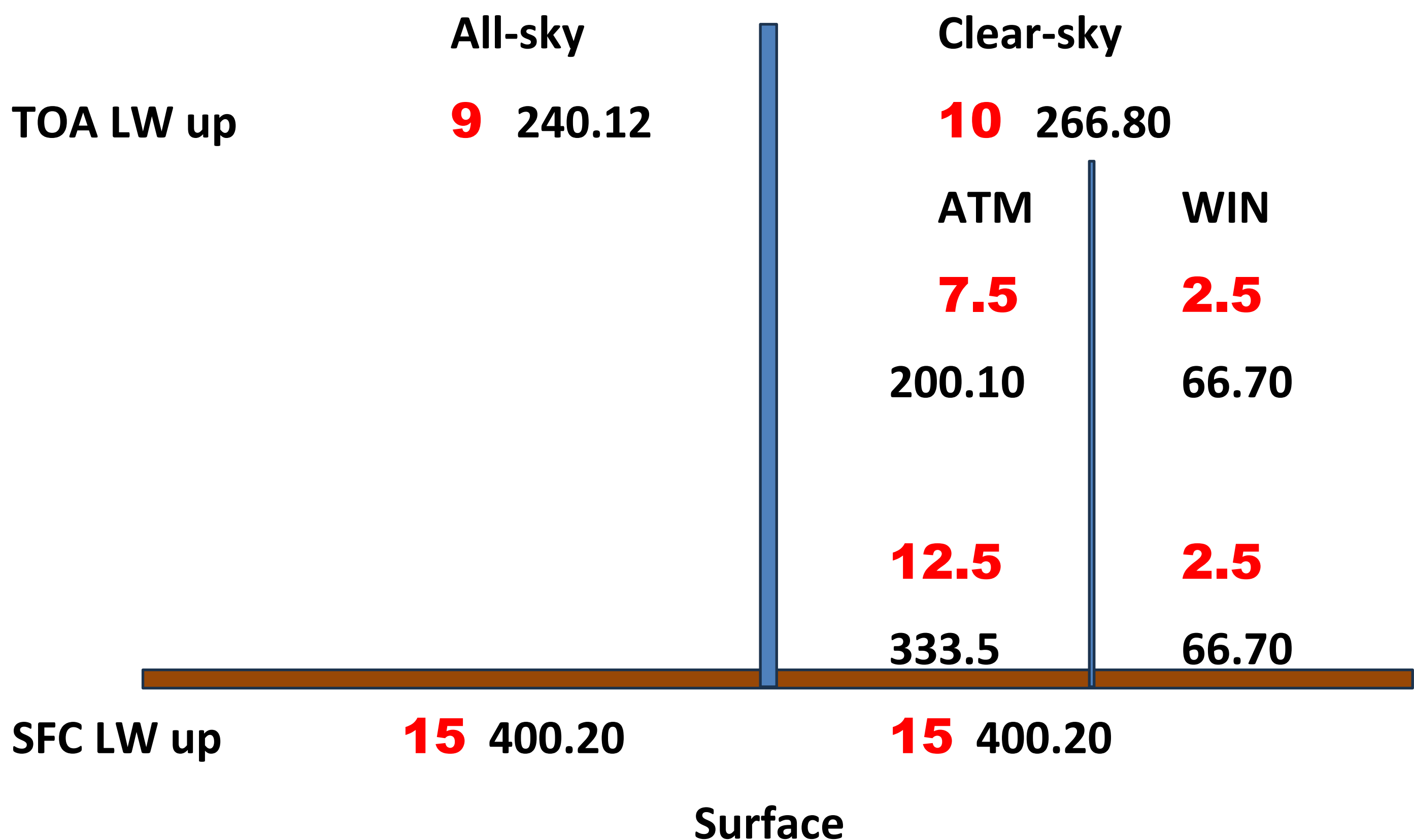


Transfer Function and Clear-Sky Atmospheric Window

Transfer function, also called planetary emissivity (Bengtsson 2012), is defined as $\epsilon_p = f = (\text{TOA LW up}) / (\text{SFC LW up})$.

In the integer system, they have definite values, $\epsilon_p (\text{all-sky}) = f (\text{all-sky}) = 9 / 15 = 0.6$, and in the clear-sky, $\epsilon_p (\text{clear-sky}) = f (\text{clear-sky}) = 10 / 15 = 2/3$.

Now let us separate clear-sky into two parts: a transparent region for the atmospheric window, and an absorbing region for GHGs.



In the transparent region, the transfer function is $f (\text{clear-sky}) = 1$. How much is it in the absorbing region?

$f (\text{clear-sky, GHG}) = 7.5 / 12.5 = 3/5 = 0.6$. And how much is the greenhouse effect, $G = (\text{SFC LW up}) - (\text{TOA LW up})$?

In the window region it is evidently zero, $G (\text{clear, WIN}) = 0$. In the absorbing region, $G (\text{clear, GHG}) = 12.5 - 7.5 = 5$ units.

That is, in the clear-sky absorbing region, the transfer function is the same as in the all-sky, $f (\text{clear, GHG}) = f (\text{all}) = 0.6$, producing the required greenhouse effect of $G (\text{clear}) = 5$ units = 133.40 Wm^{-2} . In the absorbing part, the ratios $G (\text{clear, GHG}) : \text{OLR} (\text{clear, GHG}) : \text{ULW} (\text{clear, GHG}) = 5 : 7.5 : 12.5 = 2 : 3 : 5$ are the same as the all-sky ratios.

The corresponding greenhouse factor is $g (\text{clear, GHG}) = 5 / 12.5 = 2/5 = 0.4$, same as the all-sky greenhouse factor; and the contribution to the atmospheric emission of 200.10 Wm^{-2} per area unit is $200.10 \times 6/5 = 240.12 \text{ Wm}^{-2}$, same as the all-sky OLR. [The other component of the clear-sky OLR of 66.70 Wm^{-2} comes from the surface emission of 400.20 Wm^{-2} , with an area fraction of $1/6$].

The clear-sky transfer function, $f (\text{clear}) = 10 / 15 = 2/3$ is an area-weighted sum of the transfer functions of the transparent ($1/6 \times f (\text{WIN}) = 1/6$) and the absorbing ($5/6 \times f (\text{clear, GHG}) = 5/6 \times 3/5 = 1/2$) regions.

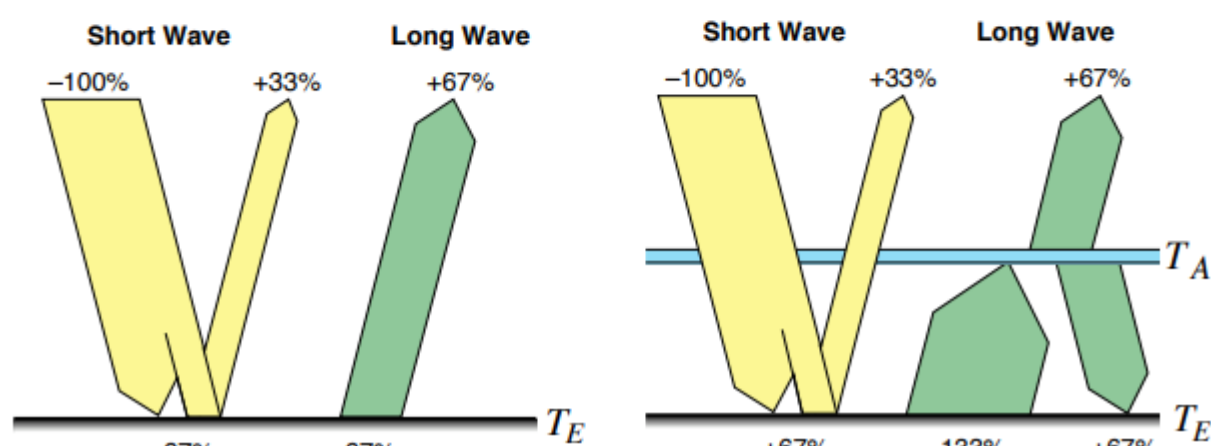
There is no “clear-sky”. Where is absorption, there are “all-sky” data; where transparent, there are direct surface-transmitted data. The absorbing part of the clear-sky atmosphere works in every respect as the all-sky, in an amazing intricate cooperation between the regions, securing an extraordinary condition of stability.

Contemplating on the Hows ...

9

Idealisierte Atmosphäre

Reale Atmosphäre



In der wirklichen Atmosphäre wirken Treibhausgase und Wolken ähnlich wie die Scheibe in einem Treibhaus:



H_2O CO_2 CH_4

Schär, ETH Zürich

In this document we showed that the 'Idealisierte Atmosphäre' provides us with an excellent theoretical reference estimate of the annual global mean energy flow system of our 'Reale Atmosphäre'.

How? In think, H_2O is the tool.

In our quasi aqua-planet — as long as there is enough open (free) ocean surface —, in a wide range of planetary temperatures H_2O is able to provide a fast and effective compensation for the changes in non-condensing greenhouse gases. By using all of its forms and available processes: evaporation (cooling the surface as CONV), water vapor (heating the surface as greenhouse gas, G), defining atmospheric LW transparency (WIN), cloud formation (shielding and blanketing effects, SW, LW and net CRE), precipitation (P), and surface snow and ice (adjusting albedo, α), H_2O generates, regulates and maintains the required atmospheric and surface properties and conditions in order to satisfy the radiative constraints expressed by the four theoretical GHG-independent stationary geometric governing equations.

... And Whys

I think the fundament is Equation (1). Under the given conditions, it may be derived from first principles (as Edward Arthur Milne noted in his *Thermodynamics of the Stars, Handbuch der Astrophysik*, Vol. 3. 1930), and prescribes surface convection as directly coupled to half of outgoing longwave radiation at TOA. But as evaporation is almost proportional to the temperature of water, a given convection defines a given surface thermal emission — hence constraining surface Planck-radiation to OLR, as given in Equation (2). From here the all-sky case is straightforward, and the basic structure is described.

In this sense, the question is not theoretical, but historical. The problem is not why are these equations valid, but that why are they omitted from the basic climate literature? Goody's essential *Atmospheric radiation: theoretical basis* (Oxford) is explicit about Eq. (1) and was published in 1964; Schwarzschild's original (1906) paper in English translation appeared in 1966. Why are they missing from Manabe and Wetherald (1964) and (1967), and from all of their follow-ups?

And if it is there in Houghton's *The physics of atmospheres* (Cambridge) in all the three editions (1977, 1986, 2002), in every university textbook on atmospheric physics and radiation and in dozens of university classroom lecture notes, why is it missing from all the IPCC Reports (1990-2021)?

And further, the integer ratio systems are apparent in every graphical arrangement of the global energy budget published in the past decade (Stevens and Schwartz 2012, Stephens et al. 2012, Wild et al. 2013, Loeb 2014, L'Ecuyer et al. 2015, Hartmann 2016 etc.). Why weren't they revealed at first glance?

The question is not, why are the $G : OLR : ULW = 1 : 2 : 3$ ratios in the clear-sky and $2 : 3 : 5$ ratios in the all-sky are valid, but that why were not these ratios deduced from the known equations much earlier?

Of course, four equations do not define every shortwave and longwave component in the all-sky and clear-sky energy flow system, therefore further logical steps are to be done. The rationale of them lies in the observational outcome, and further theoretical considerations are needed to support them.

One example is the separation of the convective flux into its components, latent heat and sensible heat, occupying integer positions individually.

Another example is the definition of clear-sky TOA imbalance as 1 (big) quantum if $TSI = 17$. The why-question here is again still unanswered.

A third case is the integer position of clear-sky atmospheric window, for which we have only a result from computation (but as that, very accurate).

And certainly, one of the most intriguing features is the role of LWCRE as the 'pacer' or 'pace-maker' of the whole integer system as the unit flux, or quantum.

New generations of theoretical physicists may find a *Fundgrube* in the geometric behavior of our greenhouse effect.

CERES_EBAF_Ed4.2.1 October 2000 – September 2024 (last 3 years are shown)

Largest difference from the N-position is 4.68 Wm⁻² in Surface total net all-sky

Click to enlarge and download table

253		98, 7074	240, 9554	2,5637	52,90444	265,6999	23,62213	-45,80284	24,74439	-21,05843	342,2266	189,6414	244,0378	23,24179	29,07158	347,8019	318,5667	400,204	400,0479	166,3996	214,9664	-52,4021	-81,48115	113,9975	133,4851
254		104,4346	238,2724	4,9966	56,10619	263,6071	27,98941	-48,32811	25,33461	-22,99351	347,703	193,2171	250,9092	26,74921	32,85757	342,1113	312,8091	394,5234	394,4719	166,4678	218,0516	-52,41211	-81,66286	114,0557	136,3887
255		107,5056	237,4099	6,2549	56,67256	262,7762	31,7214	-50,83266	25,3662	-25,46644	351,1706	192,5235	252,8553	26,60167	32,78657	339,0085	310,4919	390,9289	391,2567	165,9218	220,0688	-51,92038	-80,76502	114,0014	139,3037
256		104,8217	237,3957	9,253	55,32596	262,7736	33,37041	-49,4954	25,37786	-24,11755	351,4704	193,3327	251,7359	24,80234	30,81571	337,4441	309,6986	389,7022	390,0338	168,5303	220,9203	-52,25814	-80,33506	116,2722	140,5853
257		100,4988	238,7799	9,4367	54,44646	263,5489	30,72001	-46,05215	24,76886	-21,28329	348,7156	193,3844	248,0479	23,31385	29,34392	338,2945	311,0346	390,9992	391,1939	170,0706	218,7039	-52,70467	-80,15937	117,3659	138,5445
258		97,7993	238,5701	7,3783	54,25489	263,9326	25,56023	-43,54433	25,36258	-18,18176	343,7478	191,4149	243,3389	23,41029	29,4502	342,2765	314,8845	394,8565	395,0477	168,0046	213,8886	-52,58004	-80,16295	115,4246	133,7257
259		96,0976	240,0821	1,7949	55,47027	265,1029	17,40201	-40,62751	25,02076	-15,60676	337,9749	189,9422	239,2045	25,3512	31,49526	346,2696	318,1993	399,4394	399,9435	164,591	207,7094	-53,16977	-81,7442	111,4212	125,9651
260		96,7908	241,504	-5,2819	55,2164	266,8023	8,910278	-41,57462	25,29841	-16,27623	333,0126	183,9398	234,7318	25,06589	31,84753	350,5461	322,1613	403,8929	403,9753	158,8739	202,8843	-53,34674	-81,81413	105,5272	121,0702
261		94,2918	243,1035	-7,3893	52,42343	268,6725	9,199315	-43,09057	25,23519	-17,85538	339,0056	180,1227	230,7089	22,13565	28,73714	354,5281	327,1277	408,0301	408,2962	157,987	201,9718	-53,50202	-81,16852	104,485	120,8033
262		93,4224	244,7928	-8,6565	50,33212	270,0281	9,199315	-43,09057	25,23519	-17,85538	339,559	176,719	228,1416	19,37508	25,5568	358,5741	330,8475	409,2198	409,7949	157,3439	202,5847	-50,64572	-78,9473	106,6982	123,6374
263		91,8107	243,9578	-3,8613	48,96224	267,1224	13,8224	-42,84861	25,16452	-17,68407	331,9068	179,6492	230,4227	18,21585	24,25596	357,4669	330,2098	408,4352	408,8898	161,4333	206,1667	-50,96832	-78,68001	110,465	127,4867
264		93,3346	242,9631	0,2387	50,08413	267,9279	18,52429	-43,25048	24,96487	-18,28564	336,5364	184,3139	235,454	19,46911	25,1872	353,2803	324,7163	405,0963	405,4862	164,8448	210,2668	-51,81599	-80,76996	113,0288	129,4969
265		98,9496	240,6711	2,7428	53,15376	265,7502	23,45969	-45,7957	25,07917	-20,71652	342,3639	188,9254	243,5483	23,14738	28,91193	347,9407	318,2406	400,0871	400,2213	165,7781	214,6363	-52,14635	-81,9804	113,6317	132,6559
266		104,689	238,4728	4,6625	56,56578	263,3417	27,91626	-48,12286	24,8669	-23,25397	347,8242	192,7777	250,6648	26,84423	32,96874	341,3409	311,8542	393,6637	393,7872	165,9335	217,696	-52,32288	-81,93311	113,6106	135,763
267		106,2429	237,2914	7,6908	56,83059	262,3939	32,00045	-49,41195	25,10263	-24,30932	351,2256	193,5878	252,4548	26,50303	32,52414	337,9436	309,7894	390,5557	391,0644	167,0848	219,9305	-52,61208	-81,27502	114,4727	138,6555
268		103,8612	238,1718	9,5616	55,28458	262,8087	33,50086	-48,57627	24,63669	-23,93938	351,5945	194,0472	251,648	24,57954	30,43088	336,9802	309,3247	389,6776	390,4656	169,4676	221,2172	-52,6974	-81,14087	116,7702	140,0763
269		100,4361	238,4082	10,014	54,60859	263,3044	30,94511	-45,82726	24,89607	-20,93118	348,8583	192,7375	247,5771	23,16995	29,1373	338,9588	311,3165	391,546	392,3134	169,5676	218,4398	-52,5872	-80,99689	116,9804	137,4429
270		96,8389	238,8378	8,301	53,75555	264,0556	26,1667	-43,08337	25,21774	-17,86562	343,9779	192,2131	244,1617	23,32921	29,47409	343,0176	315,1904	395,9231	396,7707	168,8839	214,6875	-52,90546	-81,5801	115,9784	133,1074
271		95,4387	238,812	3,9093	55,06451	264,4027	18,69326	-40,37437	25,59056	-14,7838	338,1602	190,388	239,2811	25,28007	31,40031	346,5129	318,7782	399,8491	400,3909	165,108	207,8808	-53,33624	-81,61266	111,7717	126,2681
272		96,28	240,0879	-3,3144	55,04652	266,2265	11,78083	-41,23367	26,13864	-15,09504	333,0536	183,5718	234,0113	24,81425	31,73598	352,2584	324,2188	405,2886	405,2398	158,7576	202,2753	-53,05022	-81,02094	105,7074	121,2543
273		94,1155	243,9189	-7,9531	52,32	269,1089	8,65178	-41,79574	25,18998	-16,60576	330,0803	179,1258	229,6274	21,99086	28,53834	356,7723	329,5032	409,651	409,7618	157,1949	201,0891	-52,87865	-80,25866	104,3163	120,8304
274		91,9415	245,5909	-7,9875	50,36101	270,4723	8,71242	-41,58075	24,88147	-16,69928	329,5454	177,1177	226,662	19,22236	25,33484	360,2484	333,5309	411,4499	412,0339	157,8954	201,3271	-51,20147	-78,50298	106,6939	122,8241
275		90,0442	246,0138	-4,0719	48,86162	270,3517	12,77289	-41,1827	24,33787	-16,84485	331,9859	180,6093	229,242	18,09754	23,79961	359,6151	332,9008	410,9144	411,3944	162,5118	205,4424	-51,29924	-78,49373	111,2125	126,9487
276		91,8499	244,6051	0,1319	49,77739	269,1774	17,63781	-42,07256	24,56721	-17,50534	336,5875	184,6852	234,2685	19,22868	24,57043	356,68	329,0005	408,1161	408,4055	165,4566	209,698	-51,43609	-79,40533	114,0205	130,2928
277		97,7124	242,5307	2,2283	52,5686	266,8806	23,02255	-45,1436	24,35001	-20,79361	342,4721	189,1095	242,8158	22,70358	28,31689	351,3488	321,9916	402,7723	402,7569	166,4059	214,499	-51,42344	-80,76534	114,9825	133,7337
278		104,1191	239,2973	4,4884	56,20588	264,3373	27,36126	-47,91288	25,04019	-22,87269	347,905	191,8966	249,4565	26,3176	32,44026	346,1155	316,5586	396,904	396,9132	165,579	217,0163	-50,78852	-80,3543	114,7905	136,6619
279		106,3374	238,2565	6,7748	56,67485	263,6084	31,08583	-49,66216	25,35186	-24,31027	351,3696	193,2553	252,2531	26,6874	32,55133	342,2156	313,8424	393,6581	394,238	166,5679	219,7019	-51,44246	-80,39542	115,1254	139,3064
280		104,8924	238,8159	8,0029	55,36269	264,0092	32,33899	-49,52936	25,19333	-24,33604	351,7114	192,6077	251,3724	24,66777	30,7723	340,859	313,0428	392,1826	392,9261	167,9399	220,65	-51,32364	-79,788313	116,6163	140,7669
281		100,8297	239,1887	8,742	54,03152	264,4475	30,28127	-46,79798	25,25821	-15,53926	346,7605	191,705	247,7225	22,9962	28,99872	343,1651	315,163	393,9589	394,9054	168,7988	218,7237	-50,53487	-79,74237	118,0049	138,9815
282		97,8548	239,2097	6,7147	53,50908	264,6825	25,58821	-44,34574	25,47272	-18,87301	343,7798	190,219	243,4278	23,24954	29,32313	346,3315	318,2617	396,8664	397,6888	166,9694	214,1047	-50,55484	-79,95622	112,3445	127,8752
283		95,8494	239,8717	2,2767	54,33109	265,5461	18,1211	-41,5185	25,67441	-15,8441	337,9982	188,7794	238,7513	24,79462	30,9199	349,8272	322,0793	401,4675	402,0357	163,9848	207,8314	-51,64028	-79,95622	112,3445	127,8752
284		96,4398	242,4165	-5,8927	55,20716	267,5814	10,17486	-41,23293	25,16492	-16,068	332,9631	183,6233	234,0934	25,32066	32,34639	353,8289	325,9371	406,3748	406,2236	158,3027	201,7469	-52,54584	-80,28638	105,7568	121,4606
285		94,759	244,133	-8,8701	52,08978	269,4231	8,509075	-42,66945	25,28998	-17,37947	330,0214	178,1862	229,7249	21,79689	28,61031	358,2435	330,6667	410,082	410,3212	156,3893	201,1147	-51,83855	-79,65453	104,5508	121,4601
286		93,1732	245,3037	-8,7732	50,29143	270,6774	8,735243	-42,88205	25,37369	-17,50835	329,7037	175,2004	226,4833	18,91136	25,26239	360,3	333,1862	411,0113	411,5403	156,289	201,2209	-50,71124	-78,35405	105,5778	122,8668
287		90,9307	245,6309	-4,5747	49,09739	270,4989	12,39063	-41,83353	24,86801	-16,96552	331,9866	178,1705	227,5554	17,85514	23,61805	359,8003	332,7403	410,4758	410,9629	160,3154	203,9373	-50,6755	-78,22261	109,6399	125,7147
288	month	92,647	244,5557	-0,3599	49,99052	268,9713	17,88118	-42,65653	24,41561	-18,24092	336,843	182,7636	232,7271	19,10348	24,47001	356,3938	328,276	407,2179	407,6057	163,6601	208,257	-50,82407	-79,32978	112,8361	128,9273
289	mean	98,91	240,42	0,88	53,76	265,98	20,46	-45,15	25,56	-19,59	340,21	187,12	240,97	23,44	29,67	346,44	318,25	398,72	398,92	163,68	211,30	-52,28	-80,67	111,40	130,63
290	name	sw-a	lw-a	net-a	sw-cl	lw-cl	net-cl	cre-sw	cre-lw	cre-net	solar	sw-dn-a	sw-dn-c	sw-up-a	sw-up-c	lw-dn-a	lw-dn-c	lw-up-a	lw-up-c	net-sw-a	net-sw-c	net-lw-a	net-lw-c	net-tot-a	net-tot-c
291	N	15/4	9	0	2	10																			